



CMS-SMP-23-003

CERN-EP-2025-130
2025/08/12

Search for charged lepton flavor violating Z and Z' boson decays in proton-proton collisions at $\sqrt{s} = 13 \text{ TeV}$

The CMS Collaboration^{*}

Abstract

A search for flavor violating decays of the Z boson to charged leptons is performed using data from proton-proton collisions at $\sqrt{s} = 13 \text{ TeV}$ collected with the CMS detector at the LHC, corresponding to an integrated luminosity of 138 fb^{-1} . Each of the decays $Z \rightarrow e\mu$, $Z \rightarrow e\tau$, and $Z \rightarrow \mu\tau$ is considered. The data are consistent with the backgrounds expected from standard model processes. For the $Z \rightarrow e\mu$ channel the observed (expected) 95% confidence level upper limit on the branching fraction is 1.9 (2.0) $\times 10^{-7}$, which is the most stringent direct limit to date on this process; the corresponding limits for the $Z \rightarrow e\tau$ and $Z \rightarrow \mu\tau$ channels are 13.8 (11.4) $\times 10^{-6}$ and 12.0 (5.3) $\times 10^{-6}$, respectively. Additionally, the $e\mu$ final state is used to search for lepton flavor violating decays of Z' resonances in the mass range from 110 to 500 GeV. No significant excess is observed above the predicted background levels.

Submitted to Physical Review D

1 Introduction

The standard model (SM) has been highly successful in describing nature on the small distance scale. An important exception is the neutrino sector, where the observation of neutrino flavor oscillations [1–4] indicates that neutrinos have small but nonzero masses, in contrast with the SM prediction, and that their individual flavor is not a conserved quantity. Generation number violation has also been observed in the quark sector, but not to date among charged leptons. In an extended version of the SM that includes neutrino masses, the anticipated rates of charged lepton flavor violation (CLFV) induced by neutrino mixing are vanishingly small; e.g., the branching fraction $\mathcal{B}(Z \rightarrow e\mu) \approx \mathcal{O}(10^{-60})$ [5]. Therefore any observation of a CLFV process would be direct evidence of physics beyond the SM (BSM).

Potentially measurable rates of CLFV in various processes, including Z boson decay, are predicted in BSM scenarios such as the seesaw mechanism, and supersymmetry and leptoquark models [6, 7]. In addition, new particles predicted by these and other BSM models may exhibit CLFV through their decays. The new particles include additional gauge bosons such as a Z' boson, which would generally be expected to be heavier than the Z boson [8]. Axion-like particles have also been suggested as potential BSM particles that may decay into flavor-violating states [9, 10].

Searches for CLFV have been conducted in low-energy processes including $\mu \rightarrow e\gamma$ [11], $\mu \rightarrow eee$ [12], $\mu^- N(A, Z) \rightarrow e^- N(A, Z)$ [13], $e^+e^- \rightarrow \mu^+(e^-)\tau^-$ [14], $\tau \rightarrow \ell'\gamma$ ($\ell = e, \mu$) [15], and $\tau \rightarrow \ell'\ell^+\ell^-$ [16]. Limits from these reactions lead to indirect constraints on the Z boson branching fractions $\mathcal{B}(Z \rightarrow e\mu) < 10^{-12}$, $\mathcal{B}(Z \rightarrow e\tau) < 10^{-7}$, and $\mathcal{B}(Z \rightarrow \mu\tau) < 2 \times 10^{-7}$ [6]. However, direct measurements of CLFV Z decays are needed to rule out anomalous couplings or cancellations that could evade these limits [17]. Searches for such decays have been performed by experiments at the CERN LEP [18, 19] and LHC [20–22] colliders. Current limits on the branching fractions for $Z \rightarrow e\mu$, $Z \rightarrow e\tau$, and $Z \rightarrow \mu\tau$ are 2.6×10^{-7} [22], 5.0×10^{-6} [21], and 6.5×10^{-6} [21], respectively.

This paper presents a search for decays of the Z boson in the CLFV channels $Z \rightarrow e\mu$, $Z \rightarrow e\tau$, and $Z \rightarrow \mu\tau$, together with a scan of the $e\mu$ invariant mass over the range 110–500 GeV to search for potential heavy neutral resonances. The proton-proton (pp) collision data at $\sqrt{s} = 13$ TeV were collected with the CMS detector in 2016–2018, and correspond to an integrated luminosity of 138 fb^{-1} . New multivariate techniques extend the reach beyond previous results.

The signal extraction makes use of two main variables: the invariant mass of the (visible) daughters of the $Z^{(\prime)}$ boson candidate, and a multivariate discriminator, implemented as a boosted decision tree (BDT), that combines kinematic observables chosen to discriminate signal from background. For the $e\mu$ channel, where the $Z^{(\prime)}$ boson is fully reconstructed, we extract the signal yield with a fit to the $e\mu$ mass distributions, relying mainly on the sidebands to determine the background under the signal peak. These distributions are taken from separate subsamples that vary in purity, as measured by the BDT discriminator. To distinguish signal from background in the $e\tau$ and $\mu\tau$ channels, where the peak in the invariant mass distribution of the visible Z boson daughters is less sharply defined, we instead rely primarily on distributions in the BDT discriminant. These distributions are taken from subsamples defined by ranges in the visible invariant mass chosen according to the dominance of the signal or of various backgrounds.

In Section 2 we describe the CMS detector and particle reconstruction, and in Section 3 the simulation of signal and background processes. The event selection is given in Section 4, followed by the signal extraction for the $Z \rightarrow e\mu$ and $Z \rightarrow \ell\tau$ channels in Sections 5 and 6, respectively.

Systematic uncertainties are discussed in Section 7, and the results in Section 8. We conclude with a summary in Section 9. Tabulated results are provided in the HEPData record for this analysis [23].

2 The CMS detector and event reconstruction

The central feature of the CMS apparatus is a superconducting solenoid of 6 m internal diameter, providing a magnetic field of 3.8 T. Within the solenoid volume are a silicon pixel and strip tracker, a lead tungstate crystal electromagnetic calorimeter (ECAL), and a brass and scintillator hadron calorimeter (HCAL), each composed of a barrel and two endcap sections. Forward calorimeters extend the coverage in pseudorapidity (η) provided by the barrel and endcap detectors. The ECAL consists of 75 848 lead tungstate crystals, which provide pseudorapidity coverage of $|\eta| < 1.48$ in its barrel region and $1.48 < |\eta| < 3.00$ in the two endcap regions. Preshower detectors consisting of two planes of silicon sensors interleaved with a total of three radiation lengths of lead are located in front of each endcap detector. Muons are measured in gas-ionization detectors embedded in the steel flux-return yoke outside the solenoid. A more detailed description of the CMS detector, together with a definition of the coordinate system used and the relevant kinematic variables, is reported in Refs. [24, 25].

The silicon tracker used in 2016 measured charged particles within the range $|\eta| < 2.5$. For nonisolated particles of transverse momentum p_T between 1 and 10 GeV and $|\eta| < 1.4$, the track resolutions were typically 1.5% in p_T and 25–90 (45–150) μm in the transverse (longitudinal) impact parameter [26]. At the start of 2017, a new pixel detector was installed [27], which provided expanded acceptance, to $|\eta| < 3.0$, and improved transverse impact parameter resolution of 20–75 μm [28]. The primary vertex is taken to be the vertex corresponding to the hardest scattering in the event, evaluated using tracking information alone, as described in Section 9.4.1 of Ref. [29].

The global event reconstruction (also called particle-flow event reconstruction [30]) aims to reconstruct and identify each individual particle in an event, with an optimized combination of all subdetector information. In this process, the identification (ID) of the particle type (photon, electron, muon, charged hadron, neutral hadron) plays an important role in the determination of the particle direction and energy. Photons are identified as ECAL energy clusters not linked to the extrapolation of any charged-particle trajectory to the ECAL. Electrons are identified as a primary charged-particle track and potentially many ECAL energy clusters corresponding to this track extrapolation to the ECAL and to possible bremsstrahlung photons emitted along the way through the tracker material. Muons are identified as tracks in the central tracker consistent with either a track or several hits in the muon system, and associated with calorimeter deposits compatible with the muon hypothesis. Charged hadrons are identified as charged-particle tracks neither identified as electrons, nor as muons. Finally, neutral hadrons are identified as HCAL energy clusters not linked to any charged hadron trajectory, or as a combined ECAL and HCAL energy excess with respect to the expected charged-hadron energy deposit.

For each event, hadronic jets are clustered from these reconstructed particles using the infrared- and collinear-safe anti- k_T algorithm [31, 32] with a distance parameter of 0.4. Jet momentum is determined as the vectorial sum of all particle momenta in the jet, and is found from simulation to be, on average, within 5–10% of the true momentum over the entire spectrum and detector acceptance.

Additional pp interactions within the same or nearby bunch crossings (pileup) can contribute additional tracks and calorimetric energy depositions to the jet momentum. To mitigate this

effect, charged particles identified to be originating from pileup vertices are discarded, and an offset correction is applied to correct for remaining contributions [33].

Jet energy corrections are derived from simulation to bring the measured response of jets equal, on average, to that of particle-level jets. In situ measurements of the momentum balance in dijet, γ +jets, Z+jets, and strong production of jets (QCD multijet) events are used to account for any residual differences in the jet energy scale between data obtained with the detector (“data”) and simulation [34]. The jet energy resolution amounts typically to 15–20% at 30 GeV, 10% at 100 GeV, and 5% at 1 TeV [34]. Additional selection criteria are applied to each jet to remove jets potentially dominated by anomalous contributions from various subdetector component or reconstruction failures.

Jets associated with b hadron decays are identified within the tracker acceptance of $|\eta| < 2.5$ using the DEEPJET deep neural network ID algorithms [35–37]. We use both tight and loose working points of this algorithm. Their efficiencies for b jets (light-flavor quark and gluon jets) have been measured in $t\bar{t}$ events to be 84 (10)% for the loose working point and 52 (0.1)% for the tight working point.

Hadronic tau lepton decays (τ_h) are reconstructed from jets using the hadrons-plus-strips algorithm [38], which combines 1 or 3 tracks with energy deposits in the calorimeters to identify the various hadronic τ decay modes. Neutral pions are reconstructed as clusters with dynamic size in (η, ϕ) , from reconstructed electrons and photons; the size of the dimension in the azimuthal angle ϕ (“strip”) varies as a function of the p_T of the electron or photon candidate, because of the dispersion in the magnetic field. To distinguish between genuine τ_h decays and jets originating from the hadronization of quarks or gluons, and from electrons or muons, we use the DEEPTAU algorithm [39]. Information from all individual reconstructed particles near the τ_h axis is combined with properties of the τ_h candidate and the event. The rate of a jet to be misidentified as τ_h candidate depends on the p_T and quark flavor of the jet. In a data sample enriched in W+jets events this misidentification (misID) rate is measured to be about 0.25%, with an ID efficiency for genuine τ_h of 60%, at the working point and kinematic regime of our signal regions (SRs) [39]. The rate for electrons (muons) to be misidentified as τ_h is 2.60 (0.03)% for a genuine τ_h ID efficiency of 80 (>99)%.

The electron momentum is estimated by combining the energy measurement in the ECAL with the corresponding momentum measurement in the tracker [40]. The momentum resolution for electrons with $p_T \approx 45$ GeV from $Z \rightarrow ee$ decays ranges from 1.6 to 5%. The resolution is generally better in the barrel region than in the endcaps, and it also depends on the bremsstrahlung energy emitted by the electron as it traverses the material upstream of the ECAL [40, 41].

Muons are measured in the range $|\eta| < 2.4$, with detection planes made using three technologies: drift tubes, cathode strip chambers, and resistive-plate chambers. The efficiency for the reconstruction and ID of muons is greater than 96%. Once these muon candidates are matched to tracks measured in the silicon tracker, the relative p_T resolution for muons with p_T up to 100 GeV is 1% in the barrel and 3% in the endcaps. The p_T resolution in the barrel is below 7% for muons with p_T up to 1 TeV [42].

The missing transverse momentum vector \vec{p}_T^{miss} is computed as the negative vector sum of the transverse momenta of all the particle-flow candidates in an event; its magnitude is denoted as p_T^{miss} . The \vec{p}_T^{miss} is modified to account for corrections to the energy scale of the reconstructed jets in the event. To reduce the dependence of \vec{p}_T^{miss} on pileup, we apply the pileup-per-particle-identification algorithm [43], which weights the particle-flow candidates entering the \vec{p}_T^{miss} sum by their probability of originating from the primary vertex [44].

Events of interest are selected with a two-tiered trigger system. The first level, composed of custom hardware processors, uses information from the calorimeters and muon detectors to select events at a rate of around 100 kHz within a fixed latency of about 4 μ s [45]. The second level, known as the high-level trigger, comprises a farm of processors running a version of the full event reconstruction software optimized for fast processing, and reduces the event rate to around 1 kHz before data storage [46, 47].

3 Simulated event samples

Monte Carlo simulated samples are used to optimize the analysis and to model various background sources. Events arising from W+jets are simulated, for the 2016 (2017–2018) data taking periods, with the MADGRAPH5_aMC@NLO 2.2.2 (2.4.2) [48, 49] event generator at leading order (LO) accuracy. Drell–Yan (DY), $W\gamma$, and WWW events are simulated with the same generators at next-to-LO (NLO) accuracy. The POWHEG v2.0 [50–59] program at NLO is used to generate events from $t\bar{t}$, tW , single top quark, and H boson production (where H denotes the 125-GeV Higgs boson), as well as diboson events originating from WW, WH or ZH production. The WZ and ZZ events are generated at LO using the PYTHIA 8.205 [60] package. The simulated background samples are normalized using cross section calculations performed at NLO or next-to-NLO (NNLO) precision [61–65].

Signal processes are generated at LO using PYTHIA. For each CLFV decay channel ($Z \rightarrow e\mu$, $Z \rightarrow e\tau$, or $Z \rightarrow \mu\tau$), a tree-level coupling is added, with no coupling to the other decay channels. Events for the off-Z mass scan are generated with PYTHIA, including only the contribution of a vector boson Z' , and not considering any mixing with the Z boson or photon. The decay amplitude is calculated using tree-level couplings to the $e\mu$ final state with no other decay channels. The resonances are generated in the narrow-width approximation, i.e., with a width of 0.1 GeV, far below the experimental resolution. Events are simulated with masses of 100, 125, 150, 175, 200, 300, 400, and 500 GeV.

In all samples the hadronization, as well as the underlying event, are modeled with PYTHIA using the CUETP8M1 [66] (CP5 [67]) tune for the 2016 (2017–18) data-taking years. The LO (NLO) simulations use the MLM (FxFx) scheme for matching the products of the matrix-element calculations to the parton shower simulation [68]. The parton distribution functions used with the matrix-element generators are taken from the NNPDF3.0 [69] set at LO or NLO, except for the WW samples for the 2017–2018 data-taking years where NNPDF3.1[70] is used; for PYTHIA the NNPDF2.3LO [71] set is used.

The CMS detector response is simulated using GEANT4 [72]. Simulated samples are reconstructed with the same software packages as used for collision data. To account for effects of pileup, minimum-bias events simulated with PYTHIA are added to the hard scattering process, with a distribution in the number of vertices matching that in the data.

4 Event selection

An event is required to pass either a single-electron or single-muon trigger. To ensure that the trigger is fully efficient (>95%) for the events selected for analysis, an electron (muon) matched to the single-electron (muon) trigger is required to have p_T exceeding a threshold of 29 (25) GeV for data collected in 2016, 35 (28) GeV for data collected in 2017, and 34 (25) GeV for data collected in 2018.

For all three search channels we make a selection of events with two lepton candidates (e, μ ,

or τ_h) of different flavor and opposite charge. These events are sorted into three separate data channels: $e\mu$ (from which the $Z^{(i)} \rightarrow e\mu$, $Z \rightarrow e\tau_\mu$, and $Z \rightarrow \mu\tau_e$ candidates are selected), $e\tau_h$, and $\mu\tau_h$. To suppress SM backgrounds that produce pairs of leptons, events are rejected if they contain additional electrons or muons, and for the $e\tau_h$ and $\mu\tau_h$ channels, also if they contain additional τ_h candidates. In the search for the $Z \rightarrow e\tau$ or $Z \rightarrow \mu\tau$ signal we include both a hadronic τ decay category ($e\tau_h$ or $\mu\tau_h$, respectively) and a different-flavor leptonic τ decay category ($e\tau_\mu$ or $\mu\tau_e$). As each CLFV Z boson decay signal is the target of a separate search, there is no requirement that the $Z \rightarrow e\tau_\mu$, $Z \rightarrow \mu\tau_e$, and $Z \rightarrow e\mu$ samples be nonoverlapping.

To select a light lepton ℓ (e or μ) that is produced in the decay of a Z boson or tau lepton and not from a hadron within a quark jet, we construct the relative isolation variable I_{rel}^ℓ , defined as a function of the lepton's transverse momentum p_T^ℓ as

$$I_{\text{rel}}^\ell = \frac{\sum p_T^{\text{charged}} + \max[0, \sum p_T^{\text{neutral}} + \sum p_T^\gamma - p_T^{\text{PU}}]}{p_T^\ell}, \quad (1)$$

where the sums include the particles, excluding the lepton itself, within a cone of size $\Delta R \equiv \sqrt{(\Delta\eta)^2 + (\Delta\phi)^2} = 0.4$ (0.3) about the electron (muon). Here p_T^{charged} refers to charged hadrons, p_T^{neutral} to neutral hadrons, p_T^γ to photons, and p_T^{PU} to the estimated neutral contribution from pileup. Electrons and muons are required to pass a tight isolation requirement, $I_{\text{rel}}^\ell < 0.15$.

To select prompt electrons and muons we require their transverse and longitudinal impact parameters, d_{xy} and d_z , to be less than 0.2 and 0.5 cm, respectively. For further suppression of the background from nonprompt electrons (primarily from QCD multijet and $W+jets$ events), we require electrons to have $p_T > 15$ GeV. Electron candidates with ECAL clusters in the gap region between the barrel and endcap ($1.444 < |\eta| < 1.566$) are rejected.

The τ_h candidates are required to have $p_T > 20$ GeV and $|\eta| < 2.3$, with $|d_z| < 0.2$ cm. They are further required to pass the following working points of the DEEPTAU tagging algorithm [39] for the suppression of: muons (“tight”); jets (“tight” for the SR, “very loose” for the control regions (CRs) used to estimate the misID background); and electrons (“loose”, except “very tight” for the $e\tau_h$ channel SR to suppress the background from $Z \rightarrow ee$ where one of the electrons is misidentified as a τ_h candidate).

Jets are required to have $p_T > 20$ GeV and $|\eta| < 3$. Where jets are used in the event selection, jets within $\Delta R < 0.3$ of identified leptons are excluded from consideration.

Additional requirements specific to the individual channels are described in the corresponding sections below.

5 Search for $Z \rightarrow e\mu$

The $Z \rightarrow e\mu$ search uses the $e\mu$ data channel, requiring exactly one electron and one muon candidate. Both leptons are required to have $|\eta| < 2.4$, and $p_T > 20$ GeV in addition to the trigger threshold requirement noted in Section 4 above. The invariant mass $m_{e\mu}$ of the dilepton system is required to satisfy $70 < m_{e\mu} < 110$ GeV; this range includes sidebands around the Z boson mass (91.1880 ± 0.0020 GeV [73]) for estimation of the background. The sources of backgrounds near the Z boson mass are WW , $t\bar{t}$, DY production of $\tau\tau$, nonprompt $e\mu$, and $Z \rightarrow \mu\mu^* \rightarrow \mu\mu\gamma$ production.

Events from $t\bar{t}$ (as well as sub-dominant single t quark) production are suppressed by rejecting events with jets that satisfy the loose b tagging [37]. To suppress the $Z \rightarrow \tau\tau$ contribution

we require, in addition to the requirements on the track impact parameters given in Section 4, that their significances satisfy $|d_{xy}|/\sigma_{d_{xy}} < 3$ and $|d_z|/\sigma_{d_z} < 4.7$, with $\sigma_{d_{xy}}$ and σ_{d_z} the respective uncertainties. The efficiency reduction from these requirements on the track impact parameters is $\approx 5\%$ on the signal, and $\approx 20\%$ on those backgrounds that have tau leptons in the final state.

To extract the signal yield we exploit the narrow resonance peak of the signal against a mainly smoothly falling background in the $m_{e\mu}$ spectrum. The background shape arises from the sharply falling dominant contribution of $Z \rightarrow \tau_e \tau_\mu$, combined with a nearly flat spectrum from WW, $t\bar{t}$, and nonprompt $e\mu$ events. The distribution in $m_{e\mu}$ of the events surviving the baseline selection described above is shown in Fig. 1, for the data and for the simulated background components. The shape of the simulated signal, normalized to a branching fraction of 10^{-5} , is superimposed.

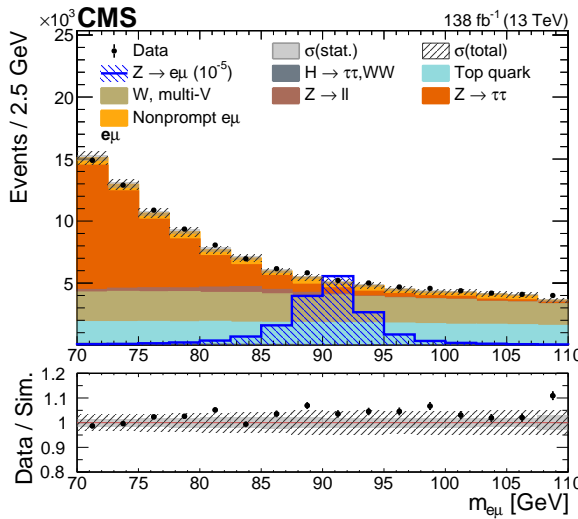


Figure 1: Invariant mass of the $e\mu$ system for data (points, with bars denoting statistical uncertainty) and simulated background (stacked filled histograms) for events passing the baseline selection. In the legend, “W, multi-V” refers to $W + \text{jets}$ events having a jet that is misidentified as a lepton, together with multiple vector boson production. The hatched histogram shows a hypothetical $Z \rightarrow e\mu$ signal normalized to a branching fraction of 10^{-5} . The lower panel shows the ratio of the data to simulated background yields, with the statistical (combined systematic and statistical) uncertainty in the simulated yield indicated by the filled (hatched) gray band.

The final selection in the $Z \rightarrow e\mu$ search makes use of a BDT trained to distinguish signal from background events. The signal is then extracted from a fit of signal and background probability density functions (pdfs) to the $m_{e\mu}$ distribution, for three SRs defined as ranges of the BDT discriminant value.

5.1 The BDT implementation for $Z \rightarrow e\mu$

While DY production of τ pairs is one of the main backgrounds, these events are concentrated in the region below the signal resonance. In our SRs, both for the Z and Z' cases, events from $t\bar{t}$ and WW production are dominant at the signal resonance mass. Therefore, a single BDT is trained using simulated events for the $Z \rightarrow e\mu$ signal and for the background. The background is represented by the WW simulation, which is similar to $t\bar{t}$ after our baseline selection. We select disjoint training and testing samples, restricting $m_{e\mu}$ for the training sample to the Z -boson peak region, 86–96 GeV, to limit the influence of any correlations of the BDT features with $m_{e\mu}$. The BDT algorithm is implemented with the XGBOOST [74] package. The hyperpa-

rameters of the BDT are optimized with a random grid search. The input features aim to exploit the difference between signal and background in p_T^{miss} and other kinematic variables. For the signal process, the Z boson is produced predominantly near threshold and decays to visible daughters, which are roughly collinear and have similar p_T , with little p_T^{miss} . Backgrounds with leptonically decaying W bosons give rise to a characteristic distribution in the transverse mass m_T formed from the W daughter lepton and p_T^{miss} . The transverse mass $m_T(1, 2)$ is defined for a system of two particles (or of two systems of particles) with transverse momenta $p_T^{(1,2)}$ and azimuthal separation $\Delta\phi$ as

$$m_T(1, 2) = \sqrt{2p_T^{(1)} p_T^{(2)} (1 - \cos \Delta\phi)}. \quad (2)$$

Since the signal extraction in the $Z \rightarrow e\mu$ search treats the BDT and $m_{e\mu}$ as independent variables, we include only features having small correlations with $m_{e\mu}$ in the BDT. From all the features tested, those that have the most discriminating power are selected:

1. $p_T^{\text{trailing}} / p_T^{\text{leading}}$;
2. $p_T^{e\mu}$;
3. $\eta_{e\mu}$;
4. $m_T(p_T^{\text{miss}}, \text{leading})$;
5. $m_T(p_T^{\text{miss}}, \text{trailing})$;
6. $|\Delta\phi(p_T^{\text{miss}}, e\mu)|$; and
7. p_T^{miss} .

The terms “leading” and “trailing” denote the higher- and lower- p_T lepton, respectively.

The resulting distributions in the discriminant value (BDT score) for the BDT test events in the range 70–110 GeV $m_{e\mu}$ are shown for signal and background in the left-hand plot of Fig. 2. We see from this plot that substantial discrimination between signal and background is achieved.

The $m_{e\mu}$ distribution for the WW background test sample confirms that no structure is introduced by the training. To check this conclusion in data, we construct a CR enriched in $t\bar{t}$ (and WW) events by applying the SR selection but replacing the veto on any loose b-tagged jet with a requirement of one tight b-tagged jet. The right-hand plot in Fig. 2 shows the $m_{e\mu}$ shape for events in this CR for each of the BDT thresholds used to define the BDT binning. The distribution is seen to be free of structure within uncertainties. The BDT-score ranges chosen to define the SRs are 0.3–0.7, 0.7–0.9, and 0.9–1.0. This binning optimized the sensitivity of the simultaneous fit to the $m_{e\mu}$ distributions in all of the SRs.

5.2 Fit model for $Z \rightarrow e\mu$

For the events within one of the BDT score categories, parametric functions of $m_{e\mu}$ are defined to describe the signal and backgrounds in that category. The parameters of these functions are then determined from a fit to the binned data distribution, performed simultaneously in all categories.

The $Z \rightarrow e\mu$ signal distribution is described by a double-sided Crystal Ball function [75, 76]. This function has a Gaussian core with independent power law tails defined such that the

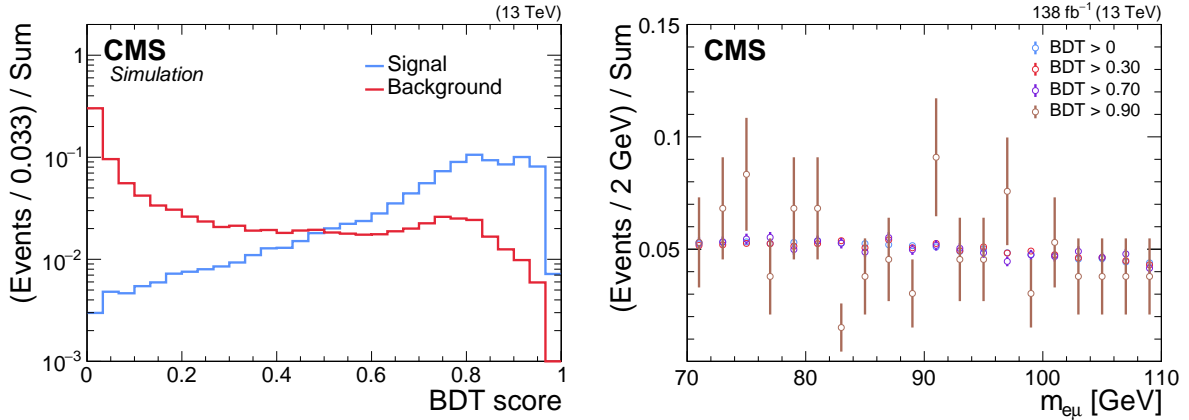


Figure 2: The left plot shows unity-normalized distributions of the $Z \rightarrow e\mu$ BDT score for simulated events from the BDT test samples satisfying $70 < m_{e\mu} < 110$ GeV. The blue and red histograms represent the signal and WW background, respectively. The right plot displays the unity-normalized distribution of $m_{e\mu}$ for events in the $t\bar{t}$ data CR used to check for BDT mass-spectrum bias, for several BDT thresholds; the vertical bars show the statistical uncertainties.

function is continuous and differentiable at all points. Its parameters are determined from a fit to simulated signal events, and fixed in the fit to the data.

The nonresonant background spectrum is modeled by analytic functions obtained directly from fits to the data, which removes from the model any dependence on simulation. The forms of these functions are established with fits to the data in the $m_{e\mu}$ sidebands, defined as $70 < m_{e\mu} < 86$ GeV and $96 < m_{e\mu} < 110$ GeV. Rather than choosing a single function that best fits the data sidebands for each region, we employ the “discrete profiling” method [77] in which an envelope of all well-fitting functions considered are included in the background model. The fit is then free to choose the background function that minimizes the likelihood at each point of the fit, profiling over the discrete nuisance parameter that represents the function choice.

Each of the individual functions included in the background model envelope is constructed from a broad, low-mass Gaussian component to represent the tail of the $Z \rightarrow \tau\tau$ spectrum, and an additional function, chosen through statistical tests based on CRs in data, for the non-resonant processes. This function has the form

$$f(x) = f_g g(x|\mu, \sigma) + (1 - f_g) h_n(x|\vec{\theta}), \quad (3)$$

where g is the Gaussian pdf with mean μ and standard deviation σ , f_g its fraction in the model, and h_n is the n th-order pdf of the function family h with parameters $\vec{\theta}$. The free parameters in the fit to the data are f_g , μ , σ , and $\vec{\theta}$. The h_n function is chosen from among the Chebychev polynomial, exponential sum, or power law sum families. The background functions that pass a χ^2 -probability test for fit consistency, $p(\chi^2) > 1\%$, are added to the model, and an F-test [78], $p(\chi_n^2 - \chi_{n+1}^2, \Delta n_d) < 5\%$, is performed to determine the maximum function order for each family. Here Δn_d is the number of degrees of freedom added by a step to the next higher-order function. Tests performed with large numbers of simulated background events confirm that the (zero) signal strength extracted from the fit is free of bias.

The model in Eq. (3) does not adequately describe the background from $Z \rightarrow \mu\mu^* \rightarrow \mu\mu\gamma$ events, which occur in cases where a muon loses a significant fraction of its energy to final-state radiation, thereby failing to reach the muon detectors, and the resulting photon is misidentified as an electron. This gives rise to a broad peak below the Z mass region that is not differentiated

by the BDT since the background comes from true Z boson decays. Therefore, this background needs to be accounted for separately in the final fit. It is modeled with a double-sided Crystal Ball function, determined from fits to simulated $Z \rightarrow \mu\mu$ events that are reconstructed as $Z \rightarrow e\mu$. We find satisfactory agreement between the simulation and data in a sample of pairs reconstructed as $e\mu$, but having the same sign (SS) of charge. These events have a large fraction of electron candidates from misID background and exhibit a shape similar to that of the opposite-sign background.

The background model envelope from the fit to the $m_{e\mu}$ sidebands is shown in Fig. 3 for each BDT category. The data points in blue in the figure are not revealed or used for the determination of the background shape.

5.3 Application to the Z' mass scan

For the $e\mu$ final state, a scan for new neutral resonances Z' above the Z boson mass is also performed, using the same strategy and selection as in the $Z \rightarrow e\mu$ search. The extended-range $m_{e\mu}$ distribution in data and simulation is shown in Fig. 4. The most important difference in procedure for this scan is that a sliding window in $m_{e\mu}$ is used for successive scan points. With this strategy, potential masses of Z' are explored from 110 to 500 GeV, the upper limit being chosen because there are not enough events for a reliable fit above that value. The size of each fit range is computed as twenty standard deviations of the mass resolution for the signal point considered. The low end of the lowest fit range is 95 GeV, which evades the $Z \rightarrow \mu\mu$ and $Z \rightarrow \tau\tau$ background components, and thus allows the model to be simplified to just the function family h of Eq. (3). For each mass point we define two BDT bins, 0.3–0.7 and 0.7–1.0, combining the upper two bins used for the $Z \rightarrow e\mu$ search because of their smaller populations.

6 Search for $Z \rightarrow e\tau$ and $Z \rightarrow \mu\tau$

The $Z \rightarrow e\tau$ and $Z \rightarrow \mu\tau$ searches each consider hadronic and leptonic τ -daughter categories. In addition to the common selection described in Section 4, in all four categories we require $40 < m_{\ell\tau} < 170$ GeV, where $m_{\ell\tau}$ is the invariant mass of the system comprising a prompt light-lepton candidate and the visible daughter(s) of a tau lepton. To reduce backgrounds from $\tau\tau$, $W + \text{jets}$, WW , and $t\bar{t}$ production, we also require $m_T(\tau, p_T^{\text{miss}})/m_{\ell\tau} < 0.8$ and $m_T(\ell\tau, p_T^{\text{miss}}) < 70$ (90) GeV, in the hadronic (leptonic) final-state categories.

To further reduce the $\tau\tau$ background, the prompt light lepton candidate must satisfy $p_T > 28$ (20) GeV in the hadronic (leptonic) final-state categories. Events are rejected if they contain b-tagged jets, based on the tight (loose) working point of the b jet ID for the hadronic (leptonic) τ -decay categories, to suppress backgrounds from t quark processes. The QCD multijet background becomes significant at low electron p_T in the $Z \rightarrow e\tau_\mu$ category, and so we require $p_T^\ell > p_T^\tau$ in that category. Additionally, the light leptons are required to have $|\eta^\ell| < 2.2$ (2.4) in the hadronic (leptonic) τ decay categories, for compatibility with the $\tau\tau$ background estimation method described in Section 6.1.1 below.

The search strategy for final states involving a tau lepton needs to take into account that the Z boson can be only partially reconstructed because of the neutrino(s) in the τ decay. The signal and background spectra in $m_{\ell\tau}$ are less distinct than those of $m_{e\mu}$. Here the background components are modeled separately, using data in CRs to the extent possible. New variables derived from the visible daughters are developed to approximate the mass of the Z boson. These and other discriminating variables are again combined into a BDT to optimize the signal extraction.

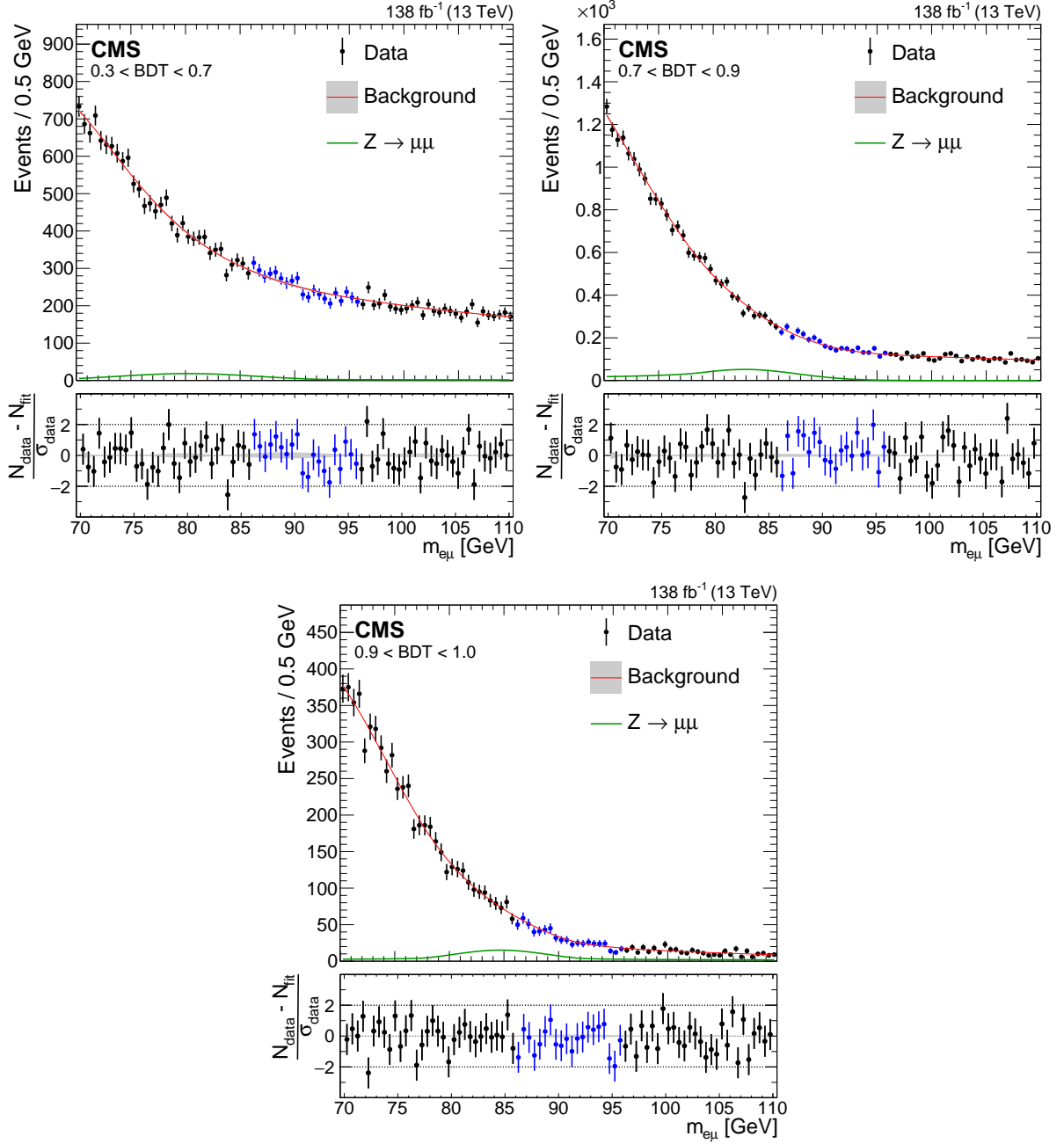


Figure 3: Fits of the data sidebands with the background functions for the BDT score ranges 0.3–0.7 (upper left), 0.7–0.9 (upper right), and 0.9–1.0 (lower). In the upper panel of each plot, the black (blue) points with bars show the data with statistical uncertainties in the sideband (signal) region, the solid red line shows the average background prediction, and the dashed green curve shows the $Z \rightarrow \mu\mu^* \rightarrow \mu\mu\gamma$ background component. The lower panel in each plot shows the ratio of the difference between the data and the average background prediction to the uncertainty in the data, and the gray band shows the spread of the background estimates from the separate families of parametric functions.

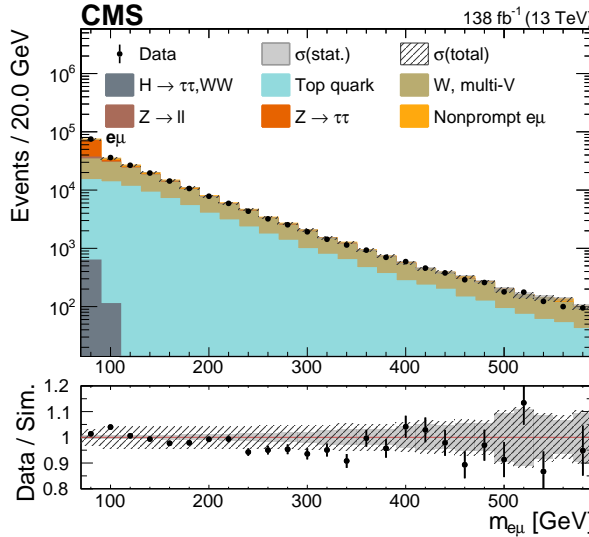


Figure 4: Invariant mass of the $e\mu$ system for data (points) and simulated background (stacked filled histograms), for events that pass the baseline selection except for that selection’s upper limit on the invariant mass. The lower panel shows the ratio of the data to simulated yields, with the statistical (combined systematic and statistical) uncertainty in the simulated yield indicated by the filled (hatched) gray band.

6.1 Background estimates for the $Z \rightarrow e\tau$ and $Z \rightarrow \mu\tau$ channels

The $Z \rightarrow e\tau$ and $Z \rightarrow \mu\tau$ searches rely on signal and background templates (binned pdfs). The dominant background sources are $\tau\tau$ production and those arising from misidentified leptons. Other sources are leptonic W boson decays, such as those from WW and $t\bar{t}$ processes.

6.1.1 Background from $\tau\tau$

The production of tau lepton pairs, most importantly from DY $Z \rightarrow \tau\tau$, is a background in all of the $Z \rightarrow \ell\tau$ channels. Neutrinos associated with the decays of both tau leptons contribute to p_T^{miss} , and the visible invariant mass spectrum of the dilepton system peaks below the Z boson mass, with a high-side tail. The τ candidate in a $Z \rightarrow e\tau$ or $Z \rightarrow \mu\tau$ signal event would be kinematically identical to one from the $Z \rightarrow \tau\tau$ decay, while the prompt lepton would have generally higher p_T than the daughter from a leptonically decaying τ lepton in the $Z \rightarrow \tau\tau$ event, and there would be no contribution to p_T^{miss} from that leg of the Z boson decay.

The SM processes that produce tau lepton pairs are identical to those that produce muon pairs, and the latter are very cleanly reconstructed in the detector. Therefore we use an “embedding” technique [79] to model $\tau\tau$ backgrounds, except for $H \rightarrow \tau\tau$ production, which is treated separately. In this method, we remove the recorded detector deposits associated with the muons from a data sample of muon pair production, and substitute those derived from simulated $\tau\tau$ events, matching the kinematic properties of the simulated tau lepton with those of the muon it replaces. The result is a hybrid data sample where the τ decay and reconstruction are simulated, but the τ production kinematics and the rest of the event (pileup, p_T^{miss} , jets, etc.) are taken directly from data. This approach significantly reduces simulation uncertainties, where the only remaining simulation-based uncertainties are those related to the decay and reconstruction of the tau leptons.

6.1.2 The τ_h misID background

The background from jets misidentified as τ_h ($j \rightarrow \tau_h$) is estimated in the $\mu\tau_h$ and $e\tau_h$ channels using a “misID-factor” method, similar to those used in Refs. [80, 81]. The method uses an application region (AR) enriched in $j \rightarrow \tau_h$ events, which has the same kinematic selection as the SR but with an inverted jet-suppression ID (“antijet-ID”) requirement (very loose and not tight, using working points of the discriminator [39]). Shape-dependent transfer factors (TFs) are used to relate the rate of the $j \rightarrow \tau_h$ events in the AR to an estimate of the corresponding background rate in the SR.

Since the TFs depend on properties that might be experimentally inaccessible (e.g., the underlying parton flavor), and depend on the background process (e.g., $W + \text{jets}$, QCD multijets), they are measured separately for each background source. An overall TF is then evaluated by combining these factors weighted by the process composition in the CR:

$$f(\vec{\beta}) = \sum_{p \in \text{processes}} c_p(\vec{\beta}) f_p(\vec{\beta}).$$

The parameters $\vec{\beta}$ are derived from the kinematic properties of the τ_h and prompt ℓ candidates along with p_T^{miss} , and the functions f , f_p , and c_p are, respectively, the overall TF to be evaluated for a given event in the AR, the TF for process p , and the expected composition fraction of process p in the AR.

The process-dependent TFs f_p are measured for $W + \text{jets}$, QCD multijet, and $t\bar{t}$ background. The $W + \text{jets}$ TFs are measured in a high- $m_T(\ell\tau, p_T^{\text{miss}})$ region, and the QCD multijet TFs are measured in a region with SS $\ell\tau_h$ pairs and $0.05 < I_{\text{rel}}^\ell < 0.15$. The $t\bar{t}$ TFs are determined using simulation, as there is not a suitable measurement region in data. These measurement regions are referred to as the determination regions. The weights c_p are estimated as functions of $m_T(\ell\tau, p_T^{\text{miss}})$, using simulated $j \rightarrow \tau_h$ events for $W + \text{jets}$ and $t\bar{t}$; for QCD multijet background we use an SS data CR, correcting for non-QCD contributions in this CR by subtracting their simulated yields.

The f_p TFs are measured as functions of the τ_h candidate p_T independently for each of four τ_h identified decay modes, one- or three-prong with zero or one π^0 . There are also subleading kinematic dependencies in the TFs. Corrections for these are derived by comparing the observation with the estimate in the tight antijet-ID subset of the determination region. This is done for the light-lepton p_T , the $\tau_h |\eta|$, and $|\Delta\phi(\ell, p_T^{\text{miss}})|$. Additional corrections to account for the CR selection bias are measured in alternate CRs and applied as functions of I_{rel}^ℓ , $m_{\ell\tau}$, and the BDT score defined in Section 6.3.

6.1.3 Light-lepton misID background

Electron and muon candidates in the $e\tau_\mu$ and $\mu\tau_e$ selections arising from misID of other particles are estimated using a method similar to the $j \rightarrow \tau_h$ estimation. This background arises mainly from $W + \text{jets}$ events, where one lepton comes from the W boson and one is a misidentified jet or a nonprompt lepton originating from a jet, and from QCD multijet events, where each lepton is either a misidentified jet or a nonprompt lepton originating from a jet.

The AR for the light-lepton misID background is the same as the SR, except with an SS selection. The determination regions for the TFs are the same as for the SRs and ARs, except with a loose isolation requirement ($0.15 < I_{\text{rel}}^\mu < 0.50$) on the muon candidate. The TFs are measured as functions of $\Delta R(e, \mu)$ separately in categories of 0, 1, and >1 jets. Subleading corrections to

the (p_T^e, p_T^μ) distribution are measured in this determination region, and CR bias corrections for the (p_T^e, p_T^μ) and BDT score (Section 6.3) distributions are measured in a loose electron isolation region.

6.1.4 Backgrounds estimated from simulation

The background from leptonic W decays in $t\bar{t}$ and WW production is relevant in all search channels, though it is most impactful at high mass in the $e\mu$ data channel, and is estimated from simulation. The embedded $\tau\tau$ samples already include the small contribution from $t\bar{t}$ and WW decays to $\tau\tau$, and so these are omitted from the simulated background model. The remaining $t\bar{t}$ and WW background processes are kept small by the event selection, which exploits several properties that distinguish them from signal. Both $t\bar{t}$ and WW have large p_T^{miss} associated with each lepton leg, unlike the signal processes, and the $t\bar{t}$ background is significantly suppressed by the veto of events with b-tagged jets.

There are also small background contributions from other diboson and triboson processes, but these have small cross sections and are suppressed by the rejection of events with additional light leptons. The $H \rightarrow \tau\tau$ and $H \rightarrow WW$ processes are also modeled with simulation, because these processes yield too few $\mu\mu p_T^{\text{miss}}$ events in data for application of the τ embedding method.

Photons misidentified as electrons and light leptons misidentified as τ_h candidates are also modeled using simulated samples. The background from DY $Z \rightarrow ee$ and $Z \rightarrow \mu\mu$ events where one light lepton is misidentified as a τ_h candidate must be carefully separated from the signal as the prompt-lepton candidate leg is identical to that of the CLFV Z signal.

6.2 Discriminating variables for $Z \rightarrow e\tau$ and $Z \rightarrow \mu\tau$

Because of the neutrinos in the τ decay, the invariant mass of the visible daughters in the $Z \rightarrow \ell\tau$ channels is a less effective discriminating variable than in the construction of $Z \rightarrow e\mu$ against the backgrounds, of which $Z \rightarrow \tau\tau$ is the largest. However, we can exploit the facts that since the decaying boson is much more massive than the τ , the τ is typically produced with a significant Lorentz boost, leading to a highly collimated decay, and that one of the Z boson daughters for the signal decay is a light lepton unaccompanied by neutrinos. We utilize two different approaches to take advantage of these features.

6.2.1 Collinear mass estimate

The first approach is the collinear mass m^{col} , derived with the collimated τ decay approximation, in which \vec{p}_T^{miss} projected onto the visible tau lepton \vec{p}_T equals the \vec{p}_T of the neutrino(s). With the further assumption that the neutrino three-momentum lies along the three-momentum of the visible τ daughter(s), we then obtain the neutrino four-vector

$$p^\nu = \frac{\vec{p}_T^{\text{miss}} \cdot \hat{p}_T^{\text{vis}}}{p_T^{\text{vis}}} p_T^{\text{vis}}, \quad (4)$$

where p^ν is the four-momentum of the visible τ daughter(s), and p_T^{vis} and \hat{p}_T^{vis} are the magnitude and direction unit vector of its transverse momentum components, respectively. The sign of $\vec{p}_T^{\text{miss}} \cdot \hat{p}_T^{\text{vis}}$ indicates whether the neutrino vector is parallel or antiparallel to the visible τ daughter's momentum. The collinear mass is then the mass of the $p^\ell + p^{\text{vis}} + p^\nu = p^\ell + p^\tau$ system. The m^{col} distribution is shown in Fig. 5 for the $Z \rightarrow \mu\tau$ search. The true $\Delta\phi$ between the visible τ decay products and the associated neutrinos is typically small, but because of uncertainties in the p_T^{miss} reconstruction this angle can be larger than $\pi/2$, leading to antiparallel neutrino configurations.

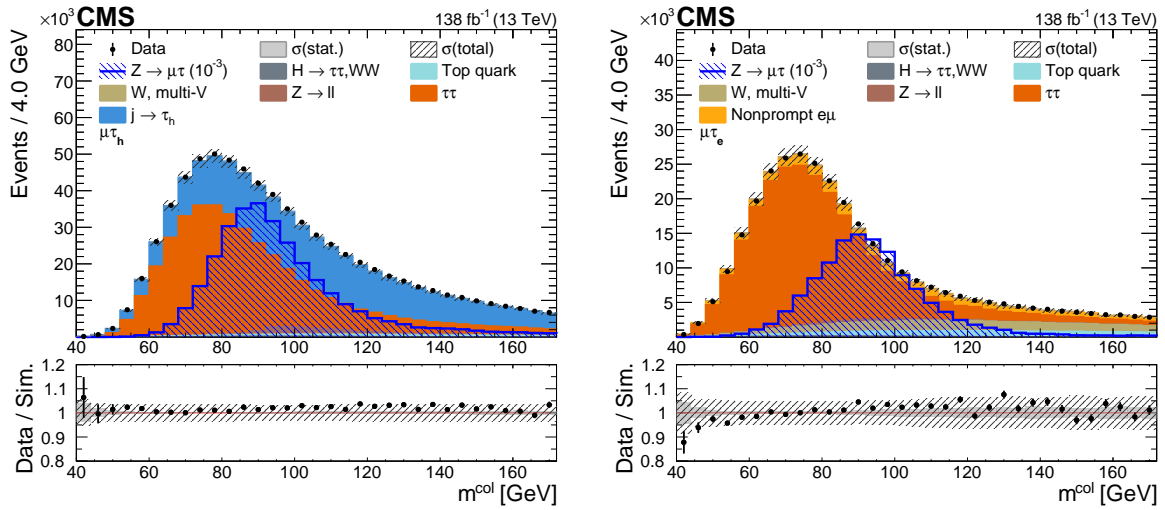


Figure 5: The $\mu\tau_h$ (left) and $\mu\tau_e$ (right) m^{col} distributions, for the data (black markers with bars showing the statistical uncertainties) and the simulated backgrounds (filled stacked histograms). The hatched blue histogram shows the shape of the signal, normalized to a branching fraction of 10^{-3} , for comparison. The lower panel shows the ratio of the data to simulated yields, with the statistical (combined systematic and statistical) uncertainty in the simulated yield indicated by the filled (hatched) gray band.

6.2.2 The tau lepton momentum scale variables $\alpha_{1,2}$

Another approach is to use collinear approximations for the τ decays along with assumptions [82] that the Z boson is on-shell and produced at threshold, i.e., that the Z boson daughters' p_T vanishes. The latter constraint implies equality of the Z daughters' p_T , $p_T^{(1)} = p_T^{(2)}$. This relation can be restated in terms of the four-momentum $p^{(i)}$ of the tau lepton and that of its daughters, defined as $p^{\text{vis},i} = p^{(i)} / \alpha_i$:

$$\alpha_1 p_T^{\text{vis},1} = \alpha_2 p_T^{\text{vis},2}. \quad (5)$$

The on-shell Z boson assumption combined with four-momentum conservation in the decay provides a second relation between the α_i :

$$m_Z^2 = m_1^2 + m_2^2 + 2p^{(1)} \cdot p^{(2)} \approx 2p^{(1)} \cdot p^{(2)} = 2\alpha_1 \alpha_2 p^{\text{vis},1} \cdot p^{\text{vis},2}. \quad (6)$$

From these equations we find

$$\alpha_{1,2} = \sqrt{\left(\frac{p_T^{\text{vis},(2,1)}}{p_T^{\text{vis},(1,2)}}\right) \frac{m_Z^2}{2p^{\text{vis},1} \cdot p^{\text{vis},2}}}. \quad (7)$$

For the signal decay $Z \rightarrow \ell\tau$ we have $\alpha_1 = \alpha_\ell = 1$, whereas for the $Z \rightarrow \tau\tau$ background we have in general $\alpha_i > 1$ for both Z boson daughters. Figure 6 shows these estimates for $Z \rightarrow \mu\tau_h$, where for the signal events α_μ is centered at one, as expected, and provides considerable discrimination against both $Z \rightarrow \tau\tau$ and τ_h misID backgrounds.

6.3 The BDTs for the $Z \rightarrow e\tau$ and $Z \rightarrow \mu\tau$ decay channels

A BDT is trained for each final state of each signal, for a total of four BDTs ($Z \rightarrow e\tau_h$, $Z \rightarrow e\tau_\mu$, $Z \rightarrow \mu\tau_h$, and $Z \rightarrow \mu\tau_e$). The ROOT TMVA toolkit [83] is used for this training. The BDTs are

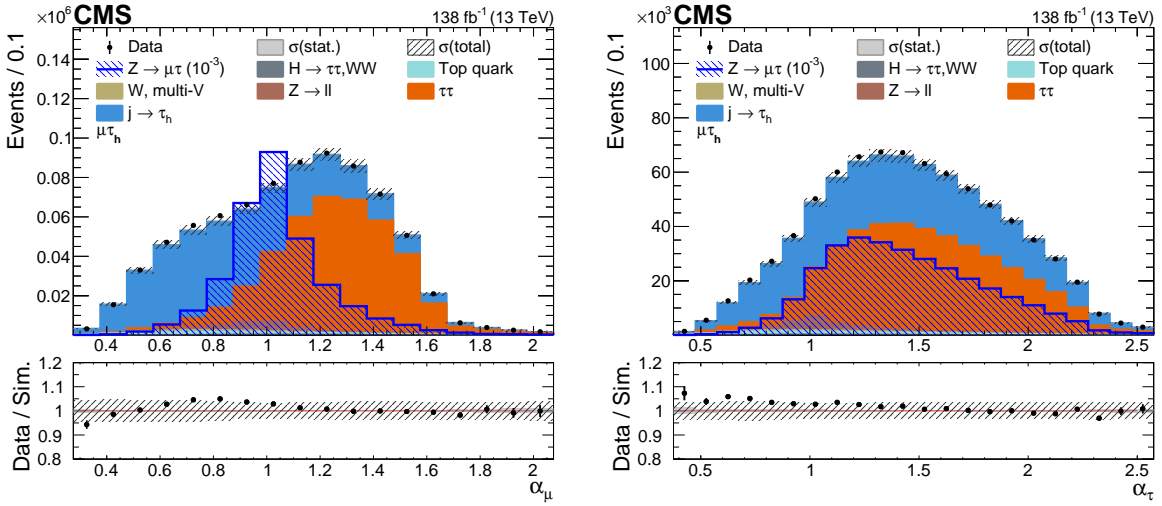


Figure 6: Distributions of $\mu\tau_h$ signal and estimated backgrounds in α_μ (left), α_τ (right), for the data (black markers with bars showing the statistical uncertainties) and the simulated backgrounds (filled stacked histograms). The hatched blue histogram shows the shape of the signal, normalized to a branching fraction of 10^{-3} , for comparison. The lower panel shows the ratio of the data to simulated yields, with the statistical (combined systematic and statistical) uncertainty in the simulated yield indicated by the filled (hatched) gray band.

constructed with input features that describe the kinematic properties of the Z boson candidate and of p_T^{miss} :

1. $m_{\ell\tau}$;
2. m^{col} ;
3. α_ℓ and α_τ ;
4. p_T^ℓ / p_T^τ ;
5. $p_T^{\ell\tau}$;
6. $\Delta\phi_{\ell\tau}$;
7. $m_T(\ell, p_T^{\text{miss}})$;
8. $\Delta\phi(\tau, p_T^{\text{miss}})$; and
9. p_T^{jet} .

The leading jet p_T is included here, as b quark initiated jets in $t\bar{t}$ decays that either fail the b tagging or are beyond the b tagging region of $|\eta| < 2.4$ typically have higher p_T than jets associated with the signal process.

The BDT training uses $\tau\tau$ simulations rather than the embedding samples. Data events from the loose antijet ID (SS) region are used in the training to model the $j \rightarrow \tau_h$ (nonprompt $e\mu$) background in the hadronic (leptonic) τ categories. Events used for training, whether simulated events or CR data, are excluded from use in the background template estimates, where the remaining events or data are scaled to compensate for the removed events. To improve the

discrimination against rare $Z \rightarrow \ell\ell$ background events in which one of the leptons is misidentified as one of a different flavor, these events are given a larger weight in the training. The BDT score distribution $O(x)$ is transformed using the signal BDT score cumulative distribution function $p(x) = \int_{-\infty}^x O(x')dx' / \int_{-\infty}^{+\infty} O(x')dx'$ to produce a useful shape that is less impacted by changes in the underlying machine-learning technique or hyperparameters.

6.4 The $Z \rightarrow e\tau$ and $Z \rightarrow \mu\tau$ mass categories

Several of the backgrounds in the $Z \rightarrow e\tau$ and $Z \rightarrow \mu\tau$ search have large systematic uncertainties that impact the search sensitivity. These are:

1. $\tau\tau$ embedding uncertainties;
2. $j \rightarrow \tau_h$ and nonprompt $e\mu$ estimates from data; and
3. $Z \rightarrow \ell\ell \rightarrow \ell\tau_h$ misID rate uncertainties.

To improve background uncertainty constraints and isolate background- or signal-enriched regions, the $Z \rightarrow e\tau$ and $Z \rightarrow \mu\tau$ fits are split into the $m_{\ell\tau}$ mass regions described in Table 1. The leptonic τ signal decays typically have lower mass than the τ_h decays because of the extra neutrino produced, which leads to differences in the $\tau\tau$ region selection. Additionally, $Z \rightarrow \ell\ell$ is a significant background only in the hadronic channels, so there is no CR for these processes in the leptonic channels. Events with low transformed BDT score are removed from the final analysis, and the transformed BDT binning is chosen to ensure that each bin contains an adequate number of events for the final fit.

Table 1: Regions in $m_{\ell\tau}$ for the $Z \rightarrow \mu\tau$ and $Z \rightarrow e\tau$ fits.

Region	$m_{\ell\tau}$ bounds [GeV]	
	$Z \rightarrow \ell\tau_h$	$Z \rightarrow \ell\tau_\ell$
$\tau\tau$	[40, 60]	[40, 50]
Signal-like	[60, 85]	[50, 100]
$Z \rightarrow \ell\ell$	[85, 100]	—
misID ($j \rightarrow \tau_h$ and nonprompt $e\mu$)	[100, 170]	[100, 170]

7 Systematic uncertainties

The main sources of systematic uncertainty arise from the simulation (e.g., simulated object reconstruction efficiency or energy scale), from the background model uncertainties (e.g., validity of the model in the SR), and statistical uncertainties because of limited event counts in the simulated samples and CRs. These uncertainties are discussed in the following paragraphs and summarized in Table 2.

In the $Z \rightarrow e\mu$ search, the most significant sources are the purely statistical uncertainties from the parameters of the background functions in the fit. These are followed by uncertainties arising from the discrete collection of background functions included in the envelope. The signal model uncertainties are negligible compared with those of the background model.

The largest sources of systematic uncertainty in the $Z \rightarrow e\tau$ and $Z \rightarrow \mu\tau$ searches are the statistical uncertainties in the background model templates and the light-lepton energy scale uncertainties. The model-template statistical uncertainties arise largely from the $Z \rightarrow ee$ and

$Z \rightarrow \mu\mu$ simulation samples used to estimate the $\ell \rightarrow \tau_h$ backgrounds, along with those from the nonprompt $e\mu$ background estimate based on CRs in the data, where the subtraction of prompt leptons from the data has a large statistical uncertainty. The statistical uncertainties in the $j \rightarrow \tau_h$ and embedded $\tau\tau$ estimates are much smaller because of their larger CR populations. The impact of the electron and muon energy scale uncertainties is large because the p_T of the prompt ℓ is highly discriminating against leptonic $Z \rightarrow \tau\tau$ decays, as well as being incorporated into several of the variables in the BDTs (dilepton mass and p_T , collinear mass, α_i , $m_T(\ell, p_T^{\text{miss}})$, and the p_T ratio). The uncertainties in the background estimate from CRs in data are also significant, mainly because of the corrections for the kinematic variation in the TF measurement regions and the statistical uncertainties in these measurement regions.

The normalization of the simulated signal and minor background yields depends on the integrated luminosity, pileup corrections, and the theoretical modeling. The integrated luminosities for the 2016, 2017, and 2018 data-taking years have individual uncertainties of 1.2–2.5% [84–86], while the overall uncertainty for the 2016–2018 period is 1.6%. To evaluate the uncertainty associated with the pileup reweighting, we vary the value of the total inelastic cross section by 5% [87]. Uncertainties arising from the theoretical model include the cross sections, the parton distribution functions, and the renormalization and factorization scales. These uncertainties are propagated to the observed signal yields and are summarized in the row labeled “Theory” in Table 2.

All uncertainties are included in the maximum likelihood fit to extract the branching fractions, which is implemented with the COMBINE statistical analysis package [88]. For an uncertainty that does not contain shape information, the uncertainty is implemented as a rate uncertainty with a log-normal pdf. Uncertainties that impact the shape of the signal or background model are handled differently in the $Z \rightarrow e\mu$ and $Z \rightarrow \ell\tau$ searches. In the $Z \rightarrow e\mu$ search, the effect is split into a rate uncertainty and an impact on the pure shape effect. A nuisance parameter is added as a shift in the corresponding model parameter drawn from a Gaussian pdf centered on zero and with a width defined by the systematic source’s effect on that model parameter. In the $Z \rightarrow e\tau$ and $Z \rightarrow \mu\tau$ searches, shape uncertainties are introduced via “continuous morphing” [89] parameterized by upward and downward uncertainty templates. In the case of the $Z \rightarrow e\mu$ background envelope, the discrete background function index parameter is treated as a free parameter. The fit selects the background function that maximizes the likelihood at any given point, profiling this discrete nuisance parameter [77].

8 Results

The branching fraction is extracted from a maximum likelihood fit of the background plus signal model to the data distribution in $m_{e\mu}$, for the $Z \rightarrow e\mu$ search, or in the BDT discriminant, for the $Z \rightarrow \ell\tau$ searches.

For the $Z \rightarrow e\mu$ search, the parameters of the background model developed from the $m_{e\mu}$ sidebands (Section 5.2) are free in the fit to the full distributions. The distributions for separate fits in each BDT region are shown along with the data in Fig. 7. No excess of events beyond the SM expectation is observed. We set upper limits on the branching fraction following the modified frequentist construction CL_s [90–92] implemented with the CMS statistical analysis tool COMBINE [88]. The observed and expected upper limits are shown in Fig. 8 and Table 3 from the fits in each BDT score category and for the joint fit combining all categories, along with the 68 and 95% uncertainties. The observed limit of $\mathcal{B}(Z \rightarrow e\mu) < 1.9 \times 10^{-7}$ represents the most stringent direct limit to date on this process.

Table 2: Sources of uncertainty and their impacts on the measured branching fraction, for each of the Z decay channels, and on the product of the production cross section and branching fraction for the Z' resonance scan. The uncertainty ranges for the Z' resonance scan are ordered from the lowest to the highest Z' mass point. Entries to which the specified uncertainty does not apply are denoted with “—”.

Uncertainty source	$\mathcal{B}(Z \rightarrow \ell\ell')$			$\sigma(pp \rightarrow Z' + X) \times \mathcal{B}(Z' \rightarrow e\mu)$ [fb]
	$e\mu$ [10 ⁻⁸]	$e\tau$ [10 ⁻⁶]	$\mu\tau$ [10 ⁻⁶]	
Electron & muon ID & trigger	0.1	0.3	0.1	0.1–0.01
Electron energy scale	0.2	3.5	0.2	0.6–0.01
Muon energy scale	0.1	0.1	0.9	0.3–0.01
Tau ID	—	0.3	0.2	—
Tau energy scale	—	0.4	0.4	—
(e, μ) $\rightarrow \tau_h$	—	0.4	0.1	—
Jet energy, p_T^{miss}	0.3	0.8	0.2	0.1–0.01
b tagging	<0.1	0.2	0.2	<(0.1–0.01)
Pileup	0.1	0.2	0.1	<(0.1–0.01)
Integrated luminosity	0.3	0.1	0.1	0.1–0.01
Theory	0.1	0.5	0.2	0.1–(<0.01)
Parametric background	7.9	—	—	0.3–0.06
Envelope	2.5	—	—	0.1–0.04
$Z \rightarrow \mu\mu$ yield	0.5	—	—	—
Embedding energy resolution	—	1.1	0.2	—
Embedding normalization	—	1.5	0.2	—
$j \rightarrow \tau_h$	—	2.8	0.9	—
Nonprompt e μ	—	2.7	0.4	—
Template event counts	<0.1	3.1	1.5	0.1–(<0.01)
Total systematic	8.3	5.7	2.2	0.8–0.08
Statistical	5.6	1.9	1.6	1.9–0.18

The transformed BDT score distributions in the invariant mass and tau lepton final-state categories are shown in Figs. 9 and 10 for the $Z \rightarrow e\tau$ search and in Figs. 11 and 12 for the $Z \rightarrow \mu\tau$ search. The pull appearing in the distributions in the lower panels for each BDT bin is the difference between the observed and fit yields divided by the uncertainty $\sqrt{\sigma_{\text{obs}}^2 - \sigma_{\text{fit}}^2}$. The minus sign in the definition of this uncertainty accounts for the correlation between the observed and fit yields, which arises because the observed yield is included in the fit [93]. The large pulls that appear in some bins in the lower row of Fig. 9 reflect non-Gaussian uncertainties in one or more of the nuisance parameters. The observed yield in the $e\tau$ ($\mu\tau$) channel is consistent with the SM background prediction at the 0.5 (2.7) σ level. The observed and expected 95% CL upper limits on the branching fractions for $Z \rightarrow e\tau$ and $Z \rightarrow \mu\tau$ are shown in Fig. 13 and Table 3, along with the 68 and 95% uncertainties in the expected limit.

Table 3: The measured branching fraction with its significance (signif.) and observed and expected 95% CL upper limits, for each of the $Z \rightarrow e\mu$, $Z \rightarrow e\tau$, and $Z \rightarrow \mu\tau$ decay channels. The prior best published limits are also given for comparison. Included are results for the separate BDT bins for $Z \rightarrow e\mu$ and the separate τ decay subchannels for $Z \rightarrow e\tau$ and $Z \rightarrow \mu\tau$.

Channel	Branching fraction	Signif. [σ]	Observed (expected) limit	Prior (expected) limit
$Z \rightarrow e\mu$	$-0.1^{+1.0}_{-1.0} \times 10^{-7}$	-0.1	$1.9(2.0^{+0.8}_{-0.6}) \times 10^{-7}$	$2.6(2.4) \times 10^{-7}$ [22]
$0.3 < \text{BDT} < 0.7$	$-3.4^{+2.8}_{-2.6} \times 10^{-7}$	-1.2	$5.7(8.2^{+2.5}_{-2.0}) \times 10^{-7}$	—
$0.7 < \text{BDT} < 0.9$	$0.4^{+1.5}_{-1.4} \times 10^{-7}$	+0.3	$3.2(2.9^{+1.2}_{-0.8}) \times 10^{-7}$	—
$0.9 < \text{BDT} < 1.0$	$0.0^{+1.5}_{-2.0} \times 10^{-7}$	+0.0	$3.0(3.0^{+1.2}_{-0.8}) \times 10^{-7}$	—
$Z \rightarrow e\tau$	$3.2^{+6.1}_{-6.0} \times 10^{-6}$	+0.5	$13.8(11.4^{+4.7}_{-3.2}) \times 10^{-6}$	$5.0(6.0) \times 10^{-6}$ [21]
$Z \rightarrow e\tau_h$	$6.3^{+8.4}_{-8.2} \times 10^{-6}$	+0.8	$21.3(16.1^{+6.7}_{-4.6}) \times 10^{-6}$	$8.1(8.1) \times 10^{-6}$ [21]
$Z \rightarrow e\tau_\mu$	$1.2^{+7.9}_{-8.1} \times 10^{-6}$	+0.2	$16.2(15.3^{+6.1}_{-4.2}) \times 10^{-6}$	$7.0(8.9) \times 10^{-6}$ [21]
$Z \rightarrow \mu\tau$	$7.5^{+2.7}_{-2.7} \times 10^{-6}$	+2.7	$12.0(5.3^{+2.1}_{-1.5}) \times 10^{-6}$	$6.5(5.3) \times 10^{-6}$ [21]
$Z \rightarrow \mu\tau_h$	$7.2^{+2.8}_{-2.8} \times 10^{-6}$	+2.5	$11.9(5.6^{+2.2}_{-1.6}) \times 10^{-6}$	$9.5(6.1) \times 10^{-6}$ [21]
$Z \rightarrow \mu\tau_e$	$7.5^{+7.1}_{-7.9} \times 10^{-6}$	+1.0	$19.5(14.4^{+5.1}_{-3.8}) \times 10^{-6}$	$7.2(10.0) \times 10^{-6}$ [21]

Figure 14 shows the $e\mu$ mass scan fit results for two example mass points. No statistically significant excess is observed over the SM background. We report 95% CL upper limits on the production cross section $\sigma(pp \rightarrow Z' + X)$ times the branching fraction $\mathcal{B}(Z' \rightarrow e\mu)$ to the $e\mu$ final state. The observed and expected limits for the entire mass scan in the $e\mu$ final state are shown in Fig. 15. All observed deviations from the background-only hypothesis have local p -values greater than 1%. The global p -value is greater than 39% after accounting for the look-elsewhere effect [94].

The search presented here for CLFV Z boson decays represents an approximately 20% improvement in sensitivity to the direct $Z \rightarrow e\mu$ decay process, with respect to the best previous search [22]. The $Z \rightarrow \mu\tau$ search has similar sensitivity as the prior limit, coming mainly from the $Z \rightarrow \mu\tau_h$ channel. The observed $Z \rightarrow \mu\tau$ limit is weaker than the expected one, mainly because of the 2.5σ excess we find in the $Z \rightarrow \mu\tau_h$ channel. The $Z \rightarrow e\tau$ search presented here is limited by high electron trigger thresholds, lower electron identification efficiencies, and large rates of $j \rightarrow \tau_h$ and $e \rightarrow \tau_h$ backgrounds, as compared with the $Z \rightarrow \mu\tau$ search, and the $Z \rightarrow e\tau$ search in Ref. [21]. Additionally, the electron energy scale has much larger uncertainties in the $\tau\tau$ embedding simulation that significantly impacts the $Z \rightarrow e\tau$ search sensitivity.

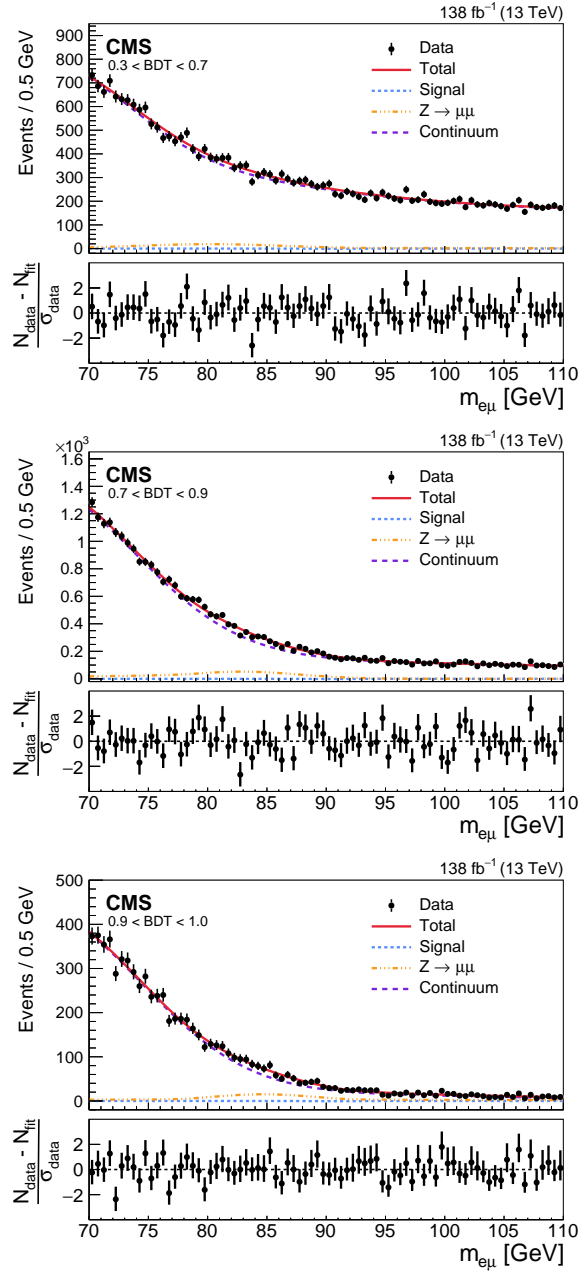


Figure 7: For the $Z \rightarrow e\mu$ search, the invariant mass fit results for the BDT score ranges 0.3–0.7 (upper), 0.7–0.9 (middle), and 0.9–1.0 (lower). In each plot, the upper panel shows the data (points with bars showing the statistical uncertainties) together with the fit distribution curve (red) and its separate signal (blue dotted) $Z \rightarrow \mu\mu$ (yellow dash-dotted) and continuum background (gray dashed) components, and the lower panel shows the deviations of the data from the fit function divided by the data uncertainty.

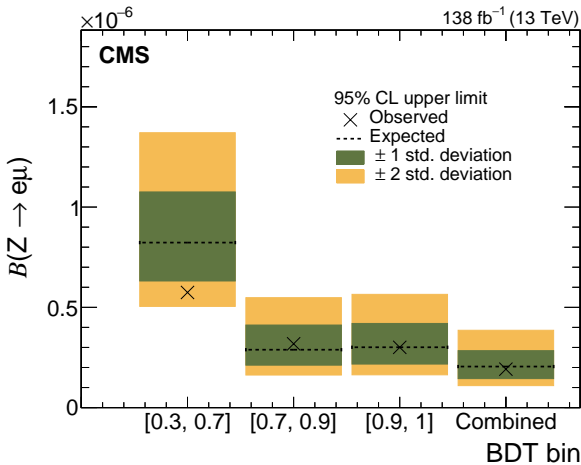


Figure 8: Upper limits at 95% CL on the branching fraction $\mathcal{B}(Z \rightarrow e\mu)$, for each BDT score range and for the final combined fit. The observed limits are denoted by the markers, while the expected limits with their 68 and 95% uncertainties are denoted by the horizontal dashed lines and green and yellow bands, respectively.

As seen in Fig. 15, the $Z' \rightarrow e\mu$ search yields an expected 95% CL upper limit on $\sigma(pp \rightarrow Z'+X)\mathcal{B}(Z' \rightarrow e\mu)$ of 4 fb at 110 GeV and 0.4 fb at 500 GeV, with an approximately exponential relation between the mass and the expected sensitivity. The observed limits are consistent with these. Searches for $Z' \rightarrow e\mu$ over various mass ranges above 200 GeV have been reported by ATLAS [95, 96] and CMS [97, 98]. Where the ranges overlap, the present limits represent an improvement of at least a factor of five over these, and are either the first or the most stringent expected limits to date on the $Z' \rightarrow e\mu$ process within the covered mass range.

9 Summary

A search is presented for flavor violating decays of the Z boson to charged leptons, and for the presence of a heavier vector boson Z' exhibiting such decays. The data from proton-proton collisions at $\sqrt{s} = 13$ TeV were collected with the CMS detector at the LHC, and correspond to an integrated luminosity of 138 fb^{-1} . The specific decay modes considered are $Z^{(\prime)} \rightarrow e\mu$, $Z \rightarrow e\tau$, and $Z \rightarrow \mu\tau$. No significant excess of events over backgrounds from standard model processes is observed. Observed (expected) upper limits of 1.9×10^{-7} , 1.38×10^{-5} , and 1.20×10^{-5} (2.0×10^{-7} , 1.14×10^{-5} , and 0.53×10^{-5}) at 95% confidence level are set on the branching fractions for $Z \rightarrow e\mu$, $Z \rightarrow e\tau$, and $Z \rightarrow \mu\tau$, respectively. The limit for $Z \rightarrow e\mu$ is the most restrictive to date, while for $Z \rightarrow \mu\tau$ the sensitivity in terms of the expected limit is the same as that of the previous best limit. All of these limits are consistent with expectations from the standard model, and with constraints inferred from low-energy experimental limits. For Z' boson masses in the range 110–500 GeV, upper limits are set on the cross section times the branching fraction to $e\mu$ that extend from 0.3 to 7 fb, and are the most restrictive to date for this mass range. Future studies can benefit from additional data, since even the systematic uncertainties arise mainly from statistical ones in control samples.

Acknowledgments

We congratulate our colleagues in the CERN accelerator departments for the excellent performance of the LHC and thank the technical and administrative staffs at CERN and at other CMS institutes for their contributions to the success of the CMS effort. In addition, we gratefully

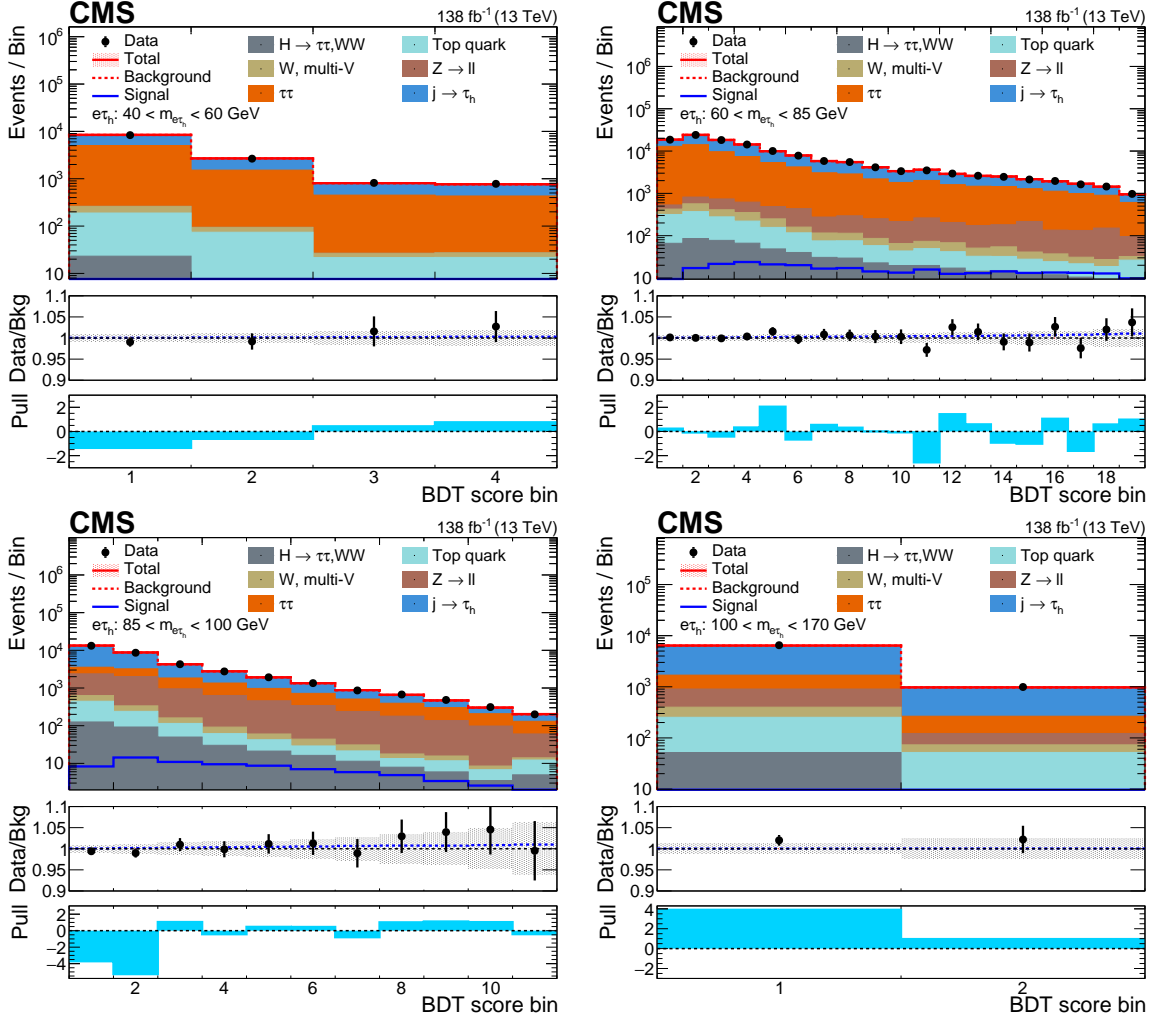


Figure 9: Transformed BDT score distributions for the $Z \rightarrow e\tau_h$ channels in the $m_{e\tau}$ ranges: (upper left) $40-60$ GeV, “ $\tau\tau$ ”; (upper right) $60-85$ GeV, “signal-like”; (lower left) $85-100$ GeV, “ $Z \rightarrow \ell\ell$ ”; (lower right) $100-170$ GeV, “misID”. In each plot, the upper panel shows the data (points), the total yield from the signal + background fit (red open histogram), the signal component (blue open histogram), and the background components (stacked filled histograms). The middle panel shows the ratio to the background of the data (points with bars showing the statistical uncertainty in the data) and the combined signal + background (blue dotted histogram). The shaded band shows the systematic uncertainty in the background estimate. The lower panel shows the pull defined in the text (light blue filled histogram).

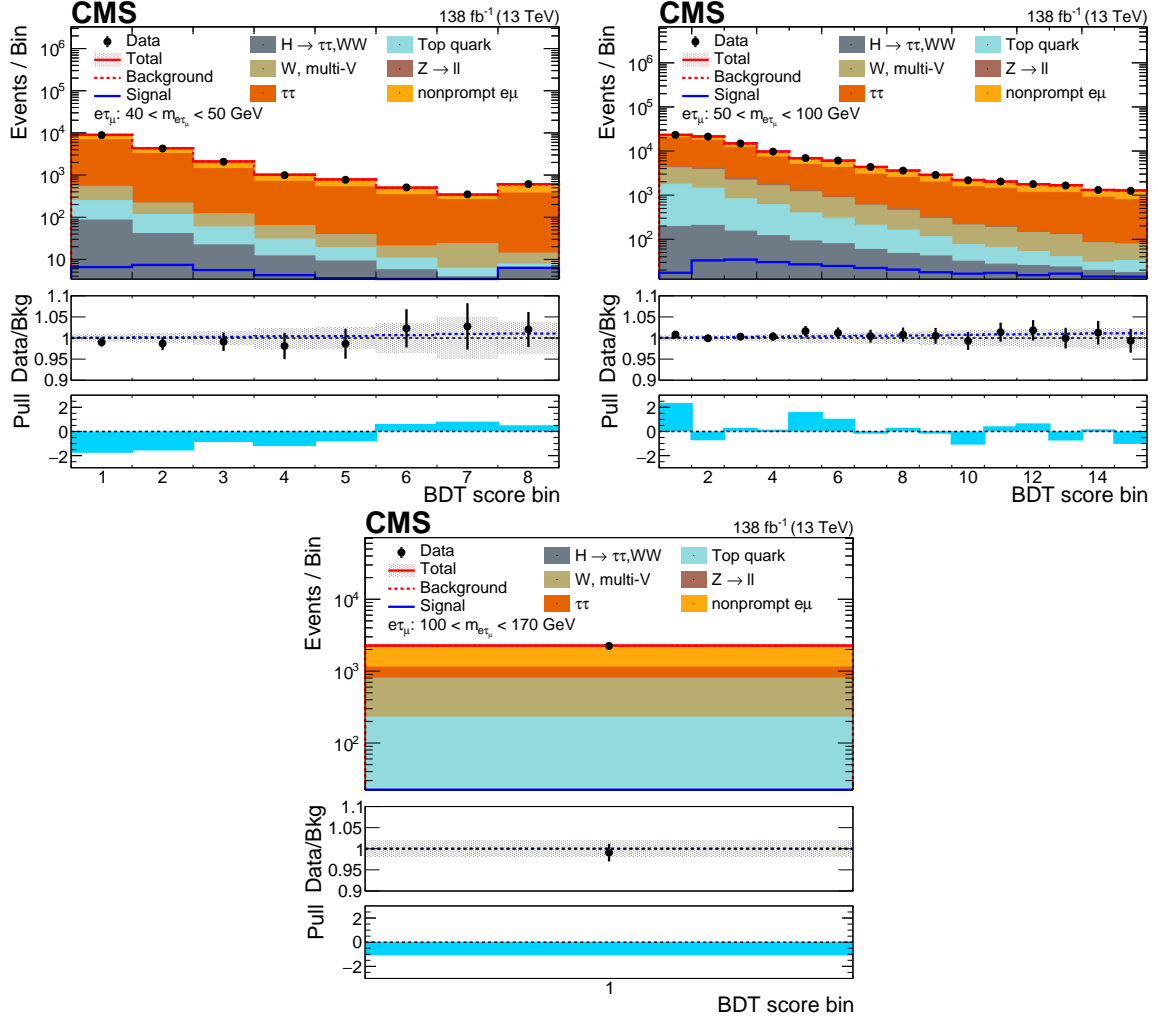


Figure 10: Transformed BDT score distributions for the $Z \rightarrow e\tau_\mu$ channels in the $m_{e\tau}$ ranges: (upper left) 40–50 GeV, “ $\tau\tau$ ”; (upper right) 50–100 GeV, “signal-like”; (lower) 100–170 GeV, “misID”. In each plot, the upper panel shows the data (points), the total yield from the signal + background fit (red open histogram), the signal component (blue open histogram), and the background components (stacked filled histograms). The middle panel shows the ratio to the background of the data (points with bars showing the statistical uncertainty in the data) and the combined signal + background (blue dotted histogram). The shaded band shows the systematic uncertainty in the background estimate. The lower panel shows the pull defined in the text (light blue filled histogram).

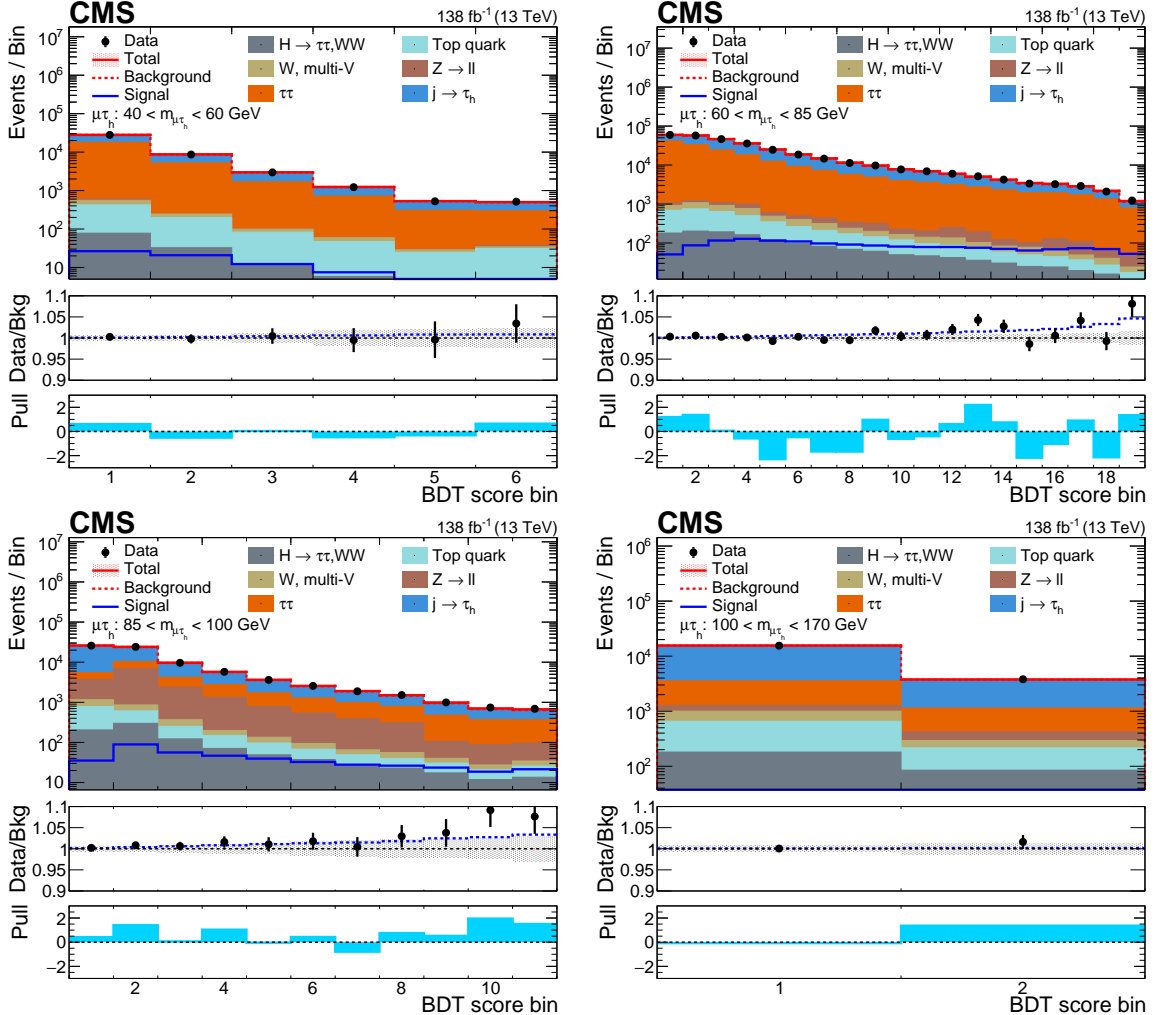


Figure 11: Transformed BDT score distributions for the $Z \rightarrow \mu\tau_h$ channels in the $m_{\mu\tau}$ ranges: (upper left) 40–60 GeV, “ $\tau\tau$ ”; (upper right) 60–85 GeV, “signal-like”; (lower left) 85–100 GeV, “ $Z \rightarrow \ell\ell$ ”; (lower right) 100–170 GeV, “misID”. In each plot, the upper panel shows the data (points), the total yield from the signal + background fit (red open histogram), the signal component (blue open histogram), and the background components (stacked filled histograms). The middle panel shows the ratio to the background of the data (points with bars showing the statistical uncertainty in the data) and the combined signal + background (blue dotted histogram). The shaded band shows the systematic uncertainty in the background estimate. The lower panel shows the pull defined in the text (light blue filled histogram).

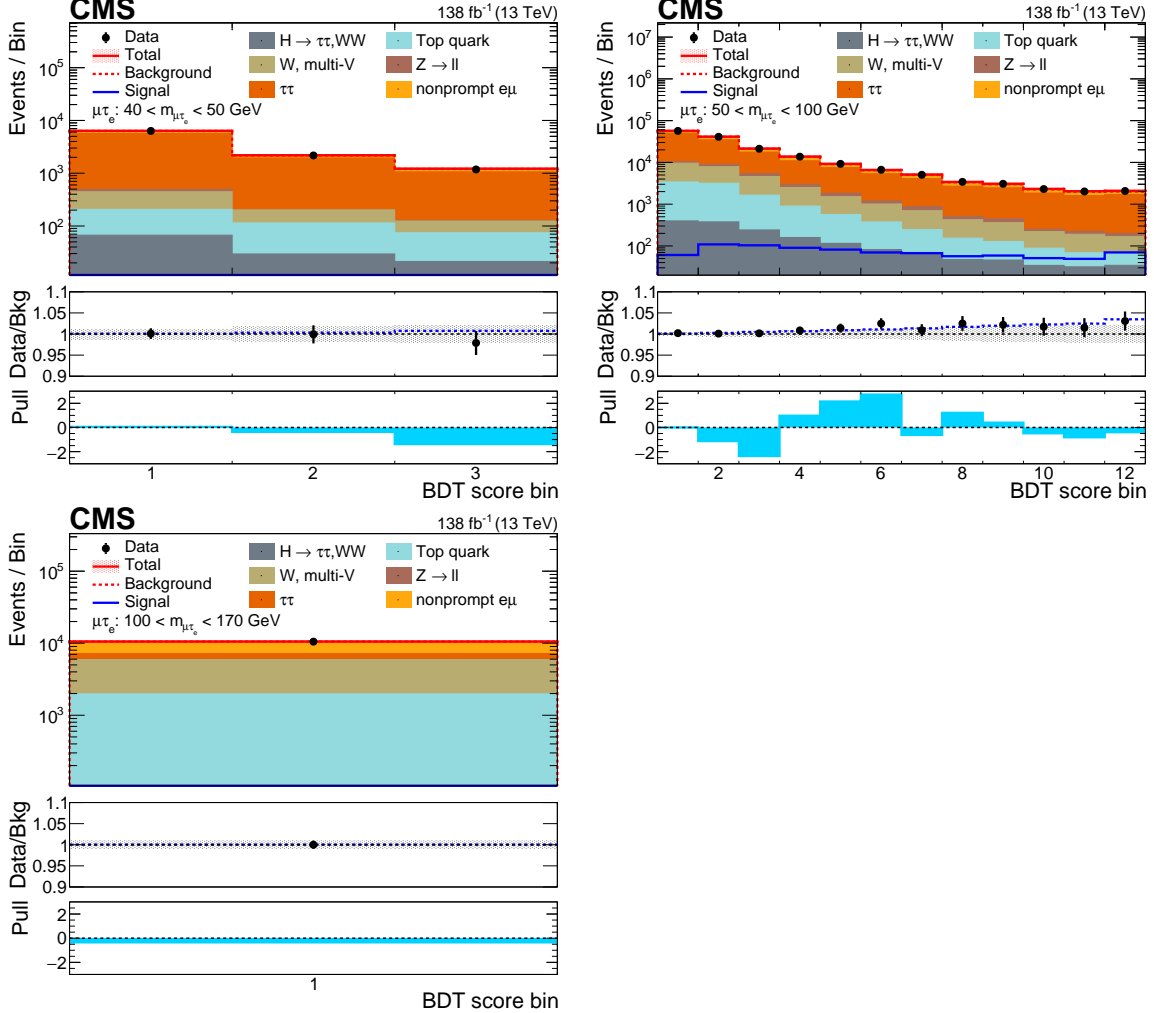


Figure 12: Transformed BDT score distributions for the $Z \rightarrow \mu\tau_e$ channels in the $m_{\mu\tau}$ ranges: (upper left) 40–50 GeV, “ $\tau\tau$ ”; (upper right) 50–100 GeV, “signal-like”; (lower) 100–170 GeV, “misID”. In each plot, the upper panel shows the data (points), the total yield from the signal + background fit (red open histogram), the signal component (blue open histogram), and the background components (stacked filled histograms). The middle panel shows the ratio to the background of the data (points with bars showing the statistical uncertainty in the data) and the combined signal + background (blue dotted histogram). The shaded band shows the systematic uncertainty in the background estimate. The lower panel shows the pull defined in the text (light blue filled histogram).

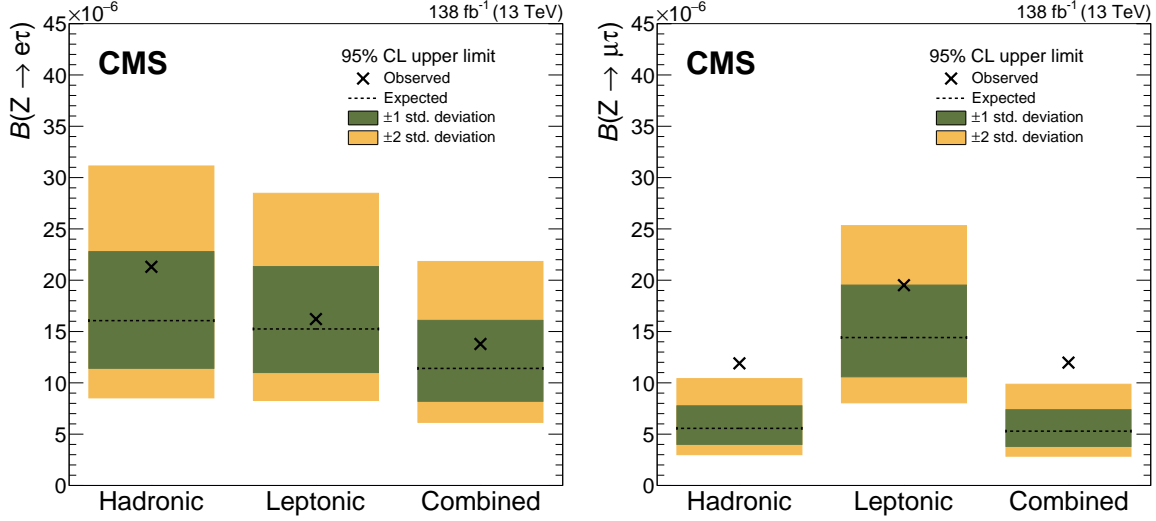


Figure 13: Observed and expected 95% CL upper limit by category, as well as for the final combined fit, for the $Z \rightarrow e\tau$ (left) and $Z \rightarrow \mu\tau$ (right) searches. The observed limits are denoted by the markers, while the expected limits with their 68 and 95% uncertainties are denoted by the horizontal dashed lines and green and yellow bands, respectively.

acknowledge the computing centers and personnel of the Worldwide LHC Computing Grid and other centers for delivering so effectively the computing infrastructure essential to our analyses. Finally, we acknowledge the enduring support for the construction and operation of the LHC, the CMS detector, and the supporting computing infrastructure provided by the following funding agencies: SC (Armenia), BMBWF and FWF (Austria); FNRS and FWO (Belgium); CNPq, CAPES, FAPERJ, FAPERGS, and FAPESP (Brazil); MES and BNSF (Bulgaria); CERN; CAS, MoST, and NSFC (China); MINCIENCIAS (Colombia); MSES and CSF (Croatia); RIF (Cyprus); SENESCYT (Ecuador); ERC PRG, TARISTU24-TK10 and MoER TK202 (Estonia); Academy of Finland, MEC, and HIP (Finland); CEA and CNRS/IN2P3 (France); SRNSF (Georgia); BMBF, DFG, and HGF (Germany); GSRI (Greece); NKFIH (Hungary); DAE and DST (India); IPM (Iran); SFI (Ireland); INFN (Italy); MSIT and NRF (Republic of Korea); MES (Latvia); LMELT (Lithuania); MOE and UM (Malaysia); BUAP, CINVESTAV, CONACYT, LNS, SEP, and UASLP-FAI (Mexico); MOS (Montenegro); MBIE (New Zealand); PAEC (Pakistan); MES and NSC (Poland); FCT (Portugal); MESTD (Serbia); MICIU/AEI and PCTI (Spain); MOSTR (Sri Lanka); Swiss Funding Agencies (Switzerland); MST (Taipei); MHESI and NSTDA (Thailand); TUBITAK and TENMAK (Türkiye); NASU (Ukraine); STFC (United Kingdom);

Individuals have received support from the Marie-Curie program and the European Research Council and Horizon 2020 Grant, contract Nos. 675440, 724704, 752730, 758316, 765710, 824093, 101115353, 101002207, 101001205, and COST Action CA16108 (European Union); the Leventis Foundation; the Alfred P. Sloan Foundation; the Alexander von Humboldt Foundation; the Science Committee, project no. 22rl-037 (Armenia); the Fonds pour la Formation à la Recherche dans l’Industrie et dans l’Agriculture (FRIA-Belgium); the Beijing Municipal Science & Technology Commission, No. Z191100007219010, the Fundamental Research Funds for the Central Universities, the Ministry of Science and Technology of China under Grant No. 2023YFA1605804, and the Natural Science Foundation of China under Grant No. 12061141002 (China); the Ministry of Education, Youth and Sports (MEYS) of the Czech Republic; the Shota Rustaveli National Science Foundation, grant FR-22-985 (Georgia); the Deutsche Forschungsgemeinschaft (DFG), among others, under Germany’s Excellence Strategy – EXC 2121 “Quan-

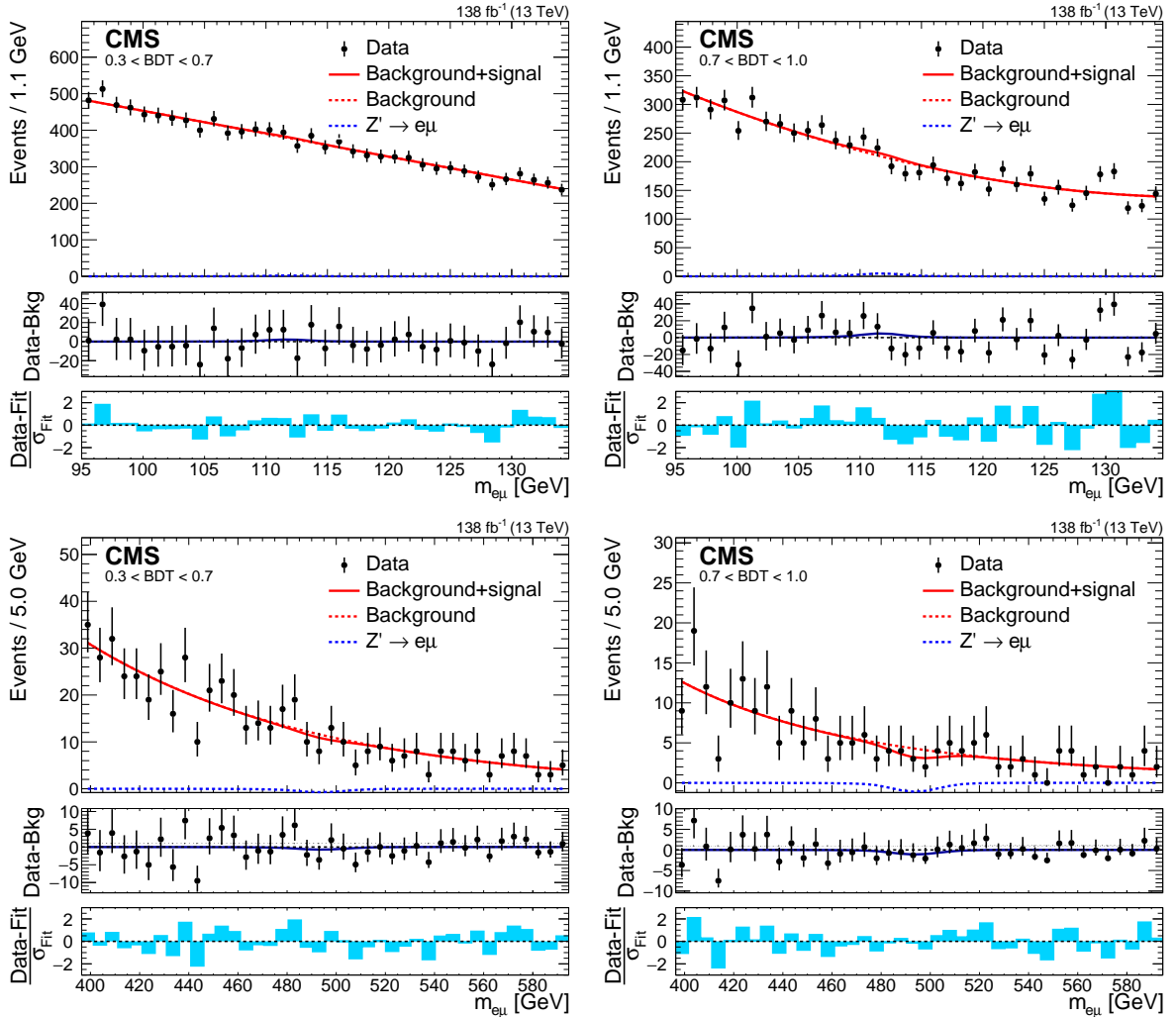


Figure 14: Distributions in $m_{e\mu}$ for the scan points 111 GeV (upper row) and 496 GeV (lower row) from the Z' search. In each row the BDT score range for the left (right) plot is 0.3–0.7 (0.7–1.0). In each plot, the upper panel shows the data (points with bars showing the statistical uncertainty) together with the fit distribution curve (red solid) and its separate signal (blue dotted) and background (red dotted) components, the middle panel shows the background subtracted data with the fit signal distribution, and the lower panel shows the deviations of the data from the fit function divided by the fit uncertainty.

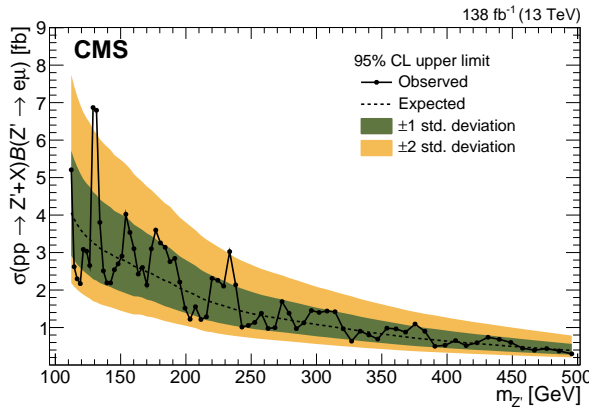


Figure 15: Expected and observed 95% CL upper limits on $\sigma(pp \rightarrow Z' + X) \mathcal{B}(Z' \rightarrow e\mu)$ for Z' masses between 110 and 500 GeV. The solid black line connects filled circles representing the observed upper limits at the scan points, and the dashed line with filled error bands shows the expected limit.

tum Universe" – 390833306, and under project number 400140256 - GRK2497; the Hellenic Foundation for Research and Innovation (HFRRI), Project Number 2288 (Greece); the Hungarian Academy of Sciences, the New National Excellence Program - ÚNKP, the NKFIH research grants K 131991, K 133046, K 138136, K 143460, K 143477, K 146913, K 146914, K 147048, 2020-2.2.1-ED-2021-00181, TKP2021-NKTA-64, and 2021-4.1.2-NEMZ-KI-2024-00036 (Hungary); the Council of Science and Industrial Research, India; ICSC – National Research Center for High Performance Computing, Big Data and Quantum Computing, FAIR – Future Artificial Intelligence Research, and CUP I53D23001070006 (Mission 4 Component 1), funded by the NextGenerationEU program (Italy); the Latvian Council of Science; the Ministry of Education and Science, project no. 2022/WK/14, and the National Science Center, contracts Opus 2021/41/B/ST2/01369 and 2021/43/B/ST2/01552 (Poland); the Fundação para a Ciência e a Tecnologia, grant CEECIND/01334/2018 (Portugal); MICIU/AEI/10.13039/501100011033, ERDF/EU, "European Union NextGenerationEU/PRTR", and Programa Severo Ochoa del Principado de Asturias (Spain); the Chulalongkorn Academic into Its 2nd Century Project Advancement Project, and the National Science, Research and Innovation Fund via the Program Management Unit for Human Resources & Institutional Development, Research and Innovation, grant B39G680009 (Thailand); the Kavli Foundation; the Nvidia Corporation; the Super-Micro Corporation; the Welch Foundation, contract C-1845; and the Weston Havens Foundation (USA).

References

- [1] Super-Kamiokande Collaboration, "Measurement of the flux and zenith angle distribution of upward through going muons by Super-Kamiokande", *Phys. Rev. Lett.* **82** (1999) 2644, doi:10.1103/PhysRevLett.82.2644, arXiv:hep-ex/9812014.
- [2] Super-Kamiokande Collaboration, "Solar B-8 and hep neutrino measurements from 1258 days of Super-Kamiokande data", *Phys. Rev. Lett.* **86** (2001) 5651, doi:10.1103/PhysRevLett.86.5651, arXiv:hep-ex/0103032.
- [3] SNO Collaboration, "Direct evidence for neutrino flavor transformation from neutral current interactions in the Sudbury Neutrino Observatory", *Phys. Rev. Lett.* **89** (2002) 011301, doi:10.1103/PhysRevLett.89.011301, arXiv:nucl-ex/0204008.

- [4] KamLAND Collaboration, “First results from KamLAND: Evidence for reactor anti-neutrino disappearance”, *Phys. Rev. Lett.* **90** (2003) 021802, doi:10.1103/PhysRevLett.90.021802, arXiv:hep-ex/0212021.
- [5] J. I. Illana and T. Riemann, “Charged lepton flavor violation from massive neutrinos in Z decays”, *Phys. Rev. D* **63** (2001) 053004, doi:10.1103/PhysRevD.63.053004, arXiv:hep-ph/0010193.
- [6] W. J. Marciano, T. Mori, and J. M. Roney, “Charged lepton flavor violation experiments”, *Ann. Rev. Nucl. Part. Sci.* **58** (2008) 315, doi:10.1146/annurev.nucl.58.110707.171126.
- [7] L. Calibbi and G. Signorelli, “Charged lepton flavour violation: An experimental and theoretical introduction”, *Riv. Nuovo Cim.* **41** (2018) 71, doi:10.1393/ncr/i2018-10144-0, arXiv:1709.00294.
- [8] P. Langacker, “The physics of heavy Z' gauge bosons”, *Rev. Mod. Phys.* **81** (2009) 1199, doi:10.1103/RevModPhys.81.1199, arXiv:0801.1345.
- [9] C. Cornellà, P. Paradisi, and O. Sumensari, “Hunting for ALPs with lepton flavor violation”, *JHEP* **01** (2020) 158, doi:10.1007/JHEP01(2020)158, arXiv:1911.06279.
- [10] M. Bauer et al., “Flavor probes of axion-like particles”, *JHEP* **09** (2022) 056, doi:10.1007/JHEP09(2022)056, arXiv:2110.10698.
- [11] MEG II Collaboration, “A search for $\mu^+ \rightarrow e^+\gamma$ with the first dataset of the MEG II experiment”, *Eur. Phys. J. C* **84** (2024) 216, doi:10.1140/epjc/s10052-024-12416-2, arXiv:2310.12614. [Erratum: doi:10.1140/epjc/s10052-024-13352-x].
- [12] SINDRUM Collaboration, “Search for the decay $\mu^+ \rightarrow e^+e^+e^-$ ”, *Nucl. Phys. B* **299** (1988) 1, doi:10.1016/0550-3213(88)90462-2.
- [13] SINDRUM II Collaboration, “A search for muon to electron conversion in muonic gold”, *Eur. Phys. J. C* **47** (2006) 337, doi:10.1140/epjc/s2006-02582-x.
- [14] BaBar Collaboration, “Search for the reactions $e^+e^- \rightarrow \mu^+\tau^-$ and $e^+e^- \rightarrow e^+\tau^-$ ”, *Phys. Rev. D* **75** (2007) 031103, doi:10.1103/PhysRevD.75.031103, arXiv:hep-ex/0607044.
- [15] BaBar Collaboration, “Searches for lepton flavor violation in the decays $\tau^\pm \rightarrow e^\pm\gamma$ and $\tau^\pm \rightarrow \mu^\pm\gamma$ ”, *Phys. Rev. Lett.* **104** (2010) 021802, doi:10.1103/PhysRevLett.104.021802, arXiv:0908.2381.
- [16] Belle Collaboration, “Search for lepton flavor violating τ decays into three leptons with 719 million produced $\tau^+\tau^-$ pairs”, *Phys. Lett. B* **687** (2010) 139, doi:10.1016/j.physletb.2010.03.037, arXiv:1001.3221.
- [17] S. Nussinov, R. D. Peccei, and X. M. Zhang, “On unitarity based relations between various lepton family violating processes”, *Phys. Rev. D* **63** (2001) 016003, doi:10.1103/PhysRevD.63.016003, arXiv:hep-ph/0004153.
- [18] OPAL Collaboration, “A search for lepton flavor violating Z^0 decays”, *Z. Phys. C* **67** (1995) 555, doi:10.1007/BF01553981.

- [19] DELPHI Collaboration, “Search for lepton flavor number violating Z^0 decays”, *Z. Phys. C* **73** (1997) 243, doi:10.1007/s002880050313.
- [20] ATLAS Collaboration, “Search for charged-lepton-flavour violation in Z -boson decays with the ATLAS detector”, *Nature Phys.* **17** (2021) 819, doi:10.1038/s41567-021-01225-z, arXiv:2010.02566.
- [21] ATLAS Collaboration, “Search for lepton-flavor-violation in Z -boson decays with τ leptons with the ATLAS detector”, *Phys. Rev. Lett.* **127** (2022) 271801, doi:10.1103/PhysRevLett.127.271801, arXiv:2105.12491.
- [22] ATLAS Collaboration, “Search for the charged-lepton-flavor-violating decay $Z \rightarrow e\mu$ in pp collisions at $\sqrt{s} = 13$ TeV with the ATLAS detector”, *Phys. Rev. D* **108** (2023) 032015, doi:10.1103/PhysRevD.108.032015, arXiv:2204.10783.
- [23] “HEPData record for this analysis”, 2025. doi:10.17182/hepdata.161021.
- [24] CMS Collaboration, “The CMS experiment at the CERN LHC”, *JINST* **3** (2008) S08004, doi:10.1088/1748-0221/3/08/S08004.
- [25] CMS Collaboration, “Development of the CMS detector for the CERN LHC Run 3”, *JINST* **19** (2024) P05064, doi:10.1088/1748-0221/19/05/P05064, arXiv:2309.05466.
- [26] CMS Tracker Collaboration, “Description and performance of track and primary-vertex reconstruction with the CMS tracker”, *JINST* **9** (2014) P10009, doi:10.1088/1748-0221/9/10/P10009, arXiv:1405.6569.
- [27] CMS Tracker Group Collaboration, “The CMS phase-1 pixel detector upgrade”, *JINST* **16** (2021) P02027, doi:10.1088/1748-0221/16/02/P02027, arXiv:2012.14304.
- [28] CMS Collaboration, “Track impact parameter resolution for the full pseudo rapidity coverage in the 2017 dataset with the CMS phase-1 pixel detector”, CMS Detector Performance Summary CMS-DP-2020-049, 2020.
- [29] CMS Collaboration, “Technical proposal for the Phase-II upgrade of the Compact Muon Solenoid”, CMS Technical Proposal CERN-LHCC-2015-010, CMS-TDR-15-02, 2015.
- [30] CMS Collaboration, “Particle-flow reconstruction and global event description with the CMS detector”, *JINST* **12** (2017) P10003, doi:10.1088/1748-0221/12/10/P10003, arXiv:1706.04965.
- [31] M. Cacciari, G. P. Salam, and G. Soyez, “The anti- k_T jet clustering algorithm”, *JHEP* **04** (2008) 063, doi:10.1088/1126-6708/2008/04/063, arXiv:0802.1189.
- [32] M. Cacciari, G. P. Salam, and G. Soyez, “FastJet user manual”, *Eur. Phys. J. C* **72** (2012) 1896, doi:10.1140/epjc/s10052-012-1896-2, arXiv:1111.6097.
- [33] CMS Collaboration, “Pileup mitigation at CMS in 13 TeV data”, *JINST* **15** (2020) P09018, doi:10.1088/1748-0221/15/09/P09018, arXiv:2003.00503.
- [34] CMS Collaboration, “Jet energy scale and resolution in the CMS experiment in pp collisions at 8 TeV”, *JINST* **12** (2017) P02014, doi:10.1088/1748-0221/12/02/P02014, arXiv:1607.03663.

- [35] CMS Collaboration, “Identification of b-quark jets with the CMS experiment”, *JINST* **8** (2013) P04013, doi:[10.1088/1748-0221/8/04/P04013](https://doi.org/10.1088/1748-0221/8/04/P04013), arXiv:[1211.4462](https://arxiv.org/abs/1211.4462).
- [36] CMS Collaboration, “Performance of the DeepJet b tagging algorithm using 41.9/fb of data from proton-proton collisions at 13 TeV with Phase 1 CMS detector”, CMS Detector Performance Summary CMS-DP-2018-058, 2018.
- [37] E. Bols et al., “Jet flavour classification using DeepJet”, *JINST* **15** (2020) P12012, doi:[10.1088/1748-0221/15/12/P12012](https://doi.org/10.1088/1748-0221/15/12/P12012), arXiv:[2008.10519](https://arxiv.org/abs/2008.10519).
- [38] CMS Collaboration, “Performance of reconstruction and identification of τ leptons decaying to hadrons and ν_τ in pp collisions at $\sqrt{s} = 13$ TeV”, *JINST* **13** (2018) P10005, doi:[10.1088/1748-0221/13/10/P10005](https://doi.org/10.1088/1748-0221/13/10/P10005), arXiv:[1809.02816](https://arxiv.org/abs/1809.02816).
- [39] CMS Collaboration, “Identification of hadronic tau lepton decays using a deep neural network”, *JINST* **17** (2022) P07023, doi:[10.1088/1748-0221/17/07/P07023](https://doi.org/10.1088/1748-0221/17/07/P07023), arXiv:[2201.08458](https://arxiv.org/abs/2201.08458).
- [40] CMS Collaboration, “ECAL 2016 refined calibration and Run 2 summary plots”, CMS Detector Performance Summary CMS-DP-2020-021, 2020.
- [41] CMS Collaboration, “Electron and photon reconstruction and identification with the CMS experiment at the CERN LHC”, *JINST* **16** (2021) P05014, doi:[10.1088/1748-0221/16/05/P05014](https://doi.org/10.1088/1748-0221/16/05/P05014), arXiv:[2012.06888](https://arxiv.org/abs/2012.06888).
- [42] CMS Collaboration, “Performance of the CMS muon detector and muon reconstruction with proton-proton collisions at $\sqrt{s} = 13$ TeV”, *JINST* **13** (2018) P06015, doi:[10.1088/1748-0221/13/06/P06015](https://doi.org/10.1088/1748-0221/13/06/P06015), arXiv:[1804.04528](https://arxiv.org/abs/1804.04528).
- [43] D. Bertolini, P. Harris, M. Low, and N. Tran, “Pileup per particle identification”, *JHEP* **10** (2014) 059, doi:[10.1007/JHEP10\(2014\)059](https://doi.org/10.1007/JHEP10(2014)059), arXiv:[1407.6013](https://arxiv.org/abs/1407.6013).
- [44] CMS Collaboration, “Performance of missing transverse momentum reconstruction in proton-proton collisions at $\sqrt{s} = 13$ TeV using the CMS detector”, *JINST* **14** (2019) P07004, doi:[10.1088/1748-0221/14/07/P07004](https://doi.org/10.1088/1748-0221/14/07/P07004), arXiv:[1903.06078](https://arxiv.org/abs/1903.06078).
- [45] CMS Collaboration, “Performance of the CMS Level-1 trigger in proton-proton collisions at $\sqrt{s} = 13$ TeV”, *JINST* **15** (2020) P10017, doi:[10.1088/1748-0221/15/10/P10017](https://doi.org/10.1088/1748-0221/15/10/P10017), arXiv:[2006.10165](https://arxiv.org/abs/2006.10165).
- [46] CMS Collaboration, “The CMS trigger system”, *JINST* **12** (2017) P01020, doi:[10.1088/1748-0221/12/01/P01020](https://doi.org/10.1088/1748-0221/12/01/P01020), arXiv:[1609.02366](https://arxiv.org/abs/1609.02366).
- [47] CMS Collaboration, “Performance of the CMS high-level trigger during LHC Run 2”, *JINST* **19** (2024) P11021, doi:[10.1088/1748-0221/19/11/P11021](https://doi.org/10.1088/1748-0221/19/11/P11021), arXiv:[2410.17038](https://arxiv.org/abs/2410.17038).
- [48] J. Alwall et al., “The automated computation of tree-level and next-to-leading order differential cross sections, and their matching to parton shower simulations”, *JHEP* **07** (2014) 079, doi:[10.1007/JHEP07\(2014\)079](https://doi.org/10.1007/JHEP07(2014)079), arXiv:[1405.0301](https://arxiv.org/abs/1405.0301).
- [49] J. Alwall et al., “Comparative study of various algorithms for the merging of parton showers and matrix elements in hadronic collisions”, *Eur. Phys. J. C* **53** (2008) 473, doi:[10.1140/epjc/s10052-007-0490-5](https://doi.org/10.1140/epjc/s10052-007-0490-5), arXiv:[0706.2569](https://arxiv.org/abs/0706.2569).

- [50] P. Nason, “A new method for combining NLO QCD with shower Monte Carlo algorithms”, *JHEP* **11** (2004) 040, doi:10.1088/1126-6708/2004/11/040, arXiv:hep-ph/0409146.
- [51] S. Frixione, P. Nason, and C. Oleari, “Matching NLO QCD computations with parton shower simulations: the POWHEG method”, *JHEP* **11** (2007) 070, doi:10.1088/1126-6708/2007/11/070, arXiv:0709.2092.
- [52] S. Alioli, P. Nason, C. Oleari, and E. Re, “A general framework for implementing NLO calculations in shower Monte Carlo programs: the POWHEG BOX”, *JHEP* **06** (2010) 043, doi:10.1007/JHEP06(2010)043, arXiv:1002.2581.
- [53] S. Alioli, P. Nason, C. Oleari, and E. Re, “NLO single-top production matched with shower in POWHEG: s - and t -channel contributions”, *JHEP* **09** (2009) 111, doi:10.1088/1126-6708/2009/09/111, arXiv:0907.4076. [Erratum: doi:10.1007/JHEP02(2010)011].
- [54] E. Re, “Single-top Wt -channel production matched with parton showers using the POWHEG method”, *Eur. Phys. J. C* **71** (2011) 1547, doi:10.1140/epjc/s10052-011-1547-z, arXiv:1009.2450.
- [55] S. Alioli, P. Nason, C. Oleari, and E. Re, “NLO Higgs boson production via gluon fusion matched with shower in POWHEG”, *JHEP* **04** (2009) 002, doi:10.1088/1126-6708/2009/04/002, arXiv:0812.0578.
- [56] P. Nason and C. Oleari, “NLO Higgs boson production via vector-boson fusion matched with shower in POWHEG”, *JHEP* **02** (2010) 037, doi:10.1007/JHEP02(2010)037, arXiv:0911.5299.
- [57] T. Melia, P. Nason, R. Rontsch, and G. Zanderighi, “ W^+W^- , WZ and ZZ production in the POWHEG BOX”, *JHEP* **11** (2011) 078, doi:10.1007/JHEP11(2011)078, arXiv:1107.5051.
- [58] P. Nason and G. Zanderighi, “ W^+W^- , WZ and ZZ production in the POWHEG-BOX-V2”, *Eur. Phys. J. C* **74** (2014) 2702, doi:10.1140/epjc/s10052-013-2702-5, arXiv:1311.1365.
- [59] G. Luisoni, P. Nason, C. Oleari, and F. Tramontano, “ $HW^\pm/HZ + 0$ and 1 jet at NLO with the POWHEG BOX interfaced to GoSam and their merging within MiNLO”, *JHEP* **10** (2013) 083, doi:10.1007/JHEP10(2013)083, arXiv:1306.2542.
- [60] T. Sjöstrand et al., “An introduction to PYTHIA 8.2”, *Comput. Phys. Commun.* **191** (2015) 159, doi:10.1016/j.cpc.2015.01.024, arXiv:1410.3012.
- [61] K. Melnikov and F. Petriello, “Electroweak gauge boson production at hadron colliders through $\mathcal{O}(\alpha_s^2)$ ”, *Phys. Rev. D* **74** (2006) 114017, doi:10.1103/PhysRevD.74.114017, arXiv:hep-ph/0609070.
- [62] M. Czakon and A. Mitov, “Top++: A program for the calculation of the top-pair cross-section at hadron colliders”, *Comput. Phys. Commun.* **185** (2014) 2930, doi:10.1016/j.cpc.2014.06.021, arXiv:1112.5675.
- [63] N. Kidonakis, “Top quark production”, in *Helmholtz International Summer School on Physics of Heavy Quarks and Hadrons*, p. 139. 2014. arXiv:1311.0283. doi:10.3204/DESY-PROC-2013-03/Kidonakis.

- [64] J. M. Campbell, R. K. Ellis, and C. Williams, “Vector boson pair production at the LHC”, *JHEP* **07** (2011) 018, doi:10.1007/JHEP07(2011)018, arXiv:1105.0020.
- [65] T. Gehrmann et al., “ W^+W^- production at hadron colliders in next to next to leading order QCD”, *Phys. Rev. Lett.* **113** (2014) 212001, doi:10.1103/PhysRevLett.113.212001, arXiv:1408.5243.
- [66] CMS Collaboration, “Event generator tunes obtained from underlying event and multiparton scattering measurements”, *Eur. Phys. J. C* **76** (2016) 155, doi:10.1140/epjc/s10052-016-3988-x, arXiv:1512.00815.
- [67] CMS Collaboration, “Extraction and validation of a new set of CMS PYTHIA8 tunes from underlying-event measurements”, *Eur. Phys. J. C* **80** (2020) 4, doi:10.1140/epjc/s10052-019-7499-4, arXiv:1903.12179.
- [68] R. Frederix and S. Frixione, “Merging meets matching in MC@NLO”, *JHEP* **12** (2012) 061, doi:10.1007/JHEP12(2012)061, arXiv:1209.6215.
- [69] NNPDF Collaboration, “Parton distributions for the LHC Run II”, *JHEP* **04** (2015) 040, doi:10.1007/JHEP04(2015)040, arXiv:1410.8849.
- [70] NNPDF Collaboration, “Parton distributions from high-precision collider data”, *Eur. Phys. J. C* **77** (2017) 663, doi:10.1140/epjc/s10052-017-5199-5, arXiv:1706.00428.
- [71] NNPDF Collaboration, “Parton distributions with QED corrections”, *Nucl. Phys. B* **877** (2013) 290, doi:10.1016/j.nuclphysb.2013.10.010, arXiv:1308.0598.
- [72] GEANT4 Collaboration, “GEANT4—a simulation toolkit”, *Nucl. Instrum. Meth. A* **506** (2003) 250, doi:10.1016/S0168-9002(03)01368-8.
- [73] Particle Data Group, S. Navas et al., “Review of particle physics”, *Phys. Rev. D* **110** (2024) 030001, doi:10.1103/PhysRevD.110.030001.
- [74] T. Chen and C. Guestrin, “XGBoost: A scalable tree boosting system”, in *Proceedings of the 22nd ACM SIGKDD International Conference on Knowledge Discovery and Data Mining*, KDD ’16, p. 785. Association for Computing Machinery, New York, NY, USA, 2016. arXiv:1603.02754. doi:10.1145/2939672.2939785.
- [75] M. J. Oreglia, “A study of the reactions $\psi' \rightarrow \gamma\gamma\psi'$ ”, Master’s thesis, Stanford University, 1980. SLAC Report SLAC-R-236.
- [76] J. E. Gaiser, “Charmonium spectroscopy from radiative decays of the J/ψ and ψ' ”, Master’s thesis, Stanford University, 1982. SLAC Report SLAC-0255.
- [77] P. D. Dauncey, M. Kenzie, N. Wardle, and G. J. Davies, “Handling uncertainties in background shapes: the discrete profiling method”, *JINST* **10** (2015) P04015, doi:10.1088/1748-0221/10/04/P04015, arXiv:1408.6865.
- [78] R. A. Fisher, “On the mathematical foundations of theoretical statistics”, *Phil. Trans. Roy. Soc. Lond.* **222** (1922) 309, doi:10.1098/rsta.1922.0009.
- [79] CMS Collaboration, “An embedding technique to determine $\tau\tau$ backgrounds in proton-proton collision data”, *JINST* **14** (2019) P06032, doi:10.1088/1748-0221/14/06/P06032, arXiv:1903.01216.

- [80] CMS Collaboration, “Measurements of Higgs boson production in the decay channel with a pair of τ leptons in proton–proton collisions at $\sqrt{s} = 13$ TeV”, *Eur. Phys. J. C* **83** (2023) 562, doi:10.1140/epjc/s10052-023-11452-8, arXiv:2204.12957.
- [81] CMS Collaboration, “Search for lepton-flavor violating decays of the Higgs boson in the $\mu\tau$ and $e\tau$ final states in proton-proton collisions at $\sqrt{s} = 13$ TeV”, *Phys. Rev. D* **104** (2021) 032013, doi:10.1103/PhysRevD.104.032013, arXiv:2105.03007.
- [82] S. Davidson, S. Lacroix, and P. Verdier, “LHC sensitivity to lepton flavour violating Z boson decays”, *JHEP* **09** (2012) 092, doi:10.1007/JHEP09(2012)092, arXiv:1207.4894.
- [83] TMVA Collaboration, “TMVA — toolkit for multivariate data analysis”, Technical Report CERN-OPEN-2007-007, 2007. arXiv:physics/0703039.
- [84] CMS Collaboration, “Precision luminosity measurement in proton-proton collisions at $\sqrt{s} = 13$ TeV in 2015 and 2016 at CMS”, *Eur. Phys. J. C* **81** (2021) 800, doi:10.1140/epjc/s10052-021-09538-2, arXiv:2104.01927.
- [85] CMS Collaboration, “CMS luminosity measurement for the 2017 data-taking period at $\sqrt{s} = 13$ TeV”, CMS Physics Analysis Summary CMS-PAS-LUM-17-004, 2018.
- [86] CMS Collaboration, “CMS luminosity measurement for the 2018 data-taking period at $\sqrt{s} = 13$ TeV”, CMS Physics Analysis Summary CMS-PAS-LUM-18-002, 2019.
- [87] CMS Collaboration, “Measurement of the inelastic proton-proton cross section at $\sqrt{s} = 13$ TeV”, *JHEP* **07** (2018) 161, doi:10.1007/JHEP07(2018)161, arXiv:1802.02613.
- [88] CMS Collaboration, “The CMS statistical analysis and combination tool: Combine”, *Comput. Softw. Big Sci.* **8** (2024) 19, doi:10.1007/s41781-024-00121-4, arXiv:2404.06614.
- [89] J. S. Conway, “Incorporating nuisance parameters in likelihoods for multisource spectra”, in *Proc. PHYSTAT 2011 Workshop*, p. 115. 2011. arXiv:1103.0354. doi:10.5170/CERN-2011-006.115.
- [90] G. Cowan, K. Cranmer, E. Gross, and O. Vitells, “Asymptotic formulae for likelihood-based tests of new physics”, *Eur. Phys. J. C* **71** (2011) 1554, doi:10.1140/epjc/s10052-011-1554-0, arXiv:1007.1727. [Erratum: doi:10.1140/epjc/s10052-013-2501-z].
- [91] T. Junk, “Confidence level computation for combining searches with small statistics”, *Nucl. Instrum. Meth. A* **434** (1999) 435, doi:10.1016/S0168-9002(99)00498-2, arXiv:hep-ex/9902006.
- [92] A. L. Read, “Presentation of search results: the CL_s technique”, *J. Phys. G* **28** (2002) 2693, doi:10.1088/0954-3899/28/10/313.
- [93] F. E. James, “Statistical Methods in Experimental Physics 2nd Edition”. World Scientific Publishing Co. Pte. Ltd., Singapore, 2006. ISBN 981-270-527-9.
- [94] G. Cowan, “Statistics for searches at the LHC”, in *LHC Phenomenology*, E. Gardi, N. Glover, and R. Aidan, eds. Springer, Cham, 2015. Scottish Graduate Series. doi:10.1007/978-3-319-05362-2_9.

- [95] ATLAS Collaboration, “Search for a heavy neutral particle decaying to $e\mu$, $e\tau$, or $\mu\tau$ in pp collisions at $\sqrt{s} = 8$ TeV with the ATLAS detector”, *Phys. Rev. Lett.* **115** (2015) 031801, doi:10.1103/PhysRevLett.115.031801, arXiv:1503.04430.
- [96] ATLAS Collaboration, “Search for new phenomena in different-flavour high-mass dilepton final states in pp collisions at $\sqrt{s} = 13$ TeV with the ATLAS detector”, *Eur. Phys. J. C* **76** (2016) 541, doi:10.1140/epjc/s10052-016-4385-1, arXiv:1607.08079.
- [97] CMS Collaboration, “Search for lepton flavour violating decays of heavy resonances and quantum black holes to an $e\mu$ pair in proton-proton collisions at $\sqrt{s} = 8$ TeV”, *Eur. Phys. J. C* **76** (2016) 317, doi:10.1140/epjc/s10052-016-4149-y, arXiv:1604.05239.
- [98] CMS Collaboration, “Search for heavy resonances and quantum black holes in $e\mu$, $e\tau$, and $\mu\tau$ final states in proton-proton collisions at $\sqrt{s} = 13$ TeV”, *JHEP* **05** (2023) 227, doi:10.1007/JHEP05(2023)227, arXiv:2205.06709.

A The CMS Collaboration

Yerevan Physics Institute, Yerevan, Armenia

A. Hayrapetyan, V. Makarenko , A. Tumasyan¹ 

Institut für Hochenergiephysik, Vienna, Austria

W. Adam , J.W. Andrejkovic, L. Benato , T. Bergauer , M. Dragicevic , C. Giordano, P.S. Hussain , M. Jeitler² , N. Krammer , A. Li , D. Liko , I. Mikulec , J. Schieck² , R. Schöfbeck² , D. Schwarz , M. Shooshtari, M. Sonawane , W. Waltenberger , C.-E. Wulz² 

Universiteit Antwerpen, Antwerpen, Belgium

T. Janssen , H. Kwon , D. Ocampo Henao , T. Van Laer , P. Van Mechelen 

Vrije Universiteit Brussel, Brussel, Belgium

J. Bierkens , N. Breugelmans, J. D'Hondt , S. Dansana , A. De Moor , M. Delcourt , F. Heyen, Y. Hong , P. Kashko , S. Lowette , I. Makarenko , D. Müller , J. Song , S. Tavernier , M. Tytgat³ , G.P. Van Onsem , S. Van Putte , D. Vannerom 

Université Libre de Bruxelles, Bruxelles, Belgium

B. Bilin , B. Clerbaux , A.K. Das, I. De Bruyn , G. De Lentdecker , H. Evard , L. Favart , P. Gianneios , A. Khalilzadeh, F.A. Khan , A. Malara , M.A. Shahzad, L. Thomas , M. Vanden Bemden , C. Vander Velde , P. Vanlaer , F. Zhang 

Ghent University, Ghent, Belgium

M. De Coen , D. Dobur , G. Gokbulut , J. Knolle , L. Lambrecht , D. Marckx , K. Skovpen , N. Van Den Bossche , J. van der Linden , J. Vandebroeck , L. Wezenbeek 

Université Catholique de Louvain, Louvain-la-Neuve, Belgium

S. Bein , A. Benecke , A. Bethani , G. Bruno , A. Cappati , J. De Favereau De Jeneret , C. Delaere , A. Giammanco , A.O. Guzel , V. Lemaitre, J. Lidrych , P. Malek , P. Mastrapasqua , S. Turkcapar 

Centro Brasileiro de Pesquisas Fisicas, Rio de Janeiro, Brazil

G.A. Alves , M. Barroso Ferreira Filho , E. Coelho , C. Hensel , T. Menezes De Oliveira , C. Mora Herrera⁴ , P. Rebello Teles , M. Soeiro , E.J. Tonelli Manganote⁵ , A. Vilela Pereira⁴ 

Universidade do Estado do Rio de Janeiro, Rio de Janeiro, Brazil

W.L. Aldá Júnior , H. Brandao Malbouisson , W. Carvalho , J. Chinellato⁶ , M. Costa Reis , E.M. Da Costa , G.G. Da Silveira⁷ , D. De Jesus Damiao , S. Fonseca De Souza , R. Gomes De Souza , S. S. Jesus , T. Laux Kuhn⁷ , M. Macedo , K. Mota Amarilo , L. Mundim , H. Nogima , J.P. Pinheiro , A. Santoro , A. Sznajder , M. Thiel , F. Torres Da Silva De Araujo⁸ 

Universidade Estadual Paulista, Universidade Federal do ABC, São Paulo, Brazil

C.A. Bernardes⁷ , T.R. Fernandez Perez Tomei , E.M. Gregores , B. Lopes Da Costa , I. Maietto Silverio , P.G. Mercadante , S.F. Novaes , B. Orzari , Sandra S. Padula , V. Scheurer

Institute for Nuclear Research and Nuclear Energy, Bulgarian Academy of Sciences, Sofia, Bulgaria

A. Aleksandrov , G. Antchev , P. Danev, R. Hadjiiska , P. Iaydjiev , M. Misheva , M. Shopova , G. Sultanov 

University of Sofia, Sofia, Bulgaria

A. Dimitrov , L. Litov , B. Pavlov , P. Petkov , A. Petrov 

Instituto De Alta Investigación, Universidad de Tarapacá, Casilla 7 D, Arica, Chile

S. Keshri , D. Laroze , S. Thakur 

Universidad Tecnica Federico Santa Maria, Valparaiso, Chile

W. Brooks 

Beihang University, Beijing, China

T. Cheng , T. Javaid , L. Wang , L. Yuan 

Department of Physics, Tsinghua University, Beijing, China

Z. Hu , Z. Liang, J. Liu, X. Wang 

Institute of High Energy Physics, Beijing, China

G.M. Chen⁹ , H.S. Chen⁹ , M. Chen⁹ , Y. Chen , Q. Hou , X. Hou, F. Iemmi , C.H. Jiang, A. Kapoor¹⁰ , H. Liao , G. Liu , Z.-A. Liu¹¹ , J.N. Song¹¹, S. Song, J. Tao , C. Wang⁹, J. Wang , H. Zhang , J. Zhao 

State Key Laboratory of Nuclear Physics and Technology, Peking University, Beijing, China

A. Agapitos , Y. Ban , A. Carvalho Antunes De Oliveira , S. Deng , B. Guo, Q. Guo, C. Jiang , A. Levin , C. Li , Q. Li , Y. Mao, S. Qian, S.J. Qian , X. Qin, X. Sun , D. Wang , J. Wang, H. Yang, M. Zhang, Y. Zhao, C. Zhou 

State Key Laboratory of Nuclear Physics and Technology, Institute of Quantum Matter, South China Normal University, Guangzhou, China

S. Yang 

Sun Yat-Sen University, Guangzhou, China

Z. You 

University of Science and Technology of China, Hefei, China

K. Jaffel , N. Lu 

Nanjing Normal University, Nanjing, China

G. Bauer¹², B. Li¹³, H. Wang , K. Yi¹⁴ , J. Zhang 

Institute of Modern Physics and Key Laboratory of Nuclear Physics and Ion-beam Application (MOE) - Fudan University, Shanghai, China

Y. Li

Zhejiang University, Hangzhou, Zhejiang, China

Z. Lin , C. Lu , M. Xiao¹⁵ 

Universidad de Los Andes, Bogota, Colombia

C. Avila , D.A. Barbosa Trujillo , A. Cabrera , C. Florez , J. Fraga , J.A. Reyes Vega

Universidad de Antioquia, Medellin, Colombia

C. Rendón , M. Rodriguez , A.A. Ruales Barbosa , J.D. Ruiz Alvarez 

University of Split, Faculty of Electrical Engineering, Mechanical Engineering and Naval Architecture, Split, Croatia

N. Godinovic , D. Lelas , A. Sculac 

University of Split, Faculty of Science, Split, Croatia

M. Kovac , A. Petkovic , T. Sculac 

Institute Rudjer Boskovic, Zagreb, Croatia

P. Bargassa , V. Brigljevic , B.K. Chitroda , D. Ferencek , K. Jakovcic, A. Starodumov , T. Susa 

University of Cyprus, Nicosia, Cyprus

A. Attikis , K. Christoforou , A. Hadjigapiou, C. Leonidou , C. Nicolaou, L. Paizanou , F. Ptochos , P.A. Razis , H. Rykaczewski, H. Saka , A. Stepenov 

Charles University, Prague, Czech Republic

M. Finger[†] , M. Finger Jr. , A. Kveton 

Escuela Politecnica Nacional, Quito, Ecuador

E. Ayala 

Universidad San Francisco de Quito, Quito, Ecuador

E. Carrera Jarrin 

Academy of Scientific Research and Technology of the Arab Republic of Egypt, Egyptian Network of High Energy Physics, Cairo, Egypt

H. Abdalla¹⁶ , Y. Assran^{17,18} 

Center for High Energy Physics (CHEP-FU), Fayoum University, El-Fayoum, Egypt

M. Abdullah Al-Mashad , A. Hussein, H. Mohammed 

National Institute of Chemical Physics and Biophysics, Tallinn, Estonia

K. Ehataht , M. Kadastik, T. Lange , C. Nielsen , J. Pata , M. Raidal , N. Seeba , L. Tani 

Department of Physics, University of Helsinki, Helsinki, Finland

A. Milieva , K. Osterberg , M. Voutilainen 

Helsinki Institute of Physics, Helsinki, Finland

N. Bin Norjoharuddeen , E. Brückner , F. Garcia , P. Inkaew , K.T.S. Kallonen , R. Kumar Verma , T. Lampén , K. Lassila-Perini , B. Lehtela , S. Lehti , T. Lindén , N.R. Mancilla Xinto , M. Myllymäki , M.m. Rantanen , S. Saariokari , N.T. Toikka , J. Tuominiemi 

Lappeenranta-Lahti University of Technology, Lappeenranta, Finland

H. Kirschenmann , P. Luukka , H. Petrow 

IRFU, CEA, Université Paris-Saclay, Gif-sur-Yvette, France

M. Besancon , F. Couderc , M. Dejardin , D. Denegri, P. Devouge, J.L. Faure , F. Ferri , S. Ganjour , P. Gras , G. Hamel de Monchenault , M. Kumar , V. Lohezic , J. Malcles , F. Orlandi , L. Portales , S. Ronchi , M.Ö. Sahin , A. Savoy-Navarro¹⁹ , P. Simkina , M. Titov , M. Tornago 

Laboratoire Leprince-Ringuet, CNRS/IN2P3, Ecole Polytechnique, Institut Polytechnique de Paris, Palaiseau, France

F. Beaudette , G. Boldrini , P. Busson , C. Charlot , M. Chiusi , T.D. Cuisset , F. Damas , O. Davignon , A. De Wit , T. Debnath , I.T. Ehle , B.A. Fontana Santos Alves , S. Ghosh , A. Gilbert , R. Granier de Cassagnac , L. Kalipoliti , M. Manoni , M. Nguyen , S. Obraztsov , C. Ochando , R. Salerno , J.B. Sauvan , Y. Sirois , G. Sokmen, L. Urda Gómez , A. Zabi , A. Zghiche 

Université de Strasbourg, CNRS, IPHC UMR 7178, Strasbourg, France

J.-L. Agram²⁰ , J. Andrea , D. Bloch , J.-M. Brom , E.C. Chabert , C. Collard 

G. Coulon, S. Falke , U. Goerlach , R. Haeberle , A.-C. Le Bihan , M. Meena , O. Poncet , G. Saha , P. Vaucelle 

Centre de Calcul de l'Institut National de Physique Nucleaire et de Physique des Particules, CNRS/IN2P3, Villeurbanne, France

A. Di Florio 

Institut de Physique des 2 Infinis de Lyon (IP2I), Villeurbanne, France

D. Amram, S. Beauceron , B. Blancon , G. Boudoul , N. Chanon , D. Contardo , P. Depasse , C. Dozen²¹ , H. El Mamouni, J. Fay , S. Gascon , M. Gouzevitch , C. Greenberg , G. Grenier , B. Ille , E. Jourd'huy, I.B. Laktineh, M. Lethuillier , B. Massoteau, L. Mirabito, A. Purohit , M. Vander Donckt , J. Xiao

Georgian Technical University, Tbilisi, Georgia

G. Adamov, I. Lomidze , Z. Tsamalaidze²² 

RWTH Aachen University, I. Physikalisches Institut, Aachen, Germany

V. Botta , S. Consuegra Rodríguez , L. Feld , K. Klein , M. Lipinski , D. Meuser , P. Nattland , V. Oppenländer, A. Pauls , D. Pérez Adán , N. Röwert , M. Teroerde 

RWTH Aachen University, III. Physikalisches Institut A, Aachen, Germany

C. Daumann, S. Diekmann , A. Dodonova , N. Eich , D. Eliseev , F. Engelke , J. Erdmann , M. Erdmann , B. Fischer , T. Hebbeker , K. Hoepfner , F. Ivone , A. Jung , N. Kumar , M.y. Lee , F. Mausolf , M. Merschmeyer , A. Meyer , F. Nowotny, A. Pozdnyakov , W. Redjeb , H. Reithler , U. Sarkar , V. Sarkisovi , A. Schmidt , C. Seth, A. Sharma , J.L. Spah , V. Vaulin, S. Zaleski

RWTH Aachen University, III. Physikalisches Institut B, Aachen, Germany

M.R. Beckers , C. Dziwok , G. Flügge , N. Hoeflich , T. Kress , A. Nowack , O. Pooth , A. Stahl , A. Zotz 

Deutsches Elektronen-Synchrotron, Hamburg, Germany

H. Aarup Petersen , A. Abel, M. Aldaya Martin , J. Alimena , S. Amoroso, Y. An , I. Andreev , J. Bach , S. Baxter , M. Bayatmakou , H. Becerril Gonzalez , O. Behnke , A. Belvedere , F. Blekman²³ , K. Borras²⁴ , A. Campbell , S. Chatterjee , L.X. Coll Saravia , G. Eckerlin, D. Eckstein , E. Gallo²³ , A. Geiser , V. Guglielmi , M. Guthoff , A. Hinzmann , L. Jeppe , M. Kasemann , C. Kleinwort , R. Kogler , M. Komm , D. Krücker , W. Lange, D. Leyva Pernia , K.-Y. Lin , K. Lipka²⁵ , W. Lohmann²⁶ , J. Malvaso , R. Mankel , I.-A. Melzer-Pellmann , M. Mendizabal Morentin , A.B. Meyer , G. Milella , K. Moral Figueroa , A. Mussgiller , L.P. Nair , J. Niedziela , A. Nürnberg , J. Park , E. Ranken , A. Raspereza , D. Rastorguev , L. Rygaard, M. Scham^{27,24} , S. Schnake²⁴ , P. Schütze , C. Schwanenberger²³ , D. Selivanova , K. Sharko , M. Shchedrolosiev , D. Stafford , M. Torkian, F. Vazzoler , A. Ventura Barroso , R. Walsh , D. Wang , Q. Wang , K. Wichmann, L. Wiens²⁴ , C. Wissing , Y. Yang , S. Zakharov, A. Zimmermann Castro Santos

University of Hamburg, Hamburg, Germany

A. Albrecht , A.R. Alves Andrade , M. Antonello , S. Bollweg, M. Bonanomi , K. El Morabit , Y. Fischer , M. Frahm, E. Garutti , A. Grohsjean , J. Haller , D. Hundhausen, H.R. Jabusch , G. Kasieczka , P. Keicher , R. Klanner , W. Korrcari , T. Kramer , C.c. Kuo, V. Kutzner , F. Labe , J. Lange , A. Lobanov , L. Moureaux , M. Mrowietz, A. Nigamova , K. Nikolopoulos , Y. Nissan, A. Paasch , K.J. Pena Rodriguez , N. Prouvost, T. Quadfasel , B. Raciti , M. Rieger , D. Savoiu

J. Schindler , P. Schleper , M. Schröder , J. Schwandt , M. Sommerhalder , H. Stadie , G. Steinbrück , A. Tews, R. Ward , B. Wiederspan, M. Wolf

Karlsruher Institut fuer Technologie, Karlsruhe, Germany

S. Brommer , E. Butz , Y.M. Chen , T. Chwalek , A. Dierlamm , G.G. Dincer , U. Elicabuk, N. Faltermann , M. Giffels , A. Gottmann , F. Hartmann²⁸ , R. Hofsaess , M. Horzela , U. Husemann , J. Kieseler , M. Klute , R. Kunnilan Muhammed Rafeek, O. Lavoryk , J.M. Lawhorn , A. Lintuluoto , S. Maier , M. Mormile , Th. Müller , E. Pfeffer , M. Presilla , G. Quast , K. Rabbertz , B. Regnery , R. Schmieder, N. Shadskiy , I. Shvetsov , H.J. Simonis , L. Sowa , L. Stockmeier, K. Tauqueer, M. Toms , B. Topko , N. Trevisani , C. Verstege , T. Voigtländer , R.F. Von Cube , J. Von Den Driesch, M. Wassmer , R. Wolf , W.D. Zeuner , X. Zuo

Institute of Nuclear and Particle Physics (INPP), NCSR Demokritos, Aghia Paraskevi, Greece

G. Anagnostou , G. Daskalakis , A. Kyriakis , A. Papadopoulos²⁸ , A. Stakia 

National and Kapodistrian University of Athens, Athens, Greece

G. Melachroinos, Z. Painesis , I. Paraskevas , N. Saoulidou , K. Theofilatos , E. Tziaferi , K. Vellidis , I. Zisopoulos 

National Technical University of Athens, Athens, Greece

T. Chatzistavrou, G. Karapostoli , K. Kousouris , E. Siamarkou, G. Tsipolitis 

University of Ioánnina, Ioánnina, Greece

I. Bestintzanos, I. Evangelou , C. Foudas, P. Katsoulis, P. Kokkas , P.G. Kosmoglou Kioseoglou , N. Manthos , I. Papadopoulos , J. Strologas 

HUN-REN Wigner Research Centre for Physics, Budapest, Hungary

D. Druzhkin , C. Hajdu , D. Horvath^{29,30} , K. Márton, A.J. Rádl³¹ , F. Sikler , V. Veszpremi 

MTA-ELTE Lendület CMS Particle and Nuclear Physics Group, Eötvös Loránd University, Budapest, Hungary

M. Csanad , K. Farkas , A. Feherkuti³² , M.M.A. Gadallah³³ , Á. Kadlecik , G. Pasztor , G.I. Veres 

Faculty of Informatics, University of Debrecen, Debrecen, Hungary

B. Ujvari , G. Zilizi 

HUN-REN ATOMKI - Institute of Nuclear Research, Debrecen, Hungary

G. Bencze, S. Czellar, J. Molnar, Z. Szillasi

Karoly Robert Campus, MATE Institute of Technology, Gyongyos, Hungary

T. Csorgo³² , F. Nemes³² , T. Novak , I. Szanyi³⁴ 

Panjab University, Chandigarh, India

S. Bansal , S.B. Beri, V. Bhatnagar , G. Chaudhary , S. Chauhan , N. Dhingra³⁵ , A. Kaur , A. Kaur , H. Kaur , M. Kaur , S. Kumar , T. Sheokand, J.B. Singh , A. Singla

University of Delhi, Delhi, India

A. Bhardwaj , A. Chhetri , B.C. Choudhary , A. Kumar , A. Kumar , M. Naimuddin , S. Phor , K. Ranjan , M.K. Saini

University of Hyderabad, Hyderabad, India

S. Acharya³⁶ , B. Gomber³⁶ , B. Sahu³⁶ 

Indian Institute of Technology Kanpur, Kanpur, India

S. Mukherjee 

Saha Institute of Nuclear Physics, HBNI, Kolkata, India

S. Baradie , S. Bhattacharya , S. Das Gupta, S. Dutta , S. Dutta, S. Sarkar

Indian Institute of Technology Madras, Madras, India

M.M. Ameen , P.K. Behera , S. Chatterjee , G. Dash , A. Dattamunsi, P. Jana , P. Kalbhor , S. Kamble , J.R. Komaragiri³⁷ , T. Mishra , P.R. Pujahari , N.R. Saha , A.K. Sikdar , R.K. Singh , P. Verma , S. Verma , A. Vijay

IISER Mohali, India, Mohali, India

B.K. Sirasva

Tata Institute of Fundamental Research-A, Mumbai, India

L. Bhatt, S. Dugad , G.B. Mohanty , M. Shelake , P. Suryadevara

Tata Institute of Fundamental Research-B, Mumbai, India

A. Bala , S. Banerjee , S. Barman³⁸ , R.M. Chatterjee, M. Guchait , Sh. Jain , A. Jaiswal, B.M. Joshi , S. Kumar , M. Maity³⁸, G. Majumder , K. Mazumdar , S. Parolia , R. Saxena , A. Thachayath

National Institute of Science Education and Research, An OCC of Homi Bhabha National Institute, Bhubaneswar, Odisha, India

S. Bahinipati³⁹ , D. Maity⁴⁰ , P. Mal , K. Naskar⁴⁰ , A. Nayak⁴⁰ , S. Nayak, K. Pal , R. Raturi, P. Sadangi, S.K. Swain , S. Varghese⁴⁰ , D. Vats⁴⁰ 

Indian Institute of Science Education and Research (IISER), Pune, India

A. Alpana , S. Dube , P. Hazarika , B. Kansal , A. Laha , R. Sharma , S. Sharma , K.Y. Vaish 

Indian Institute of Technology Hyderabad, Telangana, India

S. Ghosh 

Isfahan University of Technology, Isfahan, Iran

H. Bakhshiansohi⁴¹ , A. Jafari⁴² , V. Sedighzadeh Dalavi , M. Zeinali⁴³ 

Institute for Research in Fundamental Sciences (IPM), Tehran, Iran

S. Bashiri , S. Chenarani⁴⁴ , S.M. Etesami , Y. Hosseini , M. Khakzad , E. Khazaie , M. Mohammadi Najafabadi , S. Tizchang⁴⁵ 

University College Dublin, Dublin, Ireland

M. Felcini , M. Grunewald 

INFN Sezione di Bari^a, Università di Bari^b, Politecnico di Bari^c, Bari, Italy

M. Abbrescia^{a,b} , M. Barbieri^{a,b}, M. Buonsante^{a,b} , A. Colaleo^{a,b} , D. Creanza^{a,c} , B. D'Anzia^{a,b} , N. De Filippis^{a,c} , M. De Palma^{a,b} , W. Elmetenawee^{a,b,46} , N. Ferrara^{a,c} , L. Fiore^a , L. Longo^a , M. Louka^{a,b} , G. Maggi^{a,c} , M. Maggi^a , I. Margjeka^a , V. Mastrapasqua^{a,b} , S. My^{a,b} , F. Nenna^{a,b} , S. Nuzzo^{a,b} , A. Pellecchia^{a,b} , A. Pompili^{a,b} , G. Pugliese^{a,c} , R. Radogna^{a,b} , D. Ramos^a , A. Ranieri^a , L. Silvestris^a , F.M. Simone^{a,c} , Ü. Sözbilir^a , A. Stamerra^{a,b} , D. Troiano^{a,b} , R. Venditti^{a,b} , P. Verwilligen^a , A. Zaza^{a,b}

INFN Sezione di Bologna^a, Università di Bologna^b, Bologna, Italy

G. Abbiendi^a , C. Battilana^{a,b} , D. Bonacorsi^{a,b} , P. Capiluppi^{a,b} , F.R. Cavallo^a , M. Cuffiani^{a,b} , G.M. Dallavalle^a , T. Diotalevi^{a,b} , F. Fabbri^a , A. Fanfani^{a,b} , D. Fasanella^a , P. Giacomelli^a , C. Grandi^a , L. Guiducci^{a,b} , S. Lo Meo^{a,47} , M. Lorusso^{a,b} , L. Lunerti^a , S. Marcellini^a , F.L. Navarria^{a,b} , G. Paggi^{a,b} , A. Perrotta^a , F. Primavera^{a,b} , A.M. Rossi^{a,b} , S. Rossi Tisbeni^{a,b} , T. Rovelli^{a,b} , G.P. Siroli^{a,b}

INFN Sezione di Catania^a, Università di Catania^b, Catania, Italy

S. Costa^{a,b,48} , A. Di Mattia^a , A. Lapertosa^a , R. Potenza^{a,b} , A. Tricomi^{a,b,48} 

INFN Sezione di Firenze^a, Università di Firenze^b, Firenze, Italy

J. Altork^{a,b} , P. Assiouras^a , G. Barbagli^a , G. Bardelli^a , M. Bartolini^{a,b} , A. Calandri^{a,b} , B. Camaiani^{a,b} , A. Cassese^a , R. Ceccarelli^a , V. Ciulli^{a,b} , C. Civinini^a , R. D'Alessandro^{a,b} , L. Damenti^{a,b} , E. Focardi^{a,b} , T. Kello^a , G. Latino^{a,b} , P. Lenzi^{a,b} , M. Lizzo^a , M. Meschini^a , S. Paoletti^a , A. Papanastassiou^{a,b} , G. Sguazzoni^a , L. Viliani^a

INFN Laboratori Nazionali di Frascati, Frascati, Italy

L. Benussi , S. Colafranceschi , S. Meola⁴⁹ , D. Piccolo 

INFN Sezione di Genova^a, Università di Genova^b, Genova, Italy

M. Alves Gallo Pereira^a , F. Ferro^a , E. Robutti^a , S. Tosi^{a,b} 

INFN Sezione di Milano-Bicocca^a, Università di Milano-Bicocca^b, Milano, Italy

A. Benaglia^a , F. Brivio^a , V. Camagni^{a,b} , F. Cetorelli^{a,b} , F. De Guio^{a,b} , M.E. Dinardo^{a,b} , P. Dini^a , S. Gennai^a , R. Gerosa^{a,b} , A. Ghezzi^{a,b} , P. Govoni^{a,b} , L. Guzzi^a , G. Lavizzari^{a,b} , M.T. Lucchini^{a,b} , M. Malberti^a , S. Malvezzi^a , A. Massironi^a , D. Menasce^a , L. Moroni^a , M. Paganoni^{a,b} , S. Palluotto^{a,b} , D. Pedrini^a , A. Perego^{a,b} , B.S. Pinolini^a, G. Pizzati^{a,b} , S. Ragazzi^{a,b} , T. Tabarelli de Fatis^{a,b} 

INFN Sezione di Napoli^a, Università di Napoli 'Federico II'^b, Napoli, Italy; Università della Basilicata^c, Potenza, Italy; Scuola Superiore Meridionale (SSM)^d, Napoli, Italy

S. Buontempo^a , A. Cagnotta^{a,b} , C. Di Fraia^{a,b} , F. Fabozzi^{a,c} , L. Favilla^{a,d} , A.O.M. Iorio^{a,b} , L. Lista^{a,b,50} , P. Paolucci^{a,28} , B. Rossi^a

INFN Sezione di Padova^a, Università di Padova^b, Padova, Italy; Universita degli Studi di Cagliari^c, Cagliari, Italy

P. Azzi^a , N. Bacchetta^{a,51} , A. Bergnoli^a , P. Bortignon^a , G. Bortolato^{a,b} , A.C.M. Bulla^a , R. Carlin^{a,b} , P. Checchia^a , T. Dorigo^{a,52} , F. Gasparini^{a,b} , S. Giorgetti^a , E. Lusiani^a , M. Margoni^{a,b} , A.T. Meneguzzo^{a,b} , J. Pazzini^{a,b} , P. Ronchese^{a,b} , R. Rossin^{a,b} , F. Simonetto^{a,b} , M. Tosi^{a,b} , A. Triossi^{a,b} , S. Ventura^a , M. Zanetti^{a,b} , P. Zotto^{a,b} , A. Zucchetta^{a,b} , G. Zumerle^{a,b} 

INFN Sezione di Pavia^a, Università di Pavia^b, Pavia, Italy

A. Braghieri^a , S. Calzaferri^a , P. Montagna^{a,b} , M. Pelliccioni^a , V. Re^a , C. Riccardi^{a,b} , P. Salvini^a , I. Vai^{a,b} , P. Vitulo^{a,b}

INFN Sezione di Perugia^a, Università di Perugia^b, Perugia, Italy

S. Ajmal^{a,b} , M.E. Ascioti^{a,b} , G.M. Bilei^a , C. Carrivale^{a,b} , D. Ciangottini^{a,b} , L. Della Penna^{a,b} , L. Fanò^{a,b} , V. Mariani^{a,b} , M. Menichelli^a , F. Moscatelli^{a,53} , A. Rossi^{a,b} , A. Santocchia^{a,b} , D. Spiga^a , T. Tedeschi^{a,b}

INFN Sezione di Pisa^a, Università di Pisa^b, Scuola Normale Superiore di Pisa^c, Pisa, Italy;

Università di Siena^a, Siena, Italy

C. Aimè^{a,b} , C.A. Alexe^{a,c} , P. Asenov^{a,b} , P. Azzurri^a , G. Bagliesi^a , R. Bhattacharya^a , L. Bianchini^{a,b} , T. Boccali^a , E. Bossini^a , D. Bruschini^{a,c} , L. Calligaris^{a,b} , R. Castaldi^a , F. Cattafesta^{a,c} , M.A. Ciocci^{a,b} , M. Cipriani^{a,b} , V. D'Amante^{a,d} , R. Dell'Orso^a , S. Donato^{a,b} , R. Forti^{a,b} , A. Giassi^a , F. Ligabue^{a,c} , A.C. Marini^{a,b} , D. Matos Figueiredo^a , A. Messineo^{a,b} , S. Mishra^a , V.K. Muraleedharan Nair Bindhu^{a,b} , S. Nandan^a , F. Palla^a , M. Riggirello^{a,c} , A. Rizzi^{a,b} , G. Rolandi^{a,c} , S. Roy Chowdhury^{a,54} , T. Sarkar^a , A. Scribano^a , P. Spagnolo^a , F. Tenchini^{a,b} , R. Tenchini^a , G. Tonelli^{a,b} , N. Turini^{a,d} , F. Vaselli^{a,c} , A. Venturi^a , P.G. Verdini^a

INFN Sezione di Roma^a, Sapienza Università di Roma^b, Roma, Italy

P. Akrap^{a,b} , C. Basile^{a,b} , S.C. Behera^a , F. Cavallari^a , L. Cunqueiro Mendez^{a,b} , F. De Riggia^{a,b} , D. Del Re^{a,b} , E. Di Marco^a , M. Diemoz^a , F. Errico^a , L. Frosina^{a,b} , R. Gargiulo^{a,b} , B. Harikrishnan^{a,b} , F. Lombardi^{a,b} , E. Longo^{a,b} , L. Martikainen^{a,b} , J. Mijuskovic^{a,b} , G. Organtini^{a,b} , N. Palmeri^{a,b} , R. Paramatti^{a,b} , C. Quaranta^{a,b} , S. Rahatlou^{a,b} , C. Rovelli^a , F. Santanastasio^{a,b} , L. Soffi^a , V. Vladimirov^{a,b}

INFN Sezione di Torino^a, Università di Torino^b, Torino, Italy; Università del Piemonte Orientale^c, Novara, Italy

N. Amapane^{a,b} , R. Arcidiacono^{a,c} , S. Argiro^{a,b} , M. Arneodo^{a,c} , N. Bartosik^{a,c} , R. Bellan^{a,b} , A. Bellora^{a,b} , C. Biino^a , C. Borca^{a,b} , N. Cartiglia^a , M. Costa^{a,b} , R. Covarelli^{a,b} , N. Demaria^a , L. Finco^a , M. Grippo^{a,b} , B. Kiani^{a,b} , L. Lanteri^{a,b} , F. Legger^a , F. Luongo^{a,b} , C. Mariotti^a , S. Maselli^a , A. Mecca^{a,b} , L. Menzio^{a,b} , P. Meridiani^a , E. Migliore^{a,b} , M. Monteno^a , M.M. Obertino^{a,b} , G. Ortona^a , L. Pacher^{a,b} , N. Pastrone^a , M. Ruspa^{a,c} , F. Siviero^{a,b} , V. Sola^{a,b} , A. Solano^{a,b} , A. Staiano^a , C. Tarricone^{a,b} , D. Trocino^a , G. Umoret^{a,b} , E. Vlasov^{a,b} , R. White^{a,b}

INFN Sezione di Trieste^a, Università di Trieste^b, Trieste, Italy

J. Babbar^{a,b} , S. Belforte^a , V. Candelise^{a,b} , M. Casarsa^a , F. Cossutti^a , K. De Leo^a , G. Della Ricca^{a,b} , R. Delli Gatti^{a,b} 

Kyungpook National University, Daegu, Korea

S. Dogra , J. Hong , J. Kim, T. Kim , D. Lee, H. Lee , J. Lee, S.W. Lee , C.S. Moon , Y.D. Oh , S. Sekmen , B. Tae, Y.C. Yang

Department of Mathematics and Physics - GWNU, Gangneung, Korea

M.S. Kim 

Chonnam National University, Institute for Universe and Elementary Particles, Kwangju, Korea

G. Bak , P. Gwak , H. Kim , D.H. Moon , J. Seo 

Hanyang University, Seoul, Korea

E. Asilar , F. Carnevali , J. Choi⁵⁵ , T.J. Kim , Y. Ryou 

Korea University, Seoul, Korea

S. Ha , S. Han, B. Hong , K. Lee, K.S. Lee , S. Lee , J. Yoo 

Kyung Hee University, Department of Physics, Seoul, Korea

J. Goh , J. Shin , S. Yang 

Sejong University, Seoul, Korea

Y. Kang , H. S. Kim , Y. Kim , S. Lee 

Seoul National University, Seoul, Korea

J. Almond, J.H. Bhyun, J. Choi , J. Choi, W. Jun , J. Kim , T. Kim, Y. Kim, Y.W. Kim , S. Ko , H. Lee , J. Lee , J. Lee , B.H. Oh , S.B. Oh , H. Seo , J. Shin , U.K. Yang, I. Yoon 

University of Seoul, Seoul, Korea

W. Jang , D.Y. Kang, D. Kim , S. Kim , B. Ko, J.S.H. Lee , Y. Lee , J.A. Merlin, I.C. Park , Y. Roh, I.J. Watson 

Yonsei University, Department of Physics, Seoul, Korea

G. Cho, K. Hwang , B. Kim , S. Kim, K. Lee , H.D. Yoo 

Sungkyunkwan University, Suwon, Korea

M. Choi , M.R. Kim , Y. Lee , I. Yu 

College of Engineering and Technology, American University of the Middle East (AUM), Dasman, Kuwait

T. Beyrouthy , Y. Gharbia 

Kuwait University - College of Science - Department of Physics, Safat, Kuwait

F. Alazemi 

Riga Technical University, Riga, Latvia

K. Dreimanis , O.M. Eberlins , A. Gaile , C. Munoz Diaz , D. Osite , G. Pikurs , R. Plese , A. Potrebko , M. Seidel , D. Sidiropoulos Kontos 

University of Latvia (LU), Riga, Latvia

N.R. Strautnieks 

Vilnius University, Vilnius, Lithuania

M. Ambrozas , A. Juodagalvis , S. Nargelas , A. Rinkevicius , G. Tamulaitis 

National Centre for Particle Physics, Universiti Malaya, Kuala Lumpur, Malaysia

I. Yusuff⁵⁶ , Z. Zolkapli

Universidad de Sonora (UNISON), Hermosillo, Mexico

J.F. Benitez , A. Castaneda Hernandez , A. Cota Rodriguez , L.E. Cuevas Picos, H.A. Encinas Acosta, L.G. Gallegos Maríñez, M. León Coello , J.A. Murillo Quijada , A. Sehrawat , L. Valencia Palomo 

Centro de Investigacion y de Estudios Avanzados del IPN, Mexico City, Mexico

G. Ayala , H. Castilla-Valdez , H. Crotte Ledesma , R. Lopez-Fernandez , J. Mejia Guisao , R. Reyes-Almanza , A. Sánchez Hernández 

Universidad Iberoamericana, Mexico City, Mexico

C. Oropeza Barrera , D.L. Ramirez Guadarrama, M. Ramírez García 

Benemerita Universidad Autonoma de Puebla, Puebla, Mexico

I. Bautista , F.E. Neri Huerta , I. Pedraza , H.A. Salazar Ibarguen , C. Uribe Estrada 

University of Montenegro, Podgorica, Montenegro

I. Bubanja , N. Raicevic 

University of Canterbury, Christchurch, New Zealand

P.H. Butler 

National Centre for Physics, Quaid-I-Azam University, Islamabad, Pakistan

A. Ahmad , M.I. Asghar , A. Awais , M.I.M. Awan, W.A. Khan 

AGH University of Krakow, Krakow, Poland

V. Avati, L. Forthomme , L. Grzanka , M. Malawski , K. Piotrzkowski 

National Centre for Nuclear Research, Swierk, Poland

M. Bluj , M. Górski , M. Kazana , M. Szleper , P. Zalewski 

Institute of Experimental Physics, Faculty of Physics, University of Warsaw, Warsaw, Poland

K. Bunkowski , K. Doroba , A. Kalinowski , M. Konecki , J. Krolikowski , A. Muhammad 

Warsaw University of Technology, Warsaw, Poland

P. Fokow , K. Pozniak , W. Zabolotny 

Laboratório de Instrumentação e Física Experimental de Partículas, Lisboa, Portugal

M. Araujo , D. Bastos , C. Beirão Da Cruz E Silva , A. Boletti , M. Bozzo , T. Camporesi , G. Da Molin , P. Faccioli , M. Gallinaro , J. Hollar , N. Leonardo , G.B. Marozzo , A. Petrilli , M. Pisano , J. Seixas , J. Varela , J.W. Wulff 

Faculty of Physics, University of Belgrade, Belgrade, Serbia

P. Adzic , L. Markovic , P. Milenovic , V. Milosevic 

VINCA Institute of Nuclear Sciences, University of Belgrade, Belgrade, Serbia

D. Devetak , M. Dordevic , J. Milosevic , L. Nadderd , V. Rekovic, M. Stojanovic 

Centro de Investigaciones Energéticas Medioambientales y Tecnológicas (CIEMAT), Madrid, Spain

M. Alcalde Martinez , J. Alcaraz Maestre , Cristina F. Bedoya , J.A. Brochero Cifuentes , Oliver M. Carretero , M. Cepeda , M. Cerrada , N. Colino , J. Cuchillo Ortega, B. De La Cruz , A. Delgado Peris , A. Escalante Del Valle , D. Fernández Del Val , J.P. Fernández Ramos , J. Flix , M.C. Fouz , M. Gonzalez Hernandez , O. Gonzalez Lopez , S. Goy Lopez , J.M. Hernandez , M.I. Josa , J. Llorente Merino , C. Martin Perez , E. Martin Viscasillas , D. Moran , C. M. Morcillo Perez , R. Paz Herrera , C. Perez Dengra , A. Pérez-Calero Yzquierdo , J. Puerta Pelayo , I. Redondo , J. Vazquez Escobar 

Universidad Autónoma de Madrid, Madrid, Spain

J.F. de Trocóniz 

Universidad de Oviedo, Instituto Universitario de Ciencias y Tecnologías Espaciales de Asturias (ICTEA), Oviedo, Spain

B. Alvarez Gonzalez , J. Ayllon Torresano , A. Cardini , J. Cuevas , J. Del Riego Badas , D. Estrada Acevedo , J. Fernandez Menendez , S. Folgueras , I. Gonzalez Caballero , P. Leguina , M. Obeso Menendez , E. Palencia Cortezon , J. Prado Pico , A. Soto Rodríguez , C. Vico Villalba , P. Vischia 

Instituto de Física de Cantabria (IFCA), CSIC-Universidad de Cantabria, Santander, Spain

S. Blanco Fernández , I.J. Cabrillo , A. Calderon , J. Duarte Campderros , M. Fernandez , G. Gomez , C. Lasosa García , R. Lopez Ruiz , C. Martinez Rivero , P. Martinez Ruiz del Arbol , F. Matorras , P. Matorras Cuevas , E. Navarrete Ramos , J. Piedra Gomez , C. Quintana San Emeterio , L. Scodellaro , I. Vila , R. Vilal Cortabitarte , J.M. Vizan Garcia 

University of Colombo, Colombo, Sri Lanka

B. Kailasapathy⁵⁷ , D.D.C. Wickramarathna 

University of Ruhuna, Department of Physics, Matara, Sri Lanka

W.G.D. Dharmaratna⁵⁸ , K. Liyanage , N. Perera 

CERN, European Organization for Nuclear Research, Geneva, Switzerland

D. Abbaneo , C. Amendola , R. Ardino , E. Auffray , J. Baechler, D. Barney , M. Bianco , A. Bocci , L. Borgonovi , C. Botta , A. Bragagnolo , C.E. Brown , C. Caillol , G. Cerminara , P. Connor , D. d'Enterria , A. Dabrowski , A. David , A. De Roeck , M.M. Defranchis , M. Deile , M. Dobson , W. Funk , A. Gaddi, S. Giani, D. Gigi, K. Gill , F. Glege , M. Glowacki, A. Gruber , J. Hegeman , J.K. Heikkilä , B. Huber , V. Innocente , T. James , P. Janot , O. Kaluzinska , O. Karacheban²⁶ , G. Karathanasis , S. Laurila , P. Lecoq , C. Lourenço , A.-M. Lyon , M. Magherini , L. Malgeri , M. Mannelli , M. Matthewman, A. Mehta , F. Meijers , S. Mersi , E. Meschi , M. Migliorini , F. Monti , F. Moortgat , M. Mulders , M. Musich , I. Neutelings , S. Orfanelli, F. Pantaleo , M. Pari , G. Petrucciani , A. Pfeiffer , M. Pierini , M. Pitt , H. Qu , D. Rabady , B. Ribeiro Lopes , F. Riti , P. Rosado , M. Rovere , H. Sakulin , R. Salvatico , S. Sanchez Cruz , S. Scarfi , M. Selvaggi , A. Sharma , K. Shchelina , P. Silva , P. Sphicas⁵⁹ , A.G. Stahl Leiton , A. Steen , S. Summers , D. Treille , P. Tropea , E. Vernazza , J. Wanczyk⁶⁰ , J. Wang, S. Wuchterl , M. Zarucki , P. Zehetner , P. Zejdl , G. Zevi Della Porta 

PSI Center for Neutron and Muon Sciences, Villigen, Switzerland

T. Bevilacqua⁶¹ , L. Caminada⁶¹ , W. Erdmann , R. Horisberger , Q. Ingram , H.C. Kaestli , D. Kotlinski , C. Lange , U. Langenegger , M. Missiroli⁶¹ , L. Noehte⁶¹ , T. Rohe , A. Samalan 

ETH Zurich - Institute for Particle Physics and Astrophysics (IPA), Zurich, Switzerland

T.K. Arrestad , M. Backhaus , G. Bonomelli , C. Cazzaniga , K. Datta , P. De Bryas Dexmiers D'archiacchiac⁶⁰ , A. De Cosa , G. Dissertori , M. Dittmar, M. Donegà , F. Eble , K. Gedia , F. Glessgen , C. Grab , N. Härringer , T.G. Harte , W. Lustermann , M. Malucchi , R.A. Manzoni , M. Marchegiani , L. Marchese , A. Mascellani⁶⁰ , F. Nessi-Tedaldi , F. Pauss , V. Perovic , B. Ristic , R. Seidita , J. Steggemann⁶⁰ , A. Tarabini , D. Valsecchi , R. Wallny 

Universität Zürich, Zurich, Switzerland

C. Amsler⁶² , P. Bärtschi , F. Bilandzija , M.F. Canelli , G. Celotto , K. Cormier , M. Huwiler , W. Jin , A. Jofrehei , B. Kilminster , T.H. Kwok , S. Leontsinis , V. Lukashenko , A. Macchiolo , F. Meng , J. Motta , A. Reimers , P. Robmann, M. Senger , E. Shokr , F. Stäger , R. Tramontano 

National Central University, Chung-Li, Taiwan

D. Bhowmik, C.M. Kuo, P.K. Rout , S. Taj , P.C. Tiwari³⁷ 

National Taiwan University (NTU), Taipei, Taiwan

L. Ceard, K.F. Chen , Z.g. Chen, A. De Iorio , W.-S. Hou , T.h. Hsu, Y.w. Kao, S. Karmakar , G. Kole , Y.y. Li , R.-S. Lu , E. Paganis , X.f. Su , J. Thomas-Wilsker , L.s. Tsai, D. Tsionou, H.y. Wu , E. Yazgan 

High Energy Physics Research Unit, Department of Physics, Faculty of Science, Chulalongkorn University, Bangkok, Thailand

C. Asawatangtrakuldee , N. Srimanobhas 

Tunis El Manar University, Tunis, Tunisia

Y. Maghrbi 

Çukurova University, Physics Department, Science and Art Faculty, Adana, Turkey

D. Agyel , F. Boran , F. Dolek , I. Dumanoglu⁶³ , Y. Guler⁶⁴ , E. Gurpinar Guler⁶⁴ , C. Isik , O. Kara , A. Kayis Topaksu , Y. Komurcu , G. Onengut , K. Ozdemir⁶⁵ , B. Tali⁶⁶ , U.G. Tok , E. Uslan , I.S. Zorbakir 

Middle East Technical University, Physics Department, Ankara, Turkey

M. Yalvac⁶⁷ 

Bogazici University, Istanbul, Turkey

B. Akgun , I.O. Atakisi⁶⁸ , E. Gülmez , M. Kaya⁶⁹ , O. Kaya⁷⁰ , M.A. Sarkisla⁷¹, S. Tekten⁷² 

Istanbul Technical University, Istanbul, Turkey

A. Cakir , K. Cankocak^{63,73} , S. Sen⁷⁴ 

Istanbul University, Istanbul, Turkey

O. Aydilek⁷⁵ , B. Hacisahinoglu , I. Hos⁷⁶ , B. Kaynak , S. Ozkorucuklu , O. Potok , H. Sert , C. Simsek , C. Zorbilmez 

Yildiz Technical University, Istanbul, Turkey

S. Cerci , A.A. Guvenli , B. Isildak⁷⁷ , D. Sunar Cerci , T. Yetkin²¹ 

Institute for Scintillation Materials of National Academy of Science of Ukraine, Kharkiv, Ukraine

A. Boyaryntsev , O. Dadazhanova, B. Grynyov 

National Science Centre, Kharkiv Institute of Physics and Technology, Kharkiv, Ukraine

L. Levchuk 

University of Bristol, Bristol, United Kingdom

J.J. Brooke , A. Bundock , F. Bury , E. Clement , D. Cussans , D. Dharmender, H. Flacher , J. Goldstein , H.F. Heath , M.-L. Holmberg , L. Kreczko , S. Paramesvaran , L. Robertshaw, M.S. Sanjrani, J. Segal, V.J. Smith 

Rutherford Appleton Laboratory, Didcot, United Kingdom

A.H. Ball, K.W. Bell , A. Belyaev⁷⁸ , C. Brew , R.M. Brown , D.J.A. Cockerill , C. Cooke , A. Elliot , K.V. Ellis, J. Gajownik , K. Harder , S. Harper , J. Linacre , K. Manolopoulos, M. Moallemi , D.M. Newbold , E. Olaiya , D. Petyt , T. Reis , A.R. Sahasransu , G. Salvi , T. Schuh, C.H. Shepherd-Themistocleous , I.R. Tomalin , K.C. Whalen , T. Williams 

Imperial College, London, United Kingdom

I. Andreou , R. Bainbridge , P. Bloch , O. Buchmuller, C.A. Carrillo Montoya , D. Colling , J.S. Dancu, I. Das , P. Dauncey , G. Davies , M. Della Negra , S. Fayer, G. Fedi , G. Hall , H.R. Hoorani , A. Howard, G. Iles , C.R. Knight , P. Krueper , J. Langford , K.H. Law , J. León Holgado , E. Leutgeb , L. Lyons , A.-M. Magnan , B. Maier , S. Mallios, A. Mastronikolis , M. Mieskolainen , J. Nash⁷⁹ , M. Pesaresi , P.B. Pradeep , B.C. Radburn-Smith , A. Richards, A. Rose , L. Russell , K. Savva , C. Seez , R. Shukla , A. Tapper , K. Uchida , G.P. Uttley , T. Virdee²⁸ , M. Vojinovic , N. Wardle , D. Winterbottom 

Brunel University, Uxbridge, United Kingdom

J.E. Cole , A. Khan, P. Kyberd , I.D. Reid 

Baylor University, Waco, Texas, USA

S. Abdullin [ID](#), A. Brinkerhoff [ID](#), E. Collins [ID](#), M.R. Darwish [ID](#), J. Dittmann [ID](#), K. Hatakeyama [ID](#), V. Hegde [ID](#), J. Hiltbrand [ID](#), B. McMaster [ID](#), J. Samudio [ID](#), S. Sawant [ID](#), C. Sutantawibul [ID](#), J. Wilson [ID](#)

Bethel University, St. Paul, Minnesota, USA

J.M. Hogan⁸⁰ [ID](#)

Catholic University of America, Washington, DC, USA

R. Bartek [ID](#), A. Dominguez [ID](#), S. Raj [ID](#), A.E. Simsek [ID](#), S.S. Yu [ID](#)

The University of Alabama, Tuscaloosa, Alabama, USA

B. Bam [ID](#), A. Buchot Perraguin [ID](#), S. Campbell, R. Chudasama [ID](#), S.I. Cooper [ID](#), C. Crovella [ID](#), G. Fidalgo [ID](#), S.V. Gleyzer [ID](#), A. Khukhunaishvili [ID](#), K. Matchev [ID](#), E. Pearson, C.U. Perez [ID](#), P. Rumerio⁸¹ [ID](#), E. Usai [ID](#), R. Yi [ID](#)

Boston University, Boston, Massachusetts, USA

S. Cholak [ID](#), G. De Castro, Z. Demiragli [ID](#), C. Erice [ID](#), C. Fangmeier [ID](#), C. Fernandez Madrazo [ID](#), E. Fontanesi [ID](#), J. Fulcher [ID](#), F. Golf [ID](#), S. Jeon [ID](#), J. O'Cain, I. Reed [ID](#), J. Rohlf [ID](#), K. Salyer [ID](#), D. Sperka [ID](#), D. Spitzbart [ID](#), I. Suarez [ID](#), A. Tsatsos [ID](#), E. Wurtz, A.G. Zecchinelli [ID](#)

Brown University, Providence, Rhode Island, USA

G. Barone [ID](#), G. Benelli [ID](#), D. Cutts [ID](#), S. Ellis [ID](#), L. Gouskos [ID](#), M. Hadley [ID](#), U. Heintz [ID](#), K.W. Ho [ID](#), T. Kwon [ID](#), G. Landsberg [ID](#), K.T. Lau [ID](#), J. Luo [ID](#), S. Mondal [ID](#), J. Roloff, T. Russell [ID](#), S. Sagir⁸² [ID](#), X. Shen [ID](#), M. Stamenkovic [ID](#), N. Venkatasubramanian [ID](#)

University of California, Davis, Davis, California, USA

S. Abbott [ID](#), B. Barton [ID](#), R. Breedon [ID](#), H. Cai [ID](#), M. Calderon De La Barca Sanchez [ID](#), M. Chertok [ID](#), M. Citron [ID](#), J. Conway [ID](#), P.T. Cox [ID](#), R. Erbacher [ID](#), O. Kukral [ID](#), G. Mocellin [ID](#), S. Ostrom [ID](#), W. Wei [ID](#), S. Yoo [ID](#)

University of California, Los Angeles, California, USA

K. Adamidis, M. Bachtis [ID](#), D. Campos, R. Cousins [ID](#), A. Datta [ID](#), G. Flores Avila [ID](#), J. Hauser [ID](#), M. Ignatenko [ID](#), M.A. Iqbal [ID](#), T. Lam [ID](#), Y.f. Lo [ID](#), E. Manca [ID](#), A. Nunez Del Prado [ID](#), D. Saltzberg [ID](#), V. Valuev [ID](#)

University of California, Riverside, Riverside, California, USA

R. Clare [ID](#), J.W. Gary [ID](#), G. Hanson [ID](#)

University of California, San Diego, La Jolla, California, USA

A. Aportela [ID](#), A. Arora [ID](#), J.G. Branson [ID](#), S. Cittolin [ID](#), S. Cooperstein [ID](#), D. Diaz [ID](#), J. Duarte [ID](#), L. Giannini [ID](#), Y. Gu, J. Guiang [ID](#), V. Krutelyov [ID](#), R. Lee [ID](#), J. Letts [ID](#), H. Li, M. Masciovecchio [ID](#), F. Mokhtar [ID](#), S. Mukherjee [ID](#), M. Pieri [ID](#), D. Primosch, M. Quinnan [ID](#), V. Sharma [ID](#), M. Tadel [ID](#), E. Vourliotis [ID](#), F. Würthwein [ID](#), A. Yagil [ID](#), Z. Zhao

University of California, Santa Barbara - Department of Physics, Santa Barbara, California, USA

A. Barzdukas [ID](#), L. Brennan [ID](#), C. Campagnari [ID](#), S. Carron Montero⁸³ [ID](#), K. Downham [ID](#), C. Grieco [ID](#), M.M. Hussain, J. Incandela [ID](#), J. Kim [ID](#), M.W.K. Lai, A.J. Li [ID](#), P. Masterson [ID](#), J. Richman [ID](#), S.N. Santpur [ID](#), U. Sarica [ID](#), R. Schmitz [ID](#), F. Setti [ID](#), J. Sheplock [ID](#), D. Stuart [ID](#), T.Á. Vámi [ID](#), X. Yan [ID](#), D. Zhang [ID](#)

California Institute of Technology, Pasadena, California, USA

A. Albert [ID](#), S. Bhattacharya [ID](#), A. Bornheim [ID](#), O. Cerri, R. Kansal [ID](#), J. Mao [ID](#), H.B. New-

man [ID](#), G. Reales Gutiérrez, T. Sievert, M. Spiropulu [ID](#), J.R. Vlimant [ID](#), R.A. Wynne [ID](#), S. Xie [ID](#)

Carnegie Mellon University, Pittsburgh, Pennsylvania, USA

J. Alison [ID](#), S. An [ID](#), M. Cremonesi, V. Dutta [ID](#), E.Y. Ertorer [ID](#), T. Ferguson [ID](#), T.A. Gómez Espinosa [ID](#), A. Harilal [ID](#), A. Kallil Tharayil, M. Kanemura, C. Liu [ID](#), P. Meiring [ID](#), T. Mudholkar [ID](#), S. Murthy [ID](#), P. Palit [ID](#), K. Park [ID](#), M. Paulini [ID](#), A. Roberts [ID](#), A. Sanchez [ID](#), W. Terrill [ID](#)

University of Colorado Boulder, Boulder, Colorado, USA

J.P. Cumalat [ID](#), W.T. Ford [ID](#), A. Hart [ID](#), A. Hassani [ID](#), S. Kwan [ID](#), J. Pearkes [ID](#), C. Savard [ID](#), N. Schonbeck [ID](#), K. Stenson [ID](#), K.A. Ulmer [ID](#), S.R. Wagner [ID](#), N. Zipper [ID](#), D. Zuolo [ID](#)

Cornell University, Ithaca, New York, USA

J. Alexander [ID](#), X. Chen [ID](#), D.J. Cranshaw [ID](#), J. Dickinson [ID](#), J. Fan [ID](#), X. Fan [ID](#), J. Grassi [ID](#), S. Hogan [ID](#), P. Kotamnives [ID](#), J. Monroy [ID](#), G. Niendorf [ID](#), M. Oshiro [ID](#), J.R. Patterson [ID](#), M. Reid [ID](#), A. Ryd [ID](#), J. Thom [ID](#), P. Wittich [ID](#), R. Zou [ID](#), L. Zygalda [ID](#)

Fermi National Accelerator Laboratory, Batavia, Illinois, USA

M. Albrow [ID](#), M. Alyari [ID](#), O. Amram [ID](#), G. Apollinari [ID](#), A. Apresyan [ID](#), L.A.T. Bauerick [ID](#), D. Berry [ID](#), J. Berryhill [ID](#), P.C. Bhat [ID](#), K. Burkett [ID](#), J.N. Butler [ID](#), A. Canepa [ID](#), G.B. Cerati [ID](#), H.W.K. Cheung [ID](#), F. Chlebana [ID](#), C. Cosby [ID](#), G. Cummings [ID](#), I. Dutta [ID](#), V.D. Elvira [ID](#), J. Freeman [ID](#), A. Gandrakota [ID](#), Z. Gecse [ID](#), L. Gray [ID](#), D. Green, A. Grummer [ID](#), S. Grünendahl [ID](#), D. Guerrero [ID](#), O. Gutsche [ID](#), R.M. Harris [ID](#), T.C. Herwig [ID](#), J. Hirschauer [ID](#), B. Jayatilaka [ID](#), S. Jindariani [ID](#), M. Johnson [ID](#), U. Joshi [ID](#), T. Klijnsma [ID](#), B. Klima [ID](#), K.H.M. Kwok [ID](#), S. Lammel [ID](#), C. Lee [ID](#), D. Lincoln [ID](#), R. Lipton [ID](#), T. Liu [ID](#), K. Maeshima [ID](#), D. Mason [ID](#), P. McBride [ID](#), P. Merkel [ID](#), S. Mrenna [ID](#), S. Nahn [ID](#), J. Ngadiuba [ID](#), D. Noonan [ID](#), S. Norberg, V. Papadimitriou [ID](#), N. Pastika [ID](#), K. Pedro [ID](#), C. Pena⁸⁴ [ID](#), C.E. Perez Lara [ID](#), F. Raveria [ID](#), A. Reinsvold Hall⁸⁵ [ID](#), L. Ristori [ID](#), M. Safdari [ID](#), E. Sexton-Kennedy [ID](#), N. Smith [ID](#), A. Soha [ID](#), L. Spiegel [ID](#), S. Stoynev [ID](#), J. Strait [ID](#), L. Taylor [ID](#), S. Tkaczyk [ID](#), N.V. Tran [ID](#), L. Uplegger [ID](#), E.W. Vaandering [ID](#), C. Wang [ID](#), I. Zoi [ID](#)

University of Florida, Gainesville, Florida, USA

C. Aruta [ID](#), P. Avery [ID](#), D. Bourilkov [ID](#), P. Chang [ID](#), V. Cherepanov [ID](#), R.D. Field, C. Huh [ID](#), E. Koenig [ID](#), M. Kolosova [ID](#), J. Konigsberg [ID](#), A. Korytov [ID](#), N. Menendez [ID](#), G. Mitselmakher [ID](#), K. Mohrman [ID](#), A. Muthirakalayil Madhu [ID](#), N. Rawal [ID](#), S. Rosenzweig [ID](#), V. Sulimov [ID](#), Y. Takahashi [ID](#), J. Wang [ID](#)

Florida State University, Tallahassee, Florida, USA

T. Adams [ID](#), A. Al Kadhim [ID](#), A. Askew [ID](#), S. Bower [ID](#), R. Hashmi [ID](#), R.S. Kim [ID](#), T. Kolberg [ID](#), G. Martinez [ID](#), M. Mazza [ID](#), H. Prosper [ID](#), P.R. Prova, M. Wulansatiti [ID](#), R. Yohay [ID](#)

Florida Institute of Technology, Melbourne, Florida, USA

B. Alsufyani [ID](#), S. Butalla [ID](#), S. Das [ID](#), M. Hohlmann [ID](#), M. Lavinsky, E. Yanes

University of Illinois Chicago, Chicago, Illinois, USA

M.R. Adams [ID](#), N. Barnett, A. Baty [ID](#), C. Bennett [ID](#), R. Cavanaugh [ID](#), R. Escobar Franco [ID](#), O. Evdokimov [ID](#), C.E. Gerber [ID](#), H. Gupta [ID](#), M. Hawksworth, A. Hingrajiya, D.J. Hofman [ID](#), J.h. Lee [ID](#), D. S. Lemos [ID](#), C. Mills [ID](#), S. Nanda [ID](#), G. Nigmatkulov [ID](#), B. Ozek [ID](#), T. Phan, D. Pilipovic [ID](#), R. Pradhan [ID](#), E. Prifti, P. Roy, T. Roy [ID](#), N. Singh, M.B. Tonjes [ID](#), N. Varelas [ID](#), M.A. Wadud [ID](#), J. Yoo [ID](#)

The University of Iowa, Iowa City, Iowa, USA

M. Alhusseini [ID](#), D. Blend [ID](#), K. Dilsiz⁸⁶ [ID](#), O.K. Köseyan [ID](#), A. Mestvirishvili⁸⁷ [ID](#), O. Neogi,

H. Ogul⁸⁸ , Y. Onel , A. Penzo , C. Snyder, E. Tiras⁸⁹ 

Johns Hopkins University, Baltimore, Maryland, USA

B. Blumenfeld , J. Davis , A.V. Gritsan , L. Kang , S. Kyriacou , P. Maksimovic , M. Roguljic , S. Sekhar , M.V. Srivastav , M. Swartz 

The University of Kansas, Lawrence, Kansas, USA

A. Abreu , L.F. Alcerro Alcerro , J. Anguiano , S. Arteaga Escatel , P. Baringer , A. Bean , Z. Flowers , D. Grove , J. King , G. Krintiras , M. Lazarovits , C. Le Mahieu , J. Marquez , M. Murray , M. Nickel , S. Popescu⁹⁰ , C. Rogan , C. Royon , S. Rudrabhatla , S. Sanders , C. Smith , G. Wilson

Kansas State University, Manhattan, Kansas, USA

B. Allmond , R. Guju Gurunadha , N. Islam, A. Ivanov , K. Kaadze , Y. Maravin , J. Natoli , D. Roy , G. Sorrentino 

University of Maryland, College Park, Maryland, USA

A. Baden , A. Belloni , J. Bistany-riebman, S.C. Eno , N.J. Hadley , S. Jabeen , R.G. Kellogg , T. Koeth , B. Kronheim, S. Lascio , P. Major , A.C. Mignerey , C. Palmer , C. Papageorgakis , M.M. Paranjpe, E. Popova⁹¹ , A. Shevelev , L. Zhang 

Massachusetts Institute of Technology, Cambridge, Massachusetts, USA

C. Baldenegro Barrera , J. Bendavid , H. Bossi , S. Bright-Thonney , I.A. Cali , Y.c. Chen , P.c. Chou , M. D'Alfonso , J. Eysermans , C. Freer , G. Gomez-Ceballos , M. Goncharov, G. Grossos , P. Harris, D. Hoang , G.M. Innocentini , D. Kovalskyi , J. Krupa , L. Lavezzo , Y.-J. Lee , K. Long , C. McGinn , A. Novak , M.I. Park , C. Paus , C. Reissel , C. Roland , G. Roland , S. Rothman , T.a. Sheng , G.S.F. Stephans , D. Walter , Z. Wang , B. Wyslouch , T. J. Yang

University of Minnesota, Minneapolis, Minnesota, USA

B. Crossman , W.J. Jackson, C. Kapsiak , M. Krohn , D. Mahon , J. Mans , B. Marzocchi , R. Rusack , O. Sancar , R. Saradhy , N. Strobbe 

University of Nebraska-Lincoln, Lincoln, Nebraska, USA

K. Bloom , D.R. Claes , G. Haza , J. Hossain , C. Joo , I. Kravchenko , A. Rohilla , J.E. Siado , W. Tabb , A. Vagnerini , A. Wightman , F. Yan 

State University of New York at Buffalo, Buffalo, New York, USA

H. Bandyopadhyay , L. Hay , H.w. Hsia , I. Iashvili , A. Kalogeropoulos , A. Kharchilava , A. Mandal , M. Morris , D. Nguyen , S. Rappoccio , H. Rejeb Sfar, A. Williams , P. Young , D. Yu 

Northeastern University, Boston, Massachusetts, USA

G. Alverson , E. Barberis , J. Bonilla , B. Bylsma, M. Campana , J. Dervan , Y. Haddad , Y. Han , I. Israr , A. Krishna , M. Lu , N. Manganelli , R. McCarthy , D.M. Morse , T. Orimoto , A. Parker , L. Skinnari , C.S. Thoreson , E. Tsai , D. Wood 

Northwestern University, Evanston, Illinois, USA

S. Dittmer , K.A. Hahn , Y. Liu , M. Mackenzie , M. McGinnis , Y. Miao , D.G. Monk , M.H. Schmitt , A. Taliercio , M. Velasco , J. Wang 

University of Notre Dame, Notre Dame, Indiana, USA

G. Agarwal , R. Band , R. Bucci, S. Castells , A. Das , A. Ehnis, R. Goldouzian , M. Hildreth , K. Hurtado Anampa , T. Ivanov , C. Jessop , A. Karneyeu , K. Lannon 

J. Lawrence [ID](#), N. Loukas [ID](#), L. Lutton [ID](#), J. Mariano [ID](#), N. Marinelli, I. Mcalister, T. McCauley [ID](#), C. Mcgrady [ID](#), C. Moore [ID](#), Y. Musienko²² [ID](#), H. Nelson [ID](#), M. Osherson [ID](#), A. Piccinelli [ID](#), R. Ruchti [ID](#), A. Townsend [ID](#), Y. Wan, M. Wayne [ID](#), H. Yockey

The Ohio State University, Columbus, Ohio, USA

A. Basnet [ID](#), M. Carrigan [ID](#), R. De Los Santos [ID](#), L.S. Durkin [ID](#), C. Hill [ID](#), M. Joyce [ID](#), M. Nunez Ornelas [ID](#), D.A. Wenzl, B.L. Winer [ID](#), B. R. Yates [ID](#)

Princeton University, Princeton, New Jersey, USA

H. Bouchamaoui [ID](#), K. Coldham, P. Das [ID](#), G. Dezoort [ID](#), P. Elmer [ID](#), A. Frankenthal [ID](#), M. Galli [ID](#), B. Greenberg [ID](#), N. Haubrich [ID](#), K. Kennedy, G. Kopp [ID](#), Y. Lai [ID](#), D. Lange [ID](#), A. Loeliger [ID](#), D. Marlow [ID](#), I. Ojalvo [ID](#), J. Olsen [ID](#), F. Simpson [ID](#), D. Stickland [ID](#), C. Tully [ID](#)

University of Puerto Rico, Mayaguez, Puerto Rico, USA

S. Malik [ID](#), R. Sharma [ID](#)

Purdue University, West Lafayette, Indiana, USA

A.S. Bakshi [ID](#), S. Chandra [ID](#), R. Chawla [ID](#), A. Gu [ID](#), L. Gutay, M. Jones [ID](#), A.W. Jung [ID](#), D. Kondratyev [ID](#), M. Liu [ID](#), G. Negro [ID](#), N. Neumeister [ID](#), G. Paspalaki [ID](#), S. Piperov [ID](#), J.F. Schulte [ID](#), F. Wang [ID](#), A. Wildridge [ID](#), W. Xie [ID](#), Y. Yao [ID](#), Y. Zhong [ID](#)

Purdue University Northwest, Hammond, Indiana, USA

N. Parashar [ID](#), A. Pathak [ID](#), E. Shumka [ID](#)

Rice University, Houston, Texas, USA

D. Acosta [ID](#), A. Agrawal [ID](#), C. Arbour [ID](#), T. Carnahan [ID](#), K.M. Ecklund [ID](#), P.J. Fernández Manteca [ID](#), S. Freed, P. Gardner, F.J.M. Geurts [ID](#), T. Huang [ID](#), I. Krommydas [ID](#), N. Lewis, W. Li [ID](#), J. Lin [ID](#), O. Miguel Colin [ID](#), B.P. Padley [ID](#), R. Redjimi [ID](#), J. Rotter [ID](#), E. Yigitbasi [ID](#), Y. Zhang [ID](#)

University of Rochester, Rochester, New York, USA

O. Bessidskaia Bylund, A. Bodek [ID](#), P. de Barbaro[†] [ID](#), R. Demina [ID](#), J.L. Dulemba [ID](#), A. Garcia-Bellido [ID](#), H.S. Hare [ID](#), O. Hindrichs [ID](#), N. Parmar [ID](#), P. Parygin⁹¹ [ID](#), R. Taus [ID](#)

Rutgers, The State University of New Jersey, Piscataway, New Jersey, USA

B. Chiarito, J.P. Chou [ID](#), S.V. Clark [ID](#), S. Donnelly, D. Gadkari [ID](#), Y. Gershtein [ID](#), E. Halkiadakis [ID](#), M. Heindl [ID](#), C. Houghton [ID](#), D. Jaroslawski [ID](#), S. Konstantinou [ID](#), I. Laflotte [ID](#), A. Lath [ID](#), J. Martins [ID](#), B. Rand [ID](#), J. Reichert [ID](#), P. Saha [ID](#), S. Salur [ID](#), S. Schnetzer, S. Somalwar [ID](#), R. Stone [ID](#), S.A. Thayil [ID](#), S. Thomas, J. Vora [ID](#)

University of Tennessee, Knoxville, Tennessee, USA

D. Ally [ID](#), A.G. Delannoy [ID](#), S. Fiorendi [ID](#), J. Harris, S. Higginbotham [ID](#), T. Holmes [ID](#), A.R. Kanuganti [ID](#), N. Karunarathna [ID](#), J. Lawless, L. Lee [ID](#), E. Nibigira [ID](#), B. Skipworth, S. Spanier [ID](#)

Texas A&M University, College Station, Texas, USA

D. Aebi [ID](#), M. Ahmad [ID](#), T. Akhter [ID](#), K. Androsov [ID](#), A. Bolshov, O. Bouhalil⁹² [ID](#), R. Eusebi [ID](#), P. Flanagan [ID](#), J. Gilmore [ID](#), Y. Guo, T. Kamon [ID](#), H. Kim [ID](#), S. Luo [ID](#), R. Mueller [ID](#), A. Safonov [ID](#)

Texas Tech University, Lubbock, Texas, USA

N. Akchurin [ID](#), J. Damgov [ID](#), Y. Feng [ID](#), N. Gogate [ID](#), Y. Kazhykarim, K. Lamichhane [ID](#), S.W. Lee [ID](#), C. Madrid [ID](#), A. Mankel [ID](#), T. Peltola [ID](#), I. Volobouev [ID](#)

Vanderbilt University, Nashville, Tennessee, USA

E. Appelt , Y. Chen , S. Greene, A. Gurrola , W. Johns , R. Kunnawalkam Elayavalli , A. Melo , D. Rathjens , F. Romeo , P. Sheldon , S. Tuo , J. Velkovska , J. Viinikainen , J. Zhang

University of Virginia, Charlottesville, Virginia, USA

B. Cardwell , H. Chung , B. Cox , J. Hakala , R. Hirosky , M. Jose, A. Ledovskoy , C. Mantilla , C. Neu , C. Ramón Álvarez 

Wayne State University, Detroit, Michigan, USA

S. Bhattacharya , P.E. Karchin 

University of Wisconsin - Madison, Madison, Wisconsin, USA

A. Aravind , S. Banerjee , K. Black , T. Bose , E. Chavez , S. Dasu , P. Everaerts , C. Galloni, H. He , M. Herndon , A. Herve , C.K. Koraka , S. Lomte , R. Loveless , A. Mallampalli , A. Mohammadi , S. Mondal, T. Nelson, G. Parida , L. Pétré , D. Pinna , A. Savin, V. Shang , V. Sharma , W.H. Smith , D. Teague, H.F. Tsoi , W. Vetens , A. Warden

Authors affiliated with an international laboratory covered by a cooperation agreement with CERN

S. Afanasiev , V. Alexakhin , Yu. Andreev , T. Aushev , D. Budkouski , R. Chistov⁹³ , M. Danilov⁹³ , T. Dimova⁹³ , A. Ershov⁹³ , S. Gninenko , I. Gorbunov , A. Gribushin⁹³ , A. Kamenev , V. Karjavine , M. Kirsanov , V. Klyukhin⁹³ , O. Kodolova⁹⁴ , V. Korenkov , A. Kozyrev⁹³ , N. Krasnikov , A. Lanev , A. Malakhov , V. Matveev⁹³ , A. Nikitenko^{95,94} , V. Palichik , V. Perelygin , S. Petrushanko⁹³ , S. Polikarpov⁹³ , O. Radchenko⁹³ , M. Savina , V. Shalaev , S. Shmatov , S. Shulha , Y. Skovpen⁹³ , V. Smirnov , O. Teryaev , I. Tlisova⁹³ , A. Toropin , N. Voytishin , B.S. Yuldashev⁺⁹⁶, A. Zarubin , I. Zhizhin

Authors affiliated with an institute formerly covered by a cooperation agreement with CERN

E. Boos , V. Bunichev , M. Dubinin⁸⁴ , V. Savrin , A. Snigirev , L. Dudko , K. Ivanov , V. Kim²² , V. Murzin , V. Oreshkin , D. Sosnov 

†: Deceased

¹Also at Yerevan State University, Yerevan, Armenia

²Also at TU Wien, Vienna, Austria

³Also at Ghent University, Ghent, Belgium

⁴Also at Universidade do Estado do Rio de Janeiro, Rio de Janeiro, Brazil

⁵Also at FACAMP - Faculdades de Campinas, Sao Paulo, Brazil

⁶Also at Universidade Estadual de Campinas, Campinas, Brazil

⁷Also at Federal University of Rio Grande do Sul, Porto Alegre, Brazil

⁸Also at The University of the State of Amazonas, Manaus, Brazil

⁹Also at University of Chinese Academy of Sciences, Beijing, China

¹⁰Also at China Center of Advanced Science and Technology, Beijing, China

¹¹Also at University of Chinese Academy of Sciences, Beijing, China

¹²Now at Henan Normal University, Xinxiang, China

¹³Also at University of Shanghai for Science and Technology, Shanghai, China

¹⁴Now at The University of Iowa, Iowa City, Iowa, USA

¹⁵Also at Center for High Energy Physics, Peking University, Beijing, China

¹⁶Also at Cairo University, Cairo, Egypt

¹⁷Also at Suez University, Suez, Egypt

¹⁸Now at British University in Egypt, Cairo, Egypt

- ¹⁹Also at Purdue University, West Lafayette, Indiana, USA
²⁰Also at Université de Haute Alsace, Mulhouse, France
²¹Also at Istinye University, Istanbul, Turkey
²²Also at an institute formerly covered by a cooperation agreement with CERN
²³Also at University of Hamburg, Hamburg, Germany
²⁴Also at RWTH Aachen University, III. Physikalisches Institut A, Aachen, Germany
²⁵Also at Bergische University Wuppertal (BUW), Wuppertal, Germany
²⁶Also at Brandenburg University of Technology, Cottbus, Germany
²⁷Also at Forschungszentrum Jülich, Juelich, Germany
²⁸Also at CERN, European Organization for Nuclear Research, Geneva, Switzerland
²⁹Also at HUN-REN ATOMKI - Institute of Nuclear Research, Debrecen, Hungary
³⁰Now at Universitatea Babes-Bolyai - Facultatea de Fizica, Cluj-Napoca, Romania
³¹Also at MTA-ELTE Lendület CMS Particle and Nuclear Physics Group, Eötvös Loránd University, Budapest, Hungary
³²Also at HUN-REN Wigner Research Centre for Physics, Budapest, Hungary
³³Also at Physics Department, Faculty of Science, Assiut University, Assiut, Egypt
³⁴Also at The University of Kansas, Lawrence, Kansas, USA
³⁵Also at Punjab Agricultural University, Ludhiana, India
³⁶Also at University of Hyderabad, Hyderabad, India
³⁷Also at Indian Institute of Science (IISc), Bangalore, India
³⁸Also at University of Visva-Bharati, Santiniketan, India
³⁹Also at IIT Bhubaneswar, Bhubaneswar, India
⁴⁰Also at Institute of Physics, Bhubaneswar, India
⁴¹Also at Deutsches Elektronen-Synchrotron, Hamburg, Germany
⁴²Also at Isfahan University of Technology, Isfahan, Iran
⁴³Also at Sharif University of Technology, Tehran, Iran
⁴⁴Also at Department of Physics, University of Science and Technology of Mazandaran, Behshahr, Iran
⁴⁵Also at Department of Physics, Faculty of Science, Arak University, ARAK, Iran
⁴⁶Also at Helwan University, Cairo, Egypt
⁴⁷Also at Italian National Agency for New Technologies, Energy and Sustainable Economic Development, Bologna, Italy
⁴⁸Also at Centro Siciliano di Fisica Nucleare e di Struttura Della Materia, Catania, Italy
⁴⁹Also at Università degli Studi Guglielmo Marconi, Roma, Italy
⁵⁰Also at Scuola Superiore Meridionale, Università di Napoli 'Federico II', Napoli, Italy
⁵¹Also at Fermi National Accelerator Laboratory, Batavia, Illinois, USA
⁵²Also at Lulea University of Technology, Lulea, Sweden
⁵³Also at Consiglio Nazionale delle Ricerche - Istituto Officina dei Materiali, Perugia, Italy
⁵⁴Also at UPES - University of Petroleum and Energy Studies, Dehradun, India
⁵⁵Also at Institut de Physique des 2 Infinis de Lyon (IP2I), Villeurbanne, France
⁵⁶Also at Department of Applied Physics, Faculty of Science and Technology, Universiti Kebangsaan Malaysia, Bangi, Malaysia
⁵⁷Also at Trincomalee Campus, Eastern University, Sri Lanka, Nilaveli, Sri Lanka
⁵⁸Also at Saegis Campus, Nugegoda, Sri Lanka
⁵⁹Also at National and Kapodistrian University of Athens, Athens, Greece
⁶⁰Also at Ecole Polytechnique Fédérale Lausanne, Lausanne, Switzerland
⁶¹Also at Universität Zürich, Zurich, Switzerland
⁶²Also at Stefan Meyer Institute for Subatomic Physics, Vienna, Austria
⁶³Also at Near East University, Research Center of Experimental Health Science, Mersin,

Turkey

⁶⁴Also at Konya Technical University, Konya, Turkey

⁶⁵Also at Izmir Bakircay University, Izmir, Turkey

⁶⁶Also at Adiyaman University, Adiyaman, Turkey

⁶⁷Also at Bozok Universitetesi Rektörlüğü, Yozgat, Turkey

⁶⁸Also at Istanbul Sabahattin Zaim University, Istanbul, Turkey

⁶⁹Also at Marmara University, Istanbul, Turkey

⁷⁰Also at Milli Savunma University, Istanbul, Turkey

⁷¹Also at Informatics and Information Security Research Center, Gebze/Kocaeli, Turkey

⁷²Also at Kafkas University, Kars, Turkey

⁷³Now at Istanbul Okan University, Istanbul, Turkey

⁷⁴Also at Hacettepe University, Ankara, Turkey

⁷⁵Also at Erzincan Binali Yıldırım University, Erzincan, Turkey

⁷⁶Also at Istanbul University - Cerrahpaşa, Faculty of Engineering, Istanbul, Turkey

⁷⁷Also at Yıldız Technical University, Istanbul, Turkey

⁷⁸Also at School of Physics and Astronomy, University of Southampton, Southampton, United Kingdom

⁷⁹Also at Monash University, Faculty of Science, Clayton, Australia

⁸⁰Also at Bethel University, St. Paul, Minnesota, USA

⁸¹Also at Università di Torino, Torino, Italy

⁸²Also at Karamanoğlu Mehmetbey University, Karaman, Turkey

⁸³Also at California Lutheran University;, Thousand Oaks, California, USA

⁸⁴Also at California Institute of Technology, Pasadena, California, USA

⁸⁵Also at United States Naval Academy, Annapolis, Maryland, USA

⁸⁶Also at Bingöl University, Bingöl, Turkey

⁸⁷Also at Georgian Technical University, Tbilisi, Georgia

⁸⁸Also at Sinop University, Sinop, Turkey

⁸⁹Also at Erciyes University, Kayseri, Turkey

⁹⁰Also at Horia Hulubei National Institute of Physics and Nuclear Engineering (IFIN-HH), Bucharest, Romania

⁹¹Now at another institute formerly covered by a cooperation agreement with CERN

⁹²Also at Hamad Bin Khalifa University (HBKU), Doha, Qatar

⁹³Also at another institute formerly covered by a cooperation agreement with CERN

⁹⁴Also at Yerevan Physics Institute, Yerevan, Armenia

⁹⁵Also at Imperial College, London, United Kingdom

⁹⁶Also at Institute of Nuclear Physics of the Uzbekistan Academy of Sciences, Tashkent, Uzbekistan